ON THE VIBRATIONS OF A ROTOR WITH ROTATING INEQUALITY AND WITH VARIABLE ROTATING SPEED

Toshio YAMAMOTO, Hiroshi ŌTA and Kazutoyo KŌNO

Department of Mechanical Engineering

(Received April 14, 1972)

CONTENTS

General Introduction

It has become important in this age of high speed machinery to make clear the vibration of shaft having rotating inequality which rotates with a rotor or the vibration of a rotor with variable rotating speed.

Examples of rotating inequality, as seen in a two-pole generator or a two-bladed propeller, are an unsymmetrical rotor which has rectangular two different moments of inertia and a shaft having a key way or of rectangular section, which has two different spring constants in two directions perpendicular to each other.

In a rotating shaft system carring an unsymmetrical rotor, or in a rotating shaft system with inequality in stiffness, there are unstable regions in the neighborhood of both the major critical speed ω_c and the rotating speed ω_d at which the sum of two natural frequencies of the system (p_i+p_j) is equal to twice the rotating speed of the shaft $(2\,\omega_d)$. The unstable vibrations appearing in these unstable regions are treated for the system consisting of a rotor with unsymmetrical inertia and a shaft with unequal stiffness which rotates with the rotor.

Crandall and Brosens (1961) discussed a static unstable region of two degree-of-freedom system with regard to inclinational vibration of a rotating flat shaft with an unsymmetrical rotor. In Chapter 1, simultaneous effects of the unsymmetrical rotor and the unsymmetrical shaft in a vibratory system of four degree-

of-freedom system are appreciated and quantitative analytical results are obtained which relate the width of the unstable regions and the negative damping coefficients of the unstable vibrations to the asymmetry in inertia, the inequality in stiffness, and the relative orientation between the inequalities in inertia and stiffness. Furthermore, elimination of two kinds of unstable region is realized theoretically and experimentally.

In Chapter 2, it is described that a rotating shaft system carrying an unsymmetrical rotor and supported by rigid bearing pedestals at each end of the shaft is a four degree-of-freedom system, and so called "static unstable region" in the neighborhood of the major critical speed can be eliminated by the adoption of a flexible bearing pedestal at one end of the shaft, or by mounting an additional mass on the shaft. Additional inertia force appearing by an increase of two degree-of-freedom modifies the mode of vibration of the rotating shaft and the inclination angle θ of the rotor vanishes.

Chapter 3 deals with the physical meaning of occurrence of these unstable vibrations in the neighborhood of ω_c and ω_d by considering an input energy from shaft end into the system without solving a frequency equation numerically. The approximate results derived from taking energy into consideration coincide fairly well with the exact ones obtained by numerical calculation.

In Chapter 4, lateral forced vibrations of a rotating shaft system with a rotating anisotropy are discussed. Let the rotating speed of the shaft, the angular velocity of the anisotropy, the natural frequency of the system, and the frequency of an external periodic force exerted on the system be ω, $\lambda\omega$, p, and ω_0 respectively. Resonant phenomena can take place when $\omega_0 \fallingdotseq 2\lambda\omega - p$ as well as when $\omega_0 \fallingdotseq p$ in such a vibratory system. It can be concluded that a forced vibration with a frequency of ω_0 or $\omega_0' = 2\lambda\omega - \omega_0$ builds up remarkably according as $\omega_0 \fallingdotseq p$ or $\omega_0 = \overline{p} = 2\lambda\omega - p$. Furthermore, by using the above conclusion, elucidated physical meanings can be presented to some sorts of vibrations whose cause of occurrence is relatively difficult to understand.

In Chapter 5, when the rotating speed of a rotor varies periodically with a frequency of $\nu\omega$, the rotor is governed by differential equations having varying coefficients with time. In such a system, it is usually expected that unstable vibrations take place. It is found, however, that there occurs no unstable vibration in rotating shaft systems with a variable rotating speed. Variable inertia terms induced by the variable rotating speed result in forced vibrations with frequencies of $\omega_0 - \nu\omega$, $\omega_0 + \nu\omega$ as well as ω_0, where ω_0 is the frequency of an external force. It follows that at resonance $\omega_0 \fallingdotseq p + \nu\omega$ and $\omega_0 \fallingdotseq p - \nu\omega$, forced vibrations with frequencies of $\omega_0 - \nu\omega$ and $\omega_0 + \nu\omega$ occur respectively. Furthermore, the external force with a frequency of ω caused by unbalance of the rotor yields three forced vibrations with frequencies of ω, $(1-\nu)\omega$ and $(1+\nu)\omega$.

Chapter 1. On Vibrations of a Shaft with Unsymmetrical Stiffness Carrying an Unsymmetrical Rotor[18)~20)]

1.1. Introduction

When two principal moments of inertia I_1, I_2 about the axes perpendicular to the rotating axis of a rotor are unequal, *i.e.*, $I_1 \neq I_2$, the rotor is called an "unsymmetrical rotor". It has been reported by the authors that in a rotating

shaft system carrying an unsymmetrical rotor, there are two kinds of unstable region in the neighborhood of both the major critical speed ω_c[10)11)] and the rotating speed ω_d at which the sum of two natural frequencies p_1+p_2 is equal to twice rotating speed of the shaft $2\omega_d$[13)]. In 1961, S. H. Crandall and P. J. Brosens discussed the interaction through gyroscopic coupling between the inertia and stiffness inequalities for unstable vibrations referring to the inclination angles θ_x, θ_y of the rotor, which occur in the neighborhood of the major critical speed ω_c[8)9)].

In this chapter, a vibratory system of four-degree-of-freedom consisting of a rotating shaft with an unsymmetrical flexibility and an unsymmetrical rotor is treated, in which the deflections x, y and the inclination angles θ_x, θ_y of the rotor couple each other through gyroscopic terms; and a quantitative analysis for the unstable vibrations in the neighborhood of both ω_c and ω_d is derived, and the simultaneous effects of the diametral inertia inequality of the rotor and the unsymmetrical stiffness of the shaft on the unstable vibrations are explicitly appreciated and the relation between the relative orientation of the principal axes of moment of inertia to those of the stiffness of the shaft and the width of unstable regions is realized. The results of the analysis also show that removal of the unstable vibrations can be expected by adopting an appropriate combination of the inequalities in inertia and stiffness. The results of the analysis thus obtained were verified by experimental results through four kinds of the shaft system.

1.2. Equations of motion

In this paper a vibratory system consisting of a light elastic shaft with unequal stiffness and an unsymmetrical rigid rotor is treated, in which the deflections x and y and the inclination angles θ_x and θ_y of the rotor couple each other.

When it is assumed that there are no static and dynamic unbalance in the rotor, the center M of the rotor coincides with the center of gravity G.

Let the principal moments of inertia about the three orthogonal axes, GZ_1, GY_2, and GX_2 be I_p, I_1 and I_2 ($I_1>I_2$) respectively in Fig. 1.1 and put $I=(I_1+I_2)/2$, $\Delta I=(I_1-I_2)/2$. The orthogonal coordinate systems o-xyz, G-XYZ are parallel to each other, and those fixed on the rotor are G-$X_2Y_2Z_1$ and G-$X_3Y_3Z_1$. Eulerian angles θ, φ and ψ are used for expressing the angular position of rotor. The orthogonal coodinate system G-LKZ_1 is obtained by inclining the system G-NKZ about the axis GK by θ, which is obtainable by rotating G-XYZ about the vertical axis GZ by φ. And the orthogonal systems G-$X_2Y_2Z_1$ and G-$X_3Y_3Z_1$ are obtained by rotating the system G-LKZ_1 about the axis GZ_1 by ψ and $\psi+\zeta$. Let relative orientation $\angle X_2GX_3=\angle Y_2GY_3=\zeta$.

The angular velocities ω_{X2}, ω_{Y2}, and ω_{Z1} about the principal axes GX_2, GY_2, and GZ_1 are given as

$$\left.\begin{aligned}\omega_{X2}&=\dot{\theta}\sin\psi-\dot{\varphi}\sin\theta\cos\psi\\ \omega_{Y2}&=\dot{\theta}\cos\psi+\dot{\varphi}\sin\theta\sin\psi\\ \omega_{Z1}&=\dot{\varphi}\cos\theta+\dot{\psi}\end{aligned}\right\}\tag{1.1}$$

We may neglect the terms of powers higher than 3rd order of x, y and θ which

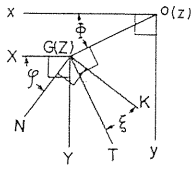

(a) Coordinates viewed from the direction *oz*.

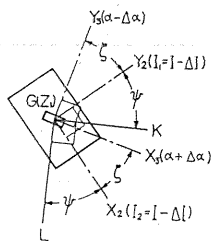

(b) Coordinates viewed from the direction GZ_1.

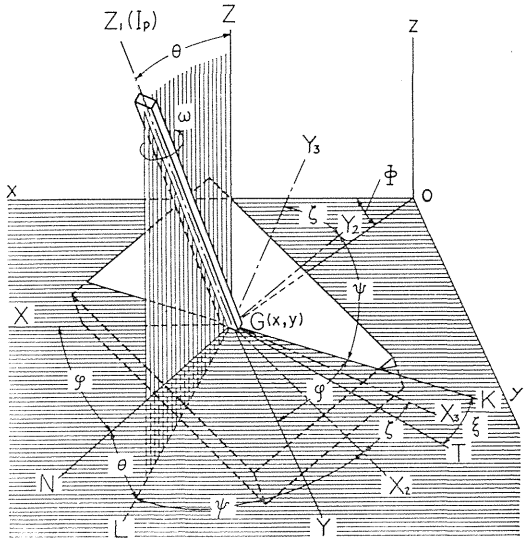

FIG. 1.1. Eulerian angles θ, φ, ψ and relative orientaion ζ.

are usually small compared with unity. We now introduce new variables as follows:

$$\Theta = \varphi + \psi, \quad \theta_x = \theta \cos \varphi, \quad \theta_y = \theta \sin \varphi \tag{1.2}$$

where θ_x, θ_y are the projectional angles of inclination θ to xz-, and yz-planes.

The total kinetic energy of the rotor is

$$T = T_1 + T_2 \tag{1.3}$$

where kinetic energy of translation T_1 is

$$T_1 = \frac{1}{2} M(\dot{x}^2 + \dot{y}^2 + \dot{z}^2) \tag{1.3.1}$$

and kinetic energy of rotation T_2 is

$$T_2 = \frac{1}{2}(I_p \omega_{Z1}^2 + I_1 \omega_{Y2}^2 + I_2 \omega_{X2}^2)$$

$$= \frac{1}{2}[I_p\{\dot{\Theta}^2 + \dot{\Theta}(\dot{\theta}_x\theta_y - \dot{\theta}_y\theta_x)\} + I(\dot{\theta}_x^2 + \dot{\theta}_y^2) + \Delta I\{(\dot{\theta}_x^2 - \dot{\theta}_y^2)\cos 2\Theta + 2\dot{\theta}_x\dot{\theta}_y \sin 2\Theta\}] \tag{1.3.2}$$

If a force P and a couple M_t are applied to the rotor which is mounted on a circular shaft with equal stiffness and they result in a deflection r and an inclination angle θ of the rotor, the following linear relationships exist:

$$P=\alpha r+\gamma\theta, \qquad M_t=\gamma r+\delta\theta \tag{1.4}$$

where α, γ, and δ are all spring constants of the shaft; α is the spring constant between the force and the deflection, γ is that between the force and the inclination or the couple and the deflection, δ between the couple and the inclination. We now denote the spring constants in GX_3-direction $\alpha+\Delta\alpha$, $\gamma+\Delta\gamma$, $\delta+\Delta\delta$, and in GY_3-direction $\alpha-\Delta\alpha$, $\gamma-\Delta\gamma$, $\delta-\Delta\delta$ in Fig. 1.1. Let the displacement of the center of gravity G be x', y', the inclination angle of GZ_1-axis be θ'_x, θ'_y in GX_3-, GY_3-directions respectively.

The potential energy of the shaft V should be represented by the following form,

$$\begin{aligned} V=&\frac{1}{2}\{(\alpha+\Delta\alpha)x'^2+2(\gamma+\Delta\gamma)x'\theta'_x+(\delta+\Delta\delta)\theta'^2_x\}\\ &+\frac{1}{2}\{(\alpha-\Delta\alpha)y'^2+2(\gamma-\Delta\gamma)y'\theta'_y+(\delta-\Delta\delta)\theta'^2_y\} \end{aligned} \tag{1.5}$$

There are the relationships (1.6) between stationary coordinates x, y, θ_x, θ_y and rotating coordinates x', y', θ'_x, θ'_y:

$$\left.\begin{aligned} \frac{x'}{\theta'_x}&=\frac{x}{\theta_x}\cos(\Theta+\zeta)+\frac{y}{\theta_y}\sin(\Theta+\zeta)\\ \frac{y'}{\theta'_y}&=-\frac{x}{\theta_x}\sin(\Theta+\zeta)+\frac{y}{\theta_y}\cos(\Theta+\zeta) \end{aligned}\right\} \tag{1.6}$$

Substituting Eq. (1.6) into Eq. (1.5) we have

$$\begin{aligned} V=&\frac{1}{2}\{\alpha(x^2+y^2)+2\gamma(x\theta_x+y\theta_y)+\delta(\theta_x^2+\theta_y^2)\}\\ &+\frac{1}{2}\{\Delta\alpha(x^2-y^2)+2\Delta\gamma(x\theta_x-y\theta_y)+\Delta\delta(\theta_x^2-\theta_y^2)\}\cos 2(\Theta+\zeta)\\ &+\{\Delta\alpha xy+\Delta\gamma(x\theta_y+y\theta_x)+\Delta\delta\theta_x\theta_y\}\sin 2(\Theta+\zeta) \end{aligned} \tag{1.7}$$

Now substituting Eqs. (1.3) and (1.7) into Lagrange's equation of motion (1.8) when the system consists of no damping and of an rotor without any static and dynamic unbalances

$$\frac{d}{dt}\left(\frac{\partial T}{\partial \dot{q}_s}\right)-\frac{\partial T}{\partial q_s}+\frac{\partial V}{\partial q_s}=0 \tag{1.8}$$

in which q_s is a generalized coordinate, we have the equations of motion. The equation of motion regarding Θ becomes

$$I_p\ddot{\Theta}=\frac{1}{2}I_p(\ddot{\theta}_y\theta_x-\ddot{\theta}_x\theta_y)+\Delta I[(\dot{\theta}_y^2-\dot{\theta}_x^2)\sin 2\Theta+2\dot{\theta}_x\dot{\theta}_y\cos 2\Theta]$$
$$+\{\Delta\alpha(x^2-y^2)+2\Delta\gamma(x\theta_x-y\theta_y)+\Delta\delta(\theta_x^2-\theta_y^2)\}\sin 2(\Theta+\zeta)$$
$$-2\{\Delta\alpha xy+\Delta\gamma(x\theta_y+y\theta_x)+\Delta\delta\theta_x\theta_y\}\cos 2(\Theta+\zeta) \tag{1.9}$$

Since all quantities of x, y, θ_x, and θ_y are enough small compared with unity, we may neglect the higher powers of them in Eq. (1.9), so Eq. (1.9) is approximately expressed as follows: $I_p\ddot{\Theta}=0$, and it leads to $\dot{\Theta}=\dot{\varphi}+\dot{\psi}=\omega$. Now putting $\Theta=\omega t-\pi/2$, we obtain the equations of motion regarding Θ, x, y, θ_x, and θ_y as follows:

$$\left.\begin{aligned}
&\dot{\Theta}=\omega=\text{constant}\\
&M\ddot{x}+\alpha x+\gamma\theta_x-\Delta\alpha\{x\cos 2(\omega t+\zeta)+y\sin 2(\omega t+\zeta)\}\\
&\quad-\Delta\gamma\{\theta_x\cos 2(\omega t+\zeta)+\theta_y\sin 2(\omega t+\zeta)\}=0\\
&M\ddot{y}+\alpha y+\gamma\theta_y-\Delta\alpha\{x\sin 2(\omega t+\zeta)-y\cos 2(\omega t+\zeta)\}\\
&\quad-\Delta\gamma\{\theta_x\sin 2(\omega t+\zeta)-\theta_y\cos 2(\omega t+\zeta)\}=0\\
&I\ddot{\theta}_x+I_p\omega\dot{\theta}_y+\gamma x+\delta\theta_x-\Delta I\cdot\frac{d}{dt}(\dot{\theta}_x\cos 2\omega t+\dot{\theta}_y\sin 2\omega t)\\
&\quad-\Delta\gamma\{x\cos 2(\omega t+\zeta)+y\sin 2(\omega t+\zeta)\}\\
&\quad-\Delta\delta\{\theta_x\cos 2(\omega t+\zeta)+\theta_y\sin 2(\omega t+\zeta)\}=0\\
&I\ddot{\theta}_y-I_p\omega\dot{\theta}_x+\gamma y+\delta\theta_y-\Delta I\cdot\frac{d}{dt}(\dot{\theta}_x\sin 2\omega t-\dot{\theta}_y\cos 2\omega t)\\
&\quad-\Delta\gamma\{x\sin 2(\omega t+\zeta)-y\cos 2(\omega t+\zeta)\}\\
&\quad-\Delta\delta\{\theta_x\sin 2(\omega t+\zeta)-\theta_y\cos 2(\omega t+\zeta)\}=0
\end{aligned}\right\} \tag{1.10}$$

Next when the advanced angles ξ and η from the axis MY_2 are the directions to which the eccentricity e and the small angle τ exist as shown in Fig. 1.2, we can express T as follows:

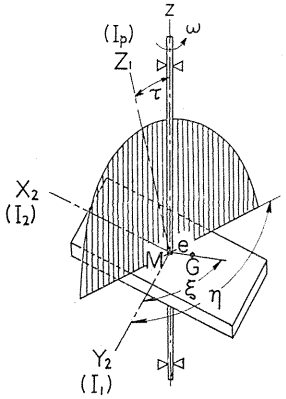

FIG. 1.2. Static unbalance e and dynamic unbalance τ.

$$T=\frac{1}{2}M[\dot{x}^2+\dot{y}^2-2e\dot{\Theta}\{\dot{x}\cos(\Theta+\xi)+\dot{y}\sin(\Theta+\xi)\}+e^2\dot{\Theta}^2]$$
$$+\frac{1}{2}I_p[(1-\tau^2)\dot{\Theta}^2-2\tau\dot{\Theta}\{\dot{\theta}_x\cos(\Theta+\eta)+\dot{\theta}_y\sin(\Theta+\eta)\}$$
$$+\dot{\Theta}(\dot{\theta}_x\theta_y-\dot{\theta}_y\theta_x)]+\frac{1}{2}I[\dot{\theta}_x^2+\dot{\theta}_y^2+\tau^2\dot{\Theta}^2+2\tau\dot{\Theta}\{\dot{\theta}_x\cos(\Theta+\eta)$$
$$+\dot{\theta}_y\sin(\Theta+\eta)\}]+\frac{1}{2}\Delta I[(\dot{\theta}_x^2-\dot{\theta}_y^2)\cos 2\Theta+2\dot{\theta}_x\dot{\theta}_y\sin 2\Theta$$
$$+\tau^2\dot{\Theta}^2\cos 2\eta+2\tau\dot{\Theta}\{\dot{\theta}_x\cos(\Theta-\eta)+\dot{\theta}_y\sin(\Theta-\eta)\}] \tag{1.3 a}$$

The potential energy V is the same as Eq. (1.7), and the dissipation function F is defined as $F=1/2\cdot c_1(\dot{x}^2+\dot{y}^2)+1/2\cdot c_2(\dot{\theta}_x^2+\dot{\theta}_y^2)$ in the system with viscous damping, where c_1 is viscous damping coefficient regarding x, y and c_2 is that regarding θ_x, θ_y.

Substituting Eqs. (1.3 a) and (1.7) and dissipation function F into Lagrange's equation of motion (1.8 a)

$$\frac{d}{dt}\left(\frac{\partial T}{\partial\dot{q}_s}\right)-\frac{\partial T}{\partial q_s}+\frac{\partial V}{\partial q_s}+\frac{\partial F}{\partial\dot{q}_s}=Q_s \tag{1.8 a}$$

in which Q_s is a generalized force besides restoring force, $I_p\ddot{\Theta}=0$, *i.e.*, $\dot{\Theta}=\omega$ is derived, and the following equations of motion are derived by putting $\Theta=\omega t-\pi/2$.

$$\left.\begin{aligned}
&M\ddot{x}+c_1\dot{x}+\alpha x+\gamma\theta_x-\Delta\alpha\{x\cos 2(\omega t+\zeta)+y\sin 2(\omega t+\zeta)\}\\
&\quad-\Delta\gamma\{\theta_x\cos 2(\omega t+\zeta)+\theta_y\sin 2(\omega t+\zeta)\}=Me\omega^2\cos(\omega t+\xi)\\
&M\ddot{y}+c_1\dot{y}+\alpha y+\gamma\theta_y-\Delta\alpha\{x\sin 2(\omega t+\zeta)-y\cos 2(\omega t+\zeta)\}\\
&\quad-\Delta\gamma\{\theta_x\sin 2(\omega t+\zeta)-\theta_y\cos 2(\omega t+\zeta)\}=Me\omega^2\sin(\omega t+\xi)\\
&I\ddot{\theta}_x+I_p\omega\dot{\theta}_y+c_2\dot{\theta}_x+\gamma x+\delta\theta_x-\Delta I\cdot\frac{d}{dt}(\dot{\theta}_x\cos 2\omega t+\dot{\theta}_y\sin 2\omega t)\\
&\quad-\Delta\gamma\{x\cos 2(\omega t+\zeta)+y\sin 2(\omega t+\zeta)\}-\Delta\delta\{\theta_x\cos 2(\omega t+\zeta)\\
&\quad+\theta_y\sin 2(\omega t+\zeta)\}=\tau\omega^2\{(I_p-I)\cos(\omega t+\eta)-\Delta I\cos(\omega t-\eta)\}\\
&I\ddot{\theta}_y-I_p\omega\dot{\theta}_x+c_2\dot{\theta}_y+\gamma y+\delta\theta_y-\Delta I\cdot\frac{d}{dt}(\dot{\theta}_x\sin 2\omega t-\dot{\theta}_y\cos 2\omega t)\\
&\quad-\Delta\gamma\{x\sin 2(\omega t+\zeta)-y\cos 2(\omega t+\zeta)\}-\Delta\delta\{\theta_x\sin 2(\omega t+\zeta)\\
&\quad-\theta_y\cos 2(\omega t+\zeta)\}=\tau\omega^2\{(I_p-I)\sin(\omega t+\eta)-\Delta I\sin(\omega t-\eta)\}
\end{aligned}\right\} \tag{1.11}$$

For convenience'sake, the following dimensionless quantities are introduced:

$$\left.\begin{aligned}
&i_p=I_p/I,\quad \Delta=\Delta I/I,\quad x'=x\sqrt{M/I},\quad y'=y\sqrt{M/I},\\
&e'=e\sqrt{M/I},\quad t'=t\sqrt{\alpha/M},\quad \omega'=\omega\sqrt{M/\alpha},\quad p'=p\sqrt{M/\alpha},\\
&\gamma'=\gamma\sqrt{M/I}/\alpha,\quad \delta'=M\delta/(\alpha I),\quad c_1'=c_1/\sqrt{M\alpha},\quad c_2'=c_2\sqrt{M/\alpha}/I,\\
&\Delta_{11}=\Delta\alpha/\alpha,\quad \Delta_{12}=\Delta\gamma/\gamma,\quad \Delta_{22}=\Delta\delta/\delta
\end{aligned}\right\} \tag{1.12}$$

Inserting Eq. (1.12) into Eq. (1.11) and omitting primes on the dimensionless

quantities, the equations of motion for the unsymmetrical rotor carried by the rotating shaft with unequal stiffness are rewritten in the form

$$\left.\begin{aligned}
&\ddot{x} + c_1\dot{x} + x + \gamma\theta_x - \Delta_{11}\{x\cos 2(\omega t+\zeta) + y\sin 2(\omega t+\zeta)\}\\
&\quad - \gamma\Delta_{12}\{\theta_x\cos 2(\omega t+\zeta) + \theta_y\sin 2(\omega t+\zeta)\} = e\omega^2\cos(\omega t+\xi)\\
&\ddot{y} + c_1\dot{y} + y + \gamma\theta_y - \Delta_{11}\{x\sin 2(\omega t+\zeta) - y\cos 2(\omega t+\zeta)\}\\
&\quad - \gamma\Delta_{12}\{\theta_x\sin 2(\omega t+\zeta) - \theta_y\cos 2(\omega t+\zeta)\} = e\omega^2\sin(\omega t+\xi)\\
&\ddot{\theta}_x + i_p\omega\dot{\theta}_y + c_2\dot{\theta}_x + \gamma x + \delta\theta_x - \Delta\cdot\frac{d}{dt}(\dot{\theta}_x\cos 2\omega t + \dot{\theta}_y\sin 2\omega t)\\
&\quad - \gamma\Delta_{12}\{x\cos 2(\omega t+\zeta) + y\sin 2(\omega t+\zeta)\}\\
&\quad - \delta\Delta_{22}\{\theta_x\cos 2(\omega t+\zeta) + \theta_y\sin 2(\omega t+\zeta)\}\\
&\quad = \tau\omega^2\{(i_p-1)\cos(\omega t+\eta) - \Delta\cos(\omega t-\eta)\}\\
&\ddot{\theta}_y - i_p\omega\dot{\theta}_x + c_2\dot{\theta}_y + \gamma y + \delta\theta_y - \Delta\cdot\frac{d}{dt}(\dot{\theta}_x\sin 2\omega t - \dot{\theta}_y\cos 2\omega t)\\
&\quad - \gamma\Delta_{12}\{x\sin 2(\omega t+\zeta) - y\cos 2(\omega t+\zeta)\}\\
&\quad - \delta\Delta_{22}\{\theta_x\sin 2(\omega t+\zeta) - \theta_y\cos 2(\omega t+\zeta)\}\\
&\quad = \tau\omega^2\{(i_p-1)\sin(\omega t+\eta) - \Delta\sin(\omega t-\eta)\}
\end{aligned}\right\} \qquad (1.13)$$

Equations of motion for a symmetrical rotor mounted on a shaft with unequal stiffness[10)11)] and an unsymmetrical rotor carried by a circular shaft[10)13)] are obtained by putting $\Delta=0$, $\zeta=0°$ and $\Delta_{ij}=0$ in Eq. (1.13) respectively.

1.3. Forced vibrations

1.3.1. Solutions of forced vibrations

Forced vibrations induced by e and τ are represented by

$$\left.\begin{aligned}
\begin{matrix}x\\y\end{matrix} &= E\begin{matrix}\cos\\\sin\end{matrix}(\omega t+\beta_1) = A\begin{matrix}\cos\\\sin\end{matrix}\omega t \mp B\begin{matrix}\sin\\\cos\end{matrix}\omega t,\\
\begin{matrix}\theta_x\\\theta_y\end{matrix} &= F\begin{matrix}\cos\\\sin\end{matrix}(\omega t+\beta_2) = C\begin{matrix}\cos\\\sin\end{matrix}\omega t \mp D\begin{matrix}\sin\\\cos\end{matrix}\omega t
\end{aligned}\right\} \qquad (1.14)$$

where β_1, β_2 are phase differences between vibrations and the axis MY_2. Inserting Eq. (1.14) into Eq. (1.13) we get the following determinant:

$$|a_{ij}| = \begin{vmatrix}
1-\Delta_{11}\cos 2\zeta-\omega^2 & -\Delta_{11}\sin 2\zeta - c_1\omega & \gamma(1-\Delta_{12}\cos 2\zeta) & -\gamma\Delta_{12}\sin 2\zeta\\
-\Delta_{11}\sin 2\zeta + c_1\omega & 1+\Delta_{11}\cos 2\zeta-\omega^2 & -\gamma\Delta_{12}\sin 2\zeta & \gamma(1+\Delta_{12}\cos 2\zeta)\\
\gamma(1-\Delta_{12}\cos 2\zeta) & -\gamma\Delta_{12}\sin 2\zeta & \delta(1-\Delta_{22}\cos 2\zeta)+(i_p-1-\Delta)\omega^2 & -\delta\Delta_{22}\sin 2\zeta - c_2\omega\\
-\gamma\Delta_{12}\sin 2\zeta & \gamma(1+\Delta_{12}\cos 2\zeta) & -\delta\Delta_{22}\sin 2\zeta + c_2\omega & \delta(1+\Delta_{22}\cos 2\zeta)+(i_p-1+\Delta)\omega^2
\end{vmatrix} \qquad (1.15)$$

It is readily seen from Eq. (1.14), (1.15) that if the cofactor of the determinant is denoted by A_{ij}, the amplitudes of forced vibrations A, B, C, D are given by the following equations:

$$\left.\begin{aligned}
A|a_{ij}| &= e\omega^2\cos\xi A_{11}+e\omega^2\sin\xi A_{21}+\tau\omega^2(i_p-1-\Delta)\cos\eta A_{31}+\tau\omega^2(i_p-1+\Delta)\sin\eta A_{41}\\
B|a_{ij}| &= e\omega^2\cos\xi A_{12}+e\omega^2\sin\xi A_{22}+\tau\omega^2(i_p-1-\Delta)\cos\eta A_{32}+\tau\omega^2(i_p-1+\Delta)\sin\eta A_{42}\\
C|a_{ij}| &= e\omega^2\cos\xi A_{13}+e\omega^2\sin\xi A_{23}+\tau\omega^2(i_p-1-\Delta)\cos\eta A_{33}+\tau\omega^2(i_p-1+\Delta)\sin\eta A_{43}\\
D|a_{ij}| &= e\omega^2\cos\xi A_{14}+e\omega^2\sin\xi A_{24}+\tau\omega^2(i_p-1-\Delta)\cos\eta A_{34}+\tau\omega^2(i_p-1+\Delta)\sin\eta A_{44}
\end{aligned}\right\} \quad (1.16)$$

1.3.2. Unstable regions of forced vibrations

When the relative orientation ζ is equal to 0° or 90° and $c_1=c_2=0$, the amplitudes A, B, C, D in Eq. (1.16) are given as follows: For the case of $\zeta=90°$

$$\left.\begin{aligned}
A &= \frac{\{\delta(1+\Delta_{22})+(i_p-1-\Delta)\omega^2\}e\omega^2\cos\xi-\gamma(1+\Delta_{12})\tau\omega^2(i_p-1-\Delta)\cos\eta}{(1+\Delta_{11}-\omega^2)\{\delta(1+\Delta_{22})+(i_p-1-\Delta)\omega^2\}-\gamma^2(1+\Delta_{12})^2}\\
B &= \frac{\{\delta(1-\Delta_{22})+(i_p-1+\Delta)\omega^2\}e\omega^2\sin\xi-\gamma(1-\Delta_{12})\tau\omega^2(i_p-1+\Delta)\sin\eta}{(1-\Delta_{11}-\omega^2)\{\delta(1-\Delta_{22})+(i_p-1+\Delta)\omega^2\}-\gamma^2(1-\Delta_{12})^2}\\
C &= \frac{(1+\Delta_{11}-\omega^2)\tau\omega^2(i_p-1-\Delta)\cos\eta-\gamma(1+\Delta_{12})e\omega^2\cos\xi}{(1+\Delta_{11}-\omega^2)\{\delta(1+\Delta_{22})+(i_p-1-\Delta)\omega^2\}-\gamma^2(1+\Delta_{12})^2}\\
D &= \frac{(1-\Delta_{11}-\omega^2)\tau\omega^2(i_p-1+\Delta)\sin\eta-\gamma(1-\Delta_{12})e\omega^2\sin\xi}{(1-\Delta_{11}-\omega^2)\{\delta(1-\Delta_{22})+(i_p-1+\Delta)\omega^2\}-\gamma^2(1-\Delta_{12})^2}
\end{aligned}\right\} \quad (1.16\,a)$$

For case of $\zeta=0°$, the sign of Δ in Eq. (1.16 a) must be changed.

And the vanishing denominators in the equations of the amplitudes A, C and B, D results in the following major critical speeds ω_{c21}, ω_{c11} and ω_{c22}, ω_{c12} separately: For the case of $\zeta=90°$

$$\left.\begin{aligned}
\frac{\omega_{c21}^2}{\omega_{c11}^2} &= \frac{\{(1+\Delta_{11})(i_p-1-\Delta)-\delta(1+\Delta_{22})\}\pm\sqrt{\{(1+\Delta_{11})(i_p-1-\Delta)+\delta(1+\Delta_{22})\}^2-4(1+\Delta_{12})^2(i_p-1-\Delta)\gamma^2}}{2(i_p-1-\Delta)}\\
\frac{\omega_{c22}^2}{\omega_{c12}^2} &= \frac{\{(1-\Delta_{11})(i_p-1+\Delta)-\delta(1-\Delta_{22})\}\pm\sqrt{\{(1-\Delta_{11})(i_p-1+\Delta)+\delta(1-\Delta_{22})\}^2-4(1-\Delta_{12})^2(i_p-1+\Delta)\gamma^2}}{2(i_p-1+\Delta)}
\end{aligned}\right\} \quad (1.17)$$

For case of $\zeta=0°$, the sign of Δ in Eq. (1.17) must be changed. It suggests that the magnitudes of the major critical speeds vary according to the value of the orientation ζ.

In the range of $|a_{ij}|<0$ the forced vibrations become statically unstable[10)11)], and the boundary rotating speeds furnished by $|a_{ij}|=0$ coincide with the major critical speeds of Eq. (1.17). Accordingly there are two static unstable regions[10)], *i.e.* the lower region $[\omega_{c21}, \omega_{c22}]$ and the higher region $[\omega_{c11}, \omega_{c12}]$.

Simultaneous effects of the asymmetry Δ of the rotor and the unsymmetrical shaft stiffness Δ_{ij} will be discussed. The unstable regions are changed with the value of Δ, ζ, c_1 and c_2 as shown in Figs. 1.3 (a), (b), (c) when $i_p=1.987$, $\delta=1.060$, $\gamma=-0.855$, $\Delta_s=\Delta_{11}=\Delta_{12}=\Delta_{22}=0.1$. Fig. 1.3 shows that elimination of the unstable region can be realized by means of an appropriate combination of Δ and Δ_s. The couple of curves when $\zeta=90°$ in Fig. 1.3 (a) cross each other in the neighborhood of $\Delta=0.25$. It shows that the unstable region vanishes even when $c_1=c_2=0$. The following condition for elimination of the unstable region is derived by putting $\omega_{c21}=\omega_{c22}$ or $\omega_{c11}=\omega_{c12}$ in Eq. (1.17).

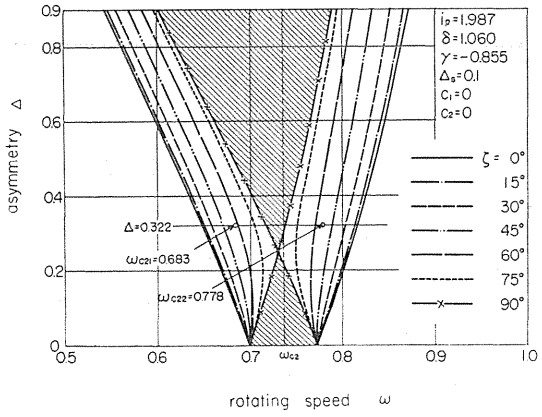

(a) $c_1=c_2=0$

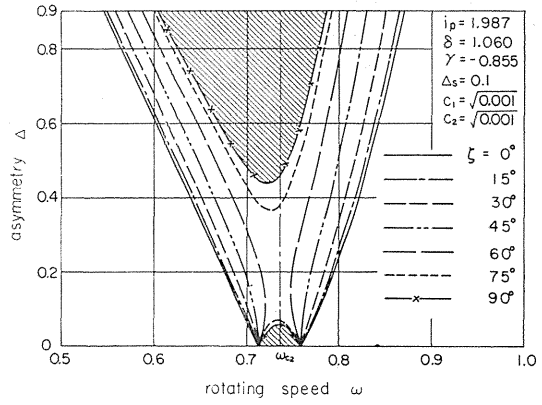

(b) $c_1=c_2=\sqrt{0.001}$

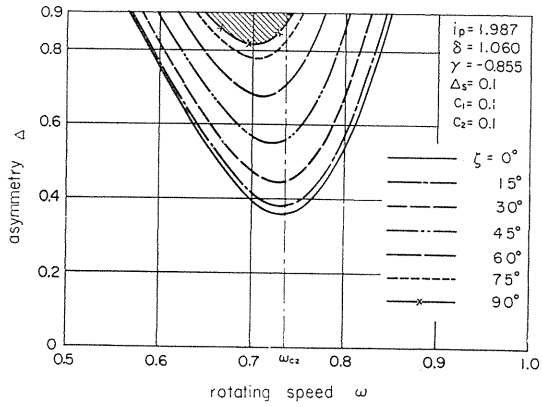

(c) $c_1=c_2=0.1$.

FIG. 1.3. Unstable region between ω_{c21} and ω_{c22} ($\omega_{c2}=0.736$).

$$\frac{1+\Delta_s}{1-\Delta_s}=g(\Delta)=\frac{(i_p-1-\Delta)\{(i_p-1+\Delta-\delta)\pm\sqrt{(i_p-1+\Delta+\delta)^2-4(i_p-1+\Delta)\gamma^2}\}}{(i_p-1+\Delta)\{(i_p-1-\Delta-\delta)\pm\sqrt{(i_p-1-\Delta+\delta)^2-4(i_p-1-\Delta)\gamma^2}\}}$$

$$\Delta_s=\frac{g(\Delta)-1}{g(\Delta)+1} \tag{1.18}$$

Eq. (1.18) for $\Delta_s=0.1$ and the upper sign results in $\Delta=0.2487$ which agrees with the results shown in Fig. 1.3 (a). For comparison the major critical speeds of the circular shaft system (*i.e.*, $\Delta_s=0$) with $\Delta=0.322$ are indicated by the symbol ○ in Fig. 1.3 (a)[10]. As is seen in Fig. 1.3, the unstable region become smaller with increasing of the damping, and finally they vanish for somewhat small asymmetry Δ as shown in Fig. 1.3 (c).

1.3.3. Response curves in the neighborhood of the major critical speed

Since there is no unstable region when $\Delta=0.322$, $\Delta_s=0.1$, $c_1=c_2=0.1$ as shown in Fig. 1.3 (c), the steady forced vibrations induced by e and τ occur in the neighborhood of the major critical speed ω_c. The amplitudes E of deflection induced by e and τ are shown by Figs. 1.4 (a) and (b) severally. Similar response curves are obtained for the amplitudes F of inclination. The maximum values of amplitude E are plotted against the orientation ζ for cases of $\xi, \eta=0°, 45°, 90°, -45°$ in Figs. 1.5 (a), (b). For comparison, the amplitudes for the system with $\Delta=0$ and $\Delta_s=0$ are indicated by the broken line curves in Figs. 1.4 and 1.5.

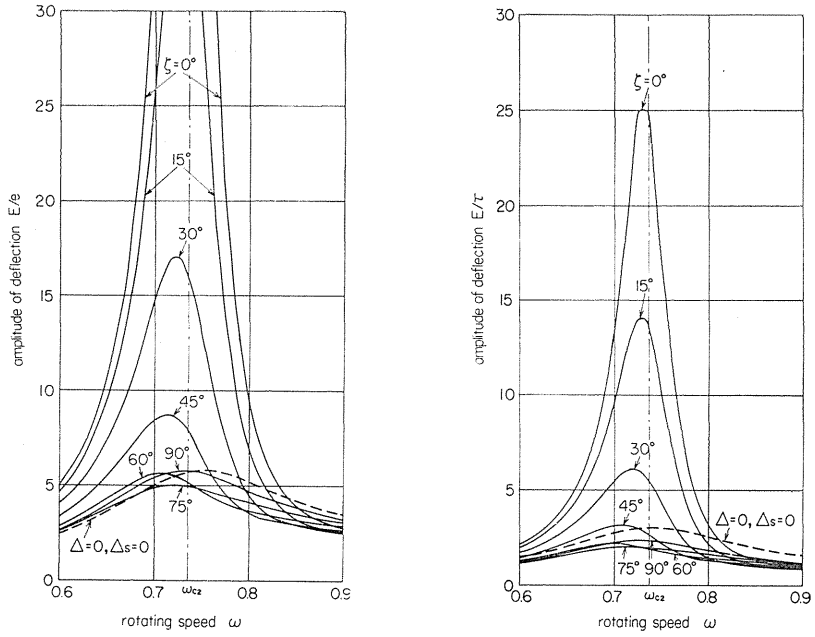

(a) $E/e-\omega$ ($\xi=0°$) (b) $E/\tau-\omega$ ($\eta=0°$)

($i_p=1.987$, $\delta=1.060$, $\gamma=-0.855$, $\Delta=0.322$, $\Delta_s=0.1$, $c_1=c_2=0.1$)

FIG. 1.4. Response curve at ω_{c2}.

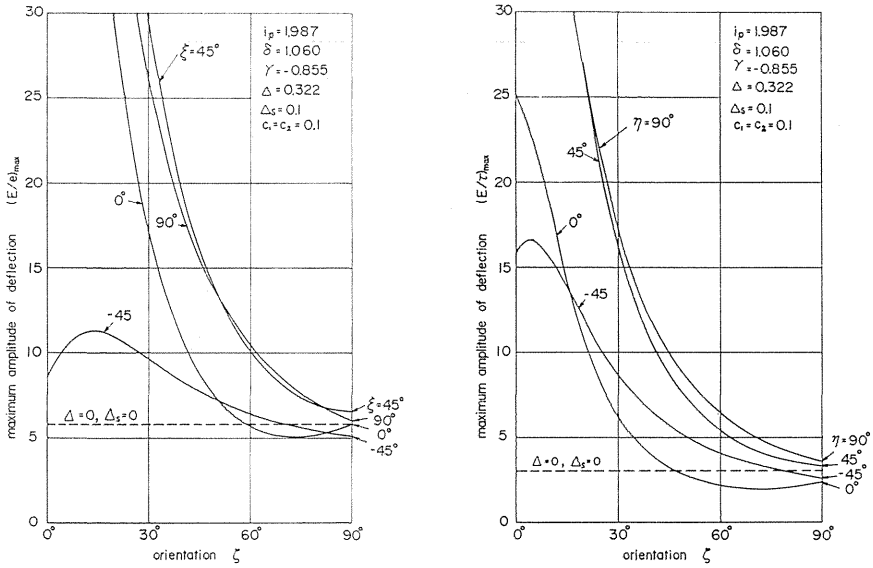

(a) $(E/e)_{max}-\zeta$ diagram (b) $(E/\tau)_{max}-\zeta$ diagram

FIG. 1.5. The relation between the maximum amplitude of deflection and the orientation ζ at ω_{c2}.

1.4. Free vibrations

1.4.1. Frequency equation and the unstable region

If $\Delta=\Delta_{11}=\Delta_{12}=\Delta_{22}=0$, $e=\tau=0$ and $c_1=c_2=0$ in Eq. (1.13), the frequency equation is

$$f=f(p)=(1-p^2)(\delta+i_p\omega p-p^2)-\gamma^2=(p-p_1)(p-p_2)(p-p_3)(p-p_4)=0 \quad (1.19)$$

where

$$p_1>1>p_2>0>p_3>-1>p_4 \quad (1.20)$$

and p_1, p_2, p_3, and p_4 are the natural frequencies of the system consisting of a symmetrical rotor and a shaft with equal stiffness α, γ, and δ.

The gyroscopic terms $i_p\omega\dot{\theta}_y$, $-i_p\omega\dot{\theta}_x$ in Eq. (1.13) result in lateral vibrations of whirling. The asymmetry in inertia Δ as well as the asymmetries in stiffness Δ_{11}, Δ_{12}, and Δ_{22} result in the coexistence of free vibrations with frequencies p and $\bar{p}=2\omega-p$[10]. Therefore, the free vibrations should be expressed in the form

$$\left.\begin{aligned} \begin{matrix} x \\ y \end{matrix} &= A \begin{matrix} \cos \\ \sin \end{matrix} pt \mp B \begin{matrix} \sin \\ \cos \end{matrix} pt + \bar{A} \begin{matrix} \cos \\ \sin \end{matrix} \bar{p}t \mp \bar{B} \begin{matrix} \sin \\ \cos \end{matrix} \bar{p}t \\ \begin{matrix} \theta_x \\ \theta_y \end{matrix} &= C \begin{matrix} \cos \\ \sin \end{matrix} pt \mp D \begin{matrix} \sin \\ \cos \end{matrix} pt + \bar{C} \begin{matrix} \cos \\ \sin \end{matrix} \bar{p}t \mp \bar{D} \begin{matrix} \sin \\ \cos \end{matrix} \bar{p}t \end{aligned}\right\} \quad (1.21)$$

Considering a rotating rectangular coordinate system o-$x'y'z$ which rotates about the z-axis with an angular velocity of ω and assuming that the x'-axis coincides with x-axis at $t=0$, we have the following relationships between coordinates x, y, θ_x, and θ_y, and coordinates x', y', θ'_x, and θ'_y with reference to this rotating coordinate axis:

$$\begin{matrix} x \\ y \end{matrix} = x' \begin{matrix} \cos \\ \sin \end{matrix} \omega t \mp y' \begin{matrix} \sin \\ \cos \end{matrix} \omega t, \quad \begin{matrix} \theta_x \\ \theta_y \end{matrix} = \theta_x' \begin{matrix} \cos \\ \sin \end{matrix} \omega t \mp \theta_y' \begin{matrix} \sin \\ \cos \end{matrix} \omega t \tag{1.22}$$

Substituting Eq. (1.22) into Eq. (1.13) and putting $e=\tau=0$, the following equations of motion are obtained with respect to x', y', θ_x', and θ_y':

$$\left.\begin{aligned}
&\ddot{x}' + c_1\dot{x}' + (1 - \Delta_{11}\cos 2\zeta - \omega^2)x' - 2\omega\dot{y}' - (c_1\omega + \Delta_{11}\sin 2\zeta)y' \\
&\quad + \gamma(1 - \Delta_{12}\cos 2\zeta)\theta_x' - \gamma\Delta_{12}\sin 2\zeta \cdot \theta_y' = 0 \\
&\ddot{y}' + c_1\dot{y}' + (1 + \Delta_{11}\cos 2\zeta - \omega^2)y' + 2\omega\dot{x}' + (c_1\omega - \Delta_{11}\sin 2\zeta)x' \\
&\quad + \gamma(1 + \Delta_{12}\cos 2\zeta)\theta_y' - \gamma\Delta_{12}\sin 2\zeta \cdot \theta_x' = 0 \\
&(1 - \Delta)\ddot{\theta}_x' + c_2\dot{\theta}_x' + \{\delta(1 - \Delta_{22}\cos 2\zeta) + (i_p - 1 - \Delta)\omega^2\}\theta_x' - (2 - i_p)\omega\dot{\theta}_y' \\
&\quad - (c_2\omega + \delta\Delta_{22}\sin 2\zeta)\theta_y' + \gamma(1 - \Delta_{12}\cos 2\zeta)x' - \gamma\Delta_{12}\sin 2\zeta \cdot y' = 0 \\
&(1 + \Delta)\ddot{\theta}_y' + c_2\dot{\theta}_y' + \{\delta(1 + \Delta_{22}\cos 2\zeta) + (i_p - 1 + \Delta)\omega^2\}\theta_y' + (2 - i_p)\omega\dot{\theta}_x' \\
&\quad + (c_2\omega - \delta\Delta_{22}\sin 2\zeta)\theta_x' + \gamma(1 + \Delta_{12}\cos 2\zeta)y' - \gamma\Delta_{12}\sin 2\zeta \cdot x' = 0
\end{aligned}\right\} \tag{1.23}$$

Assuming solutions of Eq. (1.23) to be written in the form

$$\begin{matrix} x' \\ y' \end{matrix} = \begin{matrix} A \\ B \end{matrix} e^{st}, \quad \begin{matrix} \theta_x' \\ \theta_y' \end{matrix} = \begin{matrix} C \\ D \end{matrix} e^{st} \tag{1.24}$$

and substituting Eq. (1.24) into Eq. (1.23), we have the following characteristic equation:

$$\Phi(s) = \begin{vmatrix}
s^2 + 1 - \Delta_{11}\cos 2\zeta - \omega^2 + c_1 s & -2\omega s - \Delta_{11}\sin 2\zeta - c_1\omega & \gamma(1 - \Delta_{12}\cos 2\zeta) & -\gamma\Delta_{12}\sin 2\zeta \\
2\omega s - \Delta_{11}\sin 2\zeta + c_1\omega & s^2 + 1 + \Delta_{11}\cos 2\zeta - \omega^2 + c_1 s & -\gamma\Delta_{12}\sin 2\zeta & \gamma(1 + \Delta_{12}\cos 2\zeta) \\
\gamma(1 - \Delta_{12}\cos 2\zeta) & -\gamma\Delta_{12}\sin 2\zeta & (1 - \Delta)s^2 + c_2 s + \delta(1 - \Delta_{22}\cos 2\zeta) + (i_p - 1 - \Delta)\omega^2 & -(2 - i_p)\omega s - c_2\omega - \delta\Delta_{22}\sin 2\zeta \\
-\gamma\Delta_{12}\sin 2\zeta & \gamma(1 + \Delta_{12}\cos 2\zeta) & (2 - i_p)\omega s + c_2\omega - \delta\Delta_{22}\sin 2\zeta & (1 + \Delta)s^2 + c_2 s + \delta(1 + \Delta_{22}\cos 2\zeta) + (i_p - 1 + \Delta)\omega^2
\end{vmatrix}$$

$$= K_8 s^8 + K_7 s^7 + K_6 s^6 + K_5 s^5 + K_4 s^4 + K_3 s^3 + K_2 s^2 + K_1 s + K_0 = 0 \tag{1.25}$$

where

$$\left.\begin{aligned}
&K_8 = 1 - \Delta^2 > 0 \quad (\because \quad 2 > i_p > 2\Delta > 0) \\
&K_7 = 2c_1(1 - \Delta^2) + 2c_2 \\
&K_6 = \eta_1 + (1 - \Delta^2)\nu_1 + 4c_1c_2 \\
&K_5 = 2c_1\{\eta_1 + (1 - \Delta^2)(1 + \omega^2)\} + 2c_2\{\nu_1 + (\delta + \omega^2)\} \\
&K_4 = (\omega^2 + \nu_1)\eta_1 + \eta_2 + (1 - \Delta^2)\nu_2 - \omega^2\nu_3 - 2\gamma^2(1 + \Delta_{12}^2) - c_2^2\omega^2 \\
&\quad + 4c_1c_2(1 + \delta + 2\omega^2) + 2(2\gamma^2\Delta_{12} + \delta\Delta_{22}\omega^2)\Delta\cos 2\zeta \\
&K_3 = 2c_1\{(1 + \omega^2)\eta_1 + \eta_2 + 2\gamma^2\Delta\Delta_{12}\cos 2\zeta\} + 2c_2\{(\delta + \omega^2)\nu_1 + \nu_2\} \\
&\quad - 2(c_1 + c_2)\gamma^2(1 + \Delta_{12}^2)
\end{aligned}\right\}$$

$$
\left.\begin{aligned}
K_2 &= \nu_1\eta_2+\nu_2\eta_1+2\gamma^2\{(3-\Delta_{12}^2)(2-i_p)\omega^2-(1+\delta+c_1c_2)(1+\Delta_{12}^2)\\
&\quad+2\Delta_{12}(\Delta_{11}+\delta\Delta_{22})-(\Delta_{11}-2\Delta_{12}+\Delta_{11}\Delta_{12}^2)\Delta\cos 2\zeta\}+4c_1c_2(1+\omega^2)(\delta+\omega^2)\\
K_1 &= 2c_1[(1+\omega^2)\eta_2+\gamma^2\{2(2-i_p)\omega^2-(\delta+\omega^2)(1+\Delta_{12}^2)+2\delta\Delta_{12}\Delta_{22}\\
&\quad+2\Delta\Delta_{12}\omega^2\cos 2\zeta\}]+2c_2[(\delta+\omega^2)\nu_2+\gamma^2\{4\omega^2-(1+\omega^2)(1+\Delta_{12}^2)+2\Delta_{11}\Delta_{12}\}]\\
K_0 &= \{\eta_3^2+2\eta_3\Delta\Delta_{11}\omega^2\cos 2\zeta+(\Delta\Delta_{11}\omega^2)^2\}-[\eta_4^2+2\eta_4\Delta\omega^2(1-\omega^2)\cos 2\zeta\\
&\quad+\{\Delta\omega^2(1-\omega^2)\}^2]+\omega^2\{c_1^2\eta_2+c_2^2\nu_2+2c_1c_2\gamma^2(1-\Delta_{12}^2)-c_1^2c_2^2\omega^2\}
\end{aligned}\right\} \tag{1.26}
$$

in which

$$
\left.\begin{aligned}
\nu_1 &= 2(1+\omega^2)+c_1^2\\
\nu_2 &= (1-\omega^2)^2-\Delta_{11}^2+c_1^2\omega^2\\
\nu_3 &= \{i_p(i_p-2)+2(1-\Delta^2)\}\omega^2+2\delta\\
\eta_1 &= \nu_3+c_2^2-2\delta\Delta\Delta_{22}\cos 2\zeta\\
\eta_2 &= \{(i_p-1)\omega^2+\delta\}^2-\Delta^2\omega^4-\delta^2\Delta_{22}^2+c_2^2\omega^2-2\delta\Delta\Delta_{22}\omega^2\cos 2\zeta\\
\eta_3 &= (1-\omega^2)\{(i_p-1)\omega^2+\delta\}-\gamma^2+(\delta\Delta_{11}\Delta_{22}-\gamma^2\Delta_{12}^2)\\
\eta_4 &= \{(i_p-1)\omega^2+\delta\}\Delta_{11}+\delta(1-\omega^2)\Delta_{22}-2\gamma^2\Delta_{12}
\end{aligned}\right\} \tag{1.27}
$$

The unstable regions in which vibrations mount up exponentially exist in the neighborhood of the rotating speed at which both $f(p)=0$ and $f(\bar{p})=\bar{f}(p)=0$ are satisfied, simultaneously.

If K_0 in Eq. (1.26) becomes negative, and hence the precondition for stability that all K_j ($j=0, 1, 2, \ldots, 8$) should be positive is not satisfied, Eq. (1.25) has a positive real root $s=m$ ($m>0$). Accordingly, Eq. (1.23) has solutions of $x'=Ae^{mt}$, $y'=Be^{mt}$, $\theta_x'=Ce^{mt}$, and $\theta_y'=De^{mt}$ and by substituting these solutions into Eq. (1.22) we have unstable vibrations $x=ae^{mt}\cos(\omega t+\beta)$, $y=ae^{mt}\sin(\omega t+\beta)$, $\theta_x=be^{mt}\cos(\omega t+\beta')$ and $\theta_y=be^{mt}\sin(\omega t+\beta')$ with a frequency of ω, in which m is called a negative damping coefficient. This is why the unstable region appears in the neighborhood of the major critical speed ω_c.

For stability, there is another condition that all Hurwitz's determinants H_j ($j=2, 3, \ldots, 7$) of Eq. (1.25) are positive. In the neighborhood of $\omega_d=(p_1+p_2)/2$, the Hurwitz's determinant of the highest order or that of the 7th order H_7 takes a negative value. Consequently, Eq. (1.25) has roots of conjugate complex with a positive real part, *i.e.*, $s=m\pm ip'$ ($m>0$) which leads to $x'=Ae^{mt}\cos(p't+\beta_1')$, $y'=Be^{mt}\cos(p't+\beta_2')$, $\theta_x'=Ce^{mt}\cos(p't+\beta_1'')$ and $\theta_y'=De^{mt}\cos(p't+\beta_2'')$; referring to Eq. (1.22) they can be written in the form

$$
\left.\begin{aligned}
x &= e^{mt}[a\cos\{(\omega+p')t+\beta_1\}+b\cos\{(\omega-p')t+\beta_2\}]\\
&= e^{mt}\{a\cos(P_1t+\beta_1)+b\cos(P_2t+\beta_2)\}\\
y &= e^{mt}\{a\sin(P_1t+\beta_1)+b\sin(P_2t+\beta_2)\}
\end{aligned}\right\} \tag{1.28}
$$

θ_x and θ_y are written in a similar form. In Eq. (1.28)

$$
P_1=\omega+p',\quad P_2=\omega-p'\quad\therefore\ P_1+P_2=2\omega \tag{1.29}
$$

Thus two unstable vibrations with frequencies P_1 and $P_2=2\omega-P_1$ appear simul-

taneously in the unstable region near the rotating speed $\omega_d=(p_1+p_2)/2$ ($\because$ $P_1\fallingdotseq p_1$, $P_2\fallingdotseq p_2$). On the boundary of stable and unstable region the relation $m=0$ holds.

Now we treat about the free vibration with no damping. Substituting Eq. (1.21) into Eq. (1.13) and putting $e=\tau=0$, $c_1=c_2=0$, the following equation $\Phi=0$ is obtained.

$$\Phi(p)=\begin{vmatrix}
H & \gamma & \Delta_{11}\cos 2\zeta & \gamma\Delta_{12}\cos 2\zeta & \Delta_{11}\sin 2\zeta & \gamma\Delta_{12}\sin 2\zeta & 0 & 0\\
\gamma & G & \gamma\Delta_{12}\cos 2\zeta & \Delta p\bar{p}+\delta\Delta_{22}\cos 2\zeta & \gamma\Delta_{12}\sin 2\zeta & \delta\Delta_{22}\sin 2\zeta & 0 & 0\\
\Delta_{11}\cos 2\zeta & \gamma\Delta_{12}\cos 2\zeta & \bar{H} & \gamma & 0 & 0 & -\Delta_{11}\sin 2\zeta & -\gamma\Delta_{12}\sin 2\zeta\\
\gamma\Delta_{12}\cos 2\zeta & \Delta p\bar{p}+\delta\Delta_{22}\cos 2\zeta & \gamma & \bar{G} & 0 & 0 & -\gamma\Delta_{12}\sin 2\zeta & -\delta\Delta_{22}\sin 2\zeta\\
\Delta_{11}\sin 2\zeta & \gamma\Delta_{12}\sin 2\zeta & 0 & 0 & \bar{H} & \gamma & \Delta_{11}\cos 2\zeta & \gamma\Delta_{12}\cos 2\zeta\\
\gamma\Delta_{12}\sin 2\zeta & \delta\Delta_{22}\sin 2\zeta & 0 & 0 & \gamma & \bar{G} & \gamma\Delta_{12}\cos 2\zeta & \Delta p\bar{p}+\delta\Delta_{22}\cos 2\zeta\\
0 & 0 & -\Delta_{11}\sin 2\zeta & -\gamma\Delta_{12}\sin 2\zeta & \Delta_{11}\cos 2\zeta & \gamma\Delta_{12}\cos 2\zeta & H & \gamma\\
0 & 0 & -\gamma\Delta_{12}\sin 2\zeta & -\delta\Delta_{22}\sin 2\zeta & \gamma\Delta_{12}\cos 2\zeta & \Delta p\bar{p}+\delta\Delta_{22}\cos 2\zeta & \gamma & G
\end{vmatrix}=0 \tag{1.30}$$

Some calculation shows that Eq. (1.30) can be represented by the form $\Phi=\Phi'=0$ with

$$\begin{aligned}\Phi'=&f\bar{f}+[-\Delta_{11}^2G\bar{G}-\gamma^2\Delta_{12}^2(H\bar{G}+\bar{H}G)-\delta^2\Delta_{22}^2H\bar{H}+2\gamma^2\Delta_{11}\Delta_{12}(G+\bar{G})\\&+2\delta\gamma^2\Delta_{12}\Delta_{22}(H+\bar{H})-2(\delta\Delta_{11}\Delta_{22}+\gamma^2\Delta_{12}^2)\gamma^2-\Delta^2p^2\bar{p}^2H\bar{H}\\&+2\Delta p\bar{p}\{-\gamma^2\Delta_{11}+\gamma^2\Delta_{12}(H+\bar{H})-\delta\Delta_{22}H\bar{H}\}\cos 2\zeta]+\{(\delta\Delta_{11}\Delta_{22}-\gamma^2\Delta_{12}^2)^2\\&+\Delta^2\Delta_{11}^2p^2\bar{p}^2+2\Delta\Delta_{11}p\bar{p}(\delta\Delta_{11}\Delta_{22}-\gamma^2\Delta_{12}^2)\cos 2\zeta\}=0\end{aligned} \tag{1.31}$$

in which $H=1-p^2$, $\bar{H}=1-\bar{p}^2$, $G=\delta+i_p\omega p-p^2$, $\bar{G}=\delta+i_p\omega\bar{p}-\bar{p}^2$, $f=HG-\gamma^2$ and $\bar{f}=\bar{H}\bar{G}-\gamma^2$. When $\Delta=0$ and $\Delta_{ij}=0$, Eq. (1.31) reduces to $\Phi'=f\bar{f}=0$. The unstable vibrations take place in the neighborhood of the intersecting points of the curves $f=0$ and $\bar{f}=0$ provided that Δ and Δ_{ij} are somewhat small[10)11)13)]. Accordingly the nature of Eq. (1.31) in the neighborhood of these intersecting points will be discussed. Since $f=0$ and $\bar{f}=0$ are simultaneously held in this intersecting point, *i.e.*, $HG=\bar{H}\bar{G}=\gamma^2$, Φ' in Eq. (1.31) reduces to

$$\Phi'=f\bar{f}-\varphi_2/(H\bar{H})+\varphi_4=0 \tag{1.32}$$

where

$$\left.\begin{aligned}\varphi_2&=Q^2+R^2+2QR\cos 2\zeta\geqq(|Q|-|R|)^2\geqq 0\\\varphi_4&=S^2+T^2+2ST\cos 2\zeta\geqq(|S|-|T|)^2\geqq 0\end{aligned}\right\} \tag{1.33 a}$$

$$\left.\begin{aligned}Q&=\gamma^2\Delta_{11}-\gamma^2\Delta_{12}(H+\bar{H})+\delta\Delta_{22}H\bar{H}\\R&=\Delta p\bar{p}H\bar{H},\quad S=\delta\Delta_{11}\Delta_{22}-\gamma^2\Delta_{12}^2,\quad T=\Delta\Delta_{11}p\bar{p}\end{aligned}\right\} \tag{1.33 b}$$

It should be noted from Eq. (1.33 a) that φ_2 and φ_4 take always the positive values or zero. Under the assumption that the fourth power term of Δ, Δ_{ij} in Eq. (1.32), *i.e.*, φ_4 can be neglected, it is concluded that the real roots of Eq. (1.32) exist only in the ranges where the sign of $f\bar{f}$ is the same as that of $H\bar{H}$ because of $\varphi_2\geqq 0$.

The natural frequency-the rotating speed diagram of the apparatus of the experiment IV for $\Delta=\Delta_{ij}=0$ is illustrated in Fig. 1.6 where the curves $f=0$ and $\bar{f}=0$ are shown by full and broken line curves respectively. Further the lines

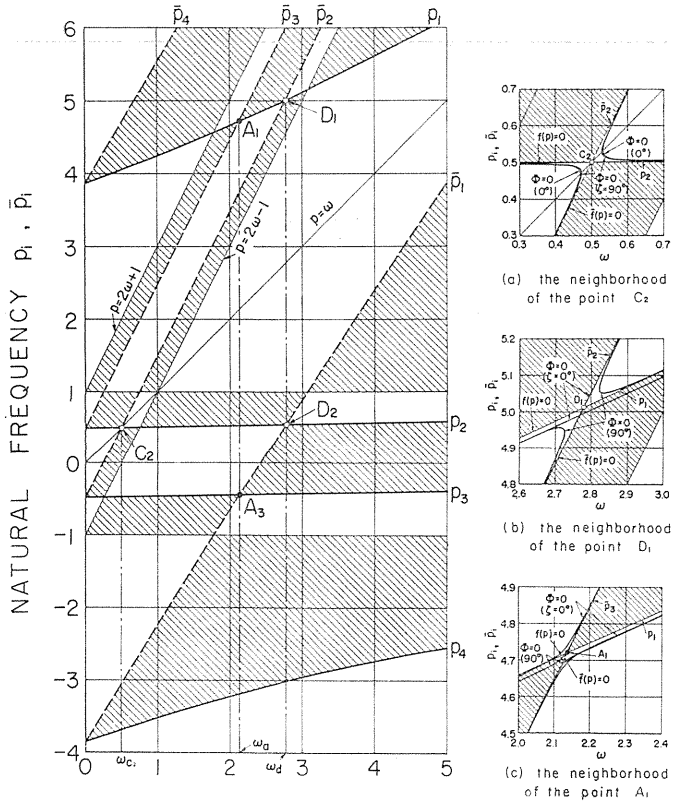

(Experiment IV, $i_p=0.7536$, $\delta=14.1786$, $\gamma=-3.2525$, $\sqrt{\alpha/M}=$ 441.9 rpm).

FIG. 1.6. The relation between the roots of $f=0$, $\bar{f}=0$ and the rotating speed ω.

$H=0$ ($p=\pm1$) and $\bar{H}=0$ ($\bar{p}=2\omega\pm1$) are added by thin lines in Fig. 1.6. In Fig. 1.6 the real roots of Eq. (1.32) can exist only in blank regions and not in hatched regions where the signs of $f\bar{f}$ and $H\bar{H}$ are different each other. In the neighborhood of the cross point of $f=0$ and $\bar{f}=0$ shown by the symbol ○, there is an unstable region because the curves $\Phi'=0$ becomes as shown in Fig. 1.6 (a), (b), and near the intersecting points shown by the symbol ● in Fig. 1.6 (c) there is no unstable region[13]. The rotating speeds of ω of the intersecting points $C_1(\omega_{c1})$, $C_2(\omega_{c2})$, $D_{1,2}(\omega_d)$, and $A_{1,3}(\omega_a)$ are as follows[11)13)24)]:

$$\frac{\omega_{c2}^2}{\omega_{c1}^2}=\{(i_p-1-\delta)\pm\sqrt{(i_p-1+\delta)^2-4(i_p-1)\gamma^2}\}/\{2(i_p-1)\} \tag{1.34}$$

$$\frac{\omega_d^2}{\omega_a^2}=\{i_p^2+4(2-i_p)(1+\delta)\pm(4-i_p)\sqrt{i_p^2+8(2-i_p)(\delta-\gamma^2)}\}/\{8(2-i_p)^2\} \tag{1.35}$$

The negative damping coefficient m takes its maximum value $m_{\max}$ at the center of unstable region $\omega=\omega_c$, and $\omega=\omega_d$. The value of m, $m_{\max}$ and the width of unstable region $2|\xi_0|$ are approximately given by means of Taylor expansion in the form (1.36)~(1 38).

When there is no daming[13],

$$m_{\max}=\sqrt{-\varphi_2\Big/\Big(\frac{\partial f}{\partial p}\frac{\partial \bar{f}}{\partial p}H\bar{H}\Big)}=\nabla \tag{1.36 a}$$

$$m=\sqrt{\nabla^2-\frac{1}{4}\Big(\frac{\partial f/\partial\omega}{\partial f/\partial p}-\frac{\partial \bar{f}/\partial\omega}{\partial \bar{f}/\partial p}\Big)^2(\omega-\omega_{c,d})^2} \tag{1.37}$$

$$2|\xi_0|=4\nabla\Big/\Big|\frac{\partial f/\partial\omega}{\partial f/\partial p}-\frac{\partial \bar{f}/\partial\omega}{\partial \bar{f}/\partial p}\Big| \tag{1.38 a}$$

When there is damping[15],

$$m_{\max}=\sqrt{\nabla^2+\Big(\frac{n_1-n_2}{2}\Big)^2}-\Big(\frac{n_1+n_2}{2}\Big) \tag{1.36 b}$$

$$2|\xi_0|=\frac{2(n_1+n_2)\sqrt{(\nabla^2-n_1n_2)/(n_1n_2)}}{\Big|\dfrac{\partial f/\partial\omega}{\partial f/\partial p}-\dfrac{\partial \bar{f}/\partial\omega}{\partial \bar{f}/\partial p}\Big|} \tag{1.38 b}$$

where for unstable vibration in the neighborhood of ω_c,

$$n_1=n_2=\frac{\gamma^2c_1+(1-\omega_c^2)^2c_2}{2\gamma^2+(2-i_p)(1-\omega_c^2)^2} \tag{1.39 a}$$

and for the unstable vibrations in the neighborhood of ω_d,

$$n_{1,2}=\frac{\gamma^2c_1+(1-p_{1,2}^2)^2c_2}{2\gamma^2+(1-p_{1,2}^2)^2\Big(2-\dfrac{i_p\omega_d}{p_{1,2}}\Big)} \tag{1.39 b}$$

1.4.2. Static unstable vibrations

The static unstable vibrations take place in the neighborhood of the intersecting points $C_1(p_1=\bar{p}_1)$ and $C_2(p_2=\bar{p}_2)$, because $R=\Delta\omega_c^2(1-\omega_c^2)^2>0$ and hence the curves $\Phi'=0$ take the form of Fig. 1.6 (a).

If the lower and upper boundaries ω_{ci1} and ω_{ci2} coincide with each other, the unstable region obviously vanishes. Thus the relation $\omega_{c21}=\omega_{c22}$ or $\omega_{c11}=\omega_{c12}$ results in the following condition for removal of the unstable region near the major critical speed ω_c:

$$\Delta=\pm\{\gamma^2\Delta_{11}-2\gamma^2\Delta_{12}(1-\omega_c^2)+\delta\Delta_{22}(1-\omega_c^2)^2\}/\{\omega_c(1-\omega_c^2)\}^2 \tag{1.40 a}$$

provided that the higher-order terms consisting of Δ, Δ_{11}, Δ_{12}, and Δ_{22} are neglected. In Eq. (1.40 a) the upper and lower signs correspond to $\zeta=90°$ and $\zeta=0°$, respectively. Eqs. (1.33), (1.36) and (1.37) show that $m_{\max}$ and $2|\xi_0|$ are functions of the orientation ζ, and $\zeta=90°$ and $\zeta=0°$ furnish their minimum and maximum values when $Q=\{\gamma^2\Delta_{11}-2\gamma^2\Delta_{12}(1-\omega_c^2)+\delta\Delta_{22}(1-\omega_c^2)^2\}>0$; vice versa when $Q<0$, because $R>0$ near ω_c.

Since $QR=\Delta\Delta_s\omega_c^2(1-\omega_c^2)^2\{\gamma^2\omega_c^4+(\delta-\gamma^2)(1-\omega_c^2)^2\}$ is always positive for the flat shaft with uniform cross section ($\Delta_{ij}\equiv\Delta_s$), the following condition of removement of unstable region can be derived from $\varphi_2=0$, *i.e.*, $Q=R(\zeta=90°)$:

$$\Delta=\Delta_s\{\gamma^2\omega_c^4+(\delta-\gamma^2)(1-\omega_c^2)^2\}/\{\omega_c(1-\omega_c^2)\}^2 \qquad (1.40\text{ b})$$

For the apparatus of Fig. 1.3 (a), Eq. (1.40 b) furnishes $\Delta_s=0.1$, $\Delta=0.2493$ which agree with the result $\Delta_s=0.1$, $\Delta=0.2487$ given by Eq. (1.18). In order to obtain condition for removal of unstable region, Eq. (1.40 b) may be more convenient than Eq. (1.18). Incidentally, if the spring constant γ vanishes, *i.e.*, $\gamma=0$, the motions of x, y and θ_x, θ_y do not couple each other, for such a system QR is always positive in the neighborhood of the higher major critical speed, *i.e.*, the point C_1 because $QR=\delta\Delta\Delta_{22}\omega_c^2(1-\omega_c^2)^4>0$[9]. For the apparatus of Fig. 1.3 with $QR>0$ the width of the unstable region $2|\xi_0|=\omega_{c22}-\omega_{c21}$ are plotted against the orientation ζ in Fig. 1.7 where the damping coefficient $c_1=c_2$ is adopted as a parameter. In Fig. 1.7, the results of approximate calculation through Eq. (1.38 a, b) are shown by full line curves and the exact values obtained from $K_0=|a_{ij}|=0$ of Eq. (1.15) are illustrated by the symbol ○; both results agree each other as is seen in Fig. 1.7. The existence of the fourth power term φ_4 in Eq. (1.32) which is assumed to be negligible gives plus effect on removal of the unstable region because $\varphi_4\geqq 0$ and $-\varphi_2/(H\bar{H})\leqq 0$ near the major critical speed.

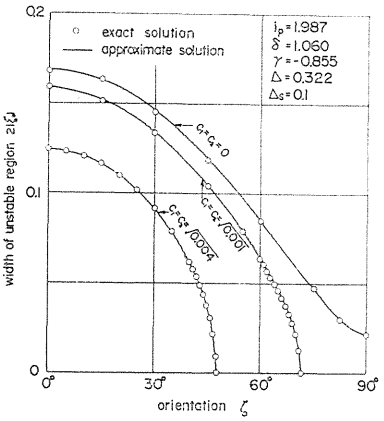

FIG. 1.7. $2|\xi_0|-\zeta$ diagram at ω_{c2}.

1.4.3. Dynamic unstable vibrations

At the points $D_1(p_1=\bar{p}_2)$ and $D_2(p_2=\bar{p}_1)$, $H\bar{H}=(1-p_1^2)(1-p_2^2)$ takes a negative value because $p_1>1>p_2>0$, and hence there is an unstable region near D_1 and D_2 because the form of the curves $\mathcal{D}'=0$ becomes of Fig. 1.6 (b). The fourth power term $\varphi_4(\geqq 0)$ gives minus effect in this case because $-\varphi_2/(H\bar{H})\geqq 0$. The negative damping coefficient m-the rotating speed ω diagrams with a parameter ζ for the system having $i_p=1$, $\delta=1.060$, $\gamma=-0.855$, $\Delta=0.3$, $\Delta_s=0.1$ and $c_1=c_2=0$, and for the system of Experiment IV are shown in Fig. 1.8 (a) and Fig. 1.9 respectively. The relation between the maximum value of m, *i.e.*, $m_{\max}$ and the orientation ζ is given in Fig. 1.8 (b) where the symbol ○ is the exact results of Fig. 1.8 (a), the full line curve is of the approximate expression (1.36 a); the former is somewhat larger than the latter[13]. Since $QR<0$ in this case the value of $m_{\max}$ takes its maximum and minimum value at $\zeta=90°$ and $\zeta=0°$ separately, the relation of which is contrary to that of the static unstable vibration. For comparison the approximate value $m_{\max}=0.1169$ and the exact value $m_{\max}=0.1214$ of the system with $\Delta=0.3$ and $\Delta_s=0$ are illustrated by horizontal full and broken line respectively in Fig. 1.8 (b). Incidentally the approximate value of $m_{\max}$ when $\Delta=0$, $\Delta_s=0.1$

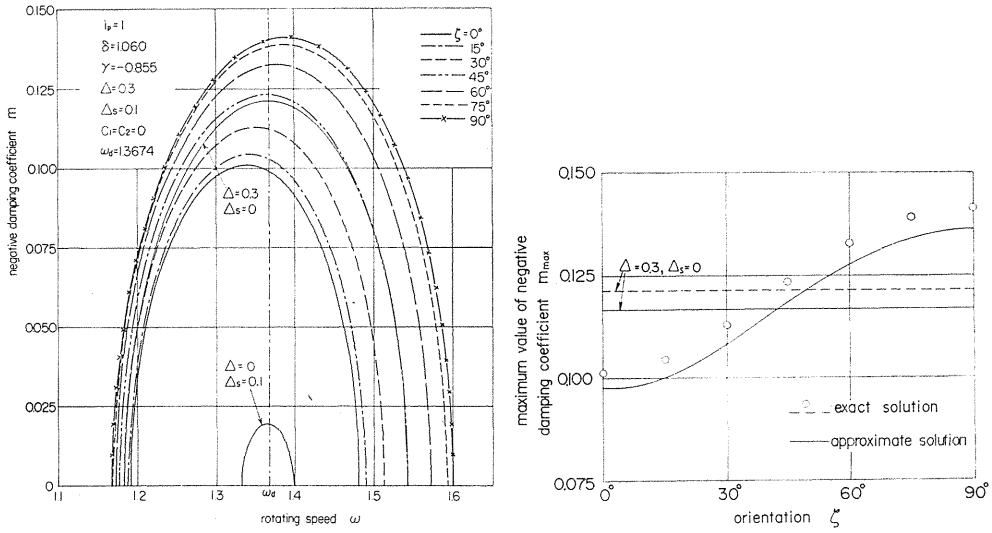

(a) $m-\omega$ diagram (exact solution) (b) $m_{\max}-\zeta$ diagram

($i_p=1$, $\delta=1.060$, $\gamma=-0.855$, $\Delta=0.3$, $\Delta_s=0.1$, $c_1=c_2=0$)

FIG. 1.8. $m-\omega$, $m_{\max}-\zeta$ diagrams at ω_d.

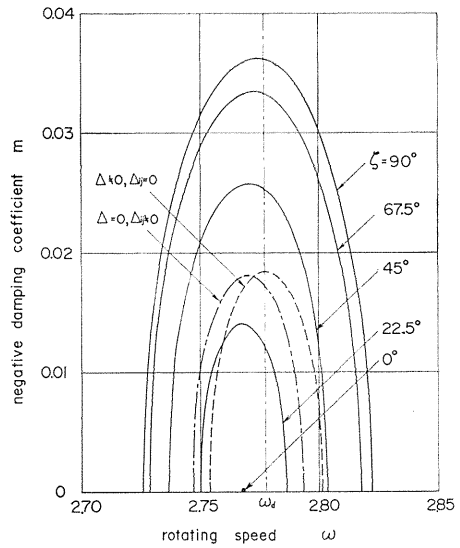

FIG. 1.9. $m-\omega$ diagram (Experiment IV, ω_d, exact solution).

is 0.0195, the result of which is not shown in the figure.

In general, the value of the orientation ζ has a remarkable effect on unstable vibrations appearing near both ω_c and ω_d, and $m_{\max}$ and the width $2|\xi_0|$ which are approximately proportional to $\sqrt{\varphi_2}=\sqrt{Q^2+R^2+2QR\cos 2\zeta}$ take their maximum and minimum values at $\zeta=0°$ and $\zeta=90°$ when $QR>0$, vice versa when $QR<0$.

Assuming $\varphi_2=0$ at ω_d, *i.e.*, $Q=\pm R$ at ω_d, the condition for removal of the unstable region near ω_d is defined approximately in terms of Δ, Δ_{11}, Δ_{12} and Δ_{22} as:

$$\Delta=\pm\{\gamma^2\Delta_{11}-\gamma^2\Delta_{12}(2-p_1^2-p_2^2)+\delta\Delta_{22}(1-p_1^2)(1-p_2^2)\}/\{p_1p_2(1-p_1^2)(1-p_2^2)\} \tag{1.41}$$

where the upper and lower signs correspond to $\zeta=90°$ and $\zeta=0°$, respectively, and p_1 and p_2 are given from the relations $f=HG-\gamma^2=0$ and $p_1+p_2=2\omega_d$ as follows:

$$p_{1,2}=\omega_d\pm\sqrt{\{(3i_p-4)\omega_d^2+(2+2\delta-i_p)\}/(4-i_p)} \tag{1.42}$$

The upper and lower signs in Eq. (1.42) correspond to p_1 and p_2, respectively,

and ω_d has already been defined in Eq. (1.35). The unstable region can be removed in the case of $\zeta=90°$ or $0°$ according to whether the value of Q is positive or negative at ω_d, because of $R<0$ at ω_d.

1.5. Experimental results

1.5.1. Experimental apparatus

The lateral vibrations take place in the vertical flat shaft S carrying an unsymmetrical rotor R as shown in Figs. 1.10 and 1.11. And the whirling of the shaft is measured optically by recording simultaneously lateral motions of the disc edge both in x-direction and y-direction as shown in Fig. 1.12.[24]

Experiments are performed using experimental apparatus shown in Table 1.1. In Experiment I, as shown in Fig. 1.10, the experimental apparatus consists of the vertical shaft of length $l=504.5$ mm with unsymmetrical stiffness supported by ball bearings at both the upper and lower shaft ends and the unsymmetrical rotor having $i_p \fallingdotseq 2$ and $\Delta=0.3041$. The length a between the lower shaft end and the rotor is 121.0 mm, and hence the length b between the upper end and the rotor is 383.5 mm. As shown in Table 1.1, the shaft used in Experiment I has unequal stiffness, *i.e.*, $\Delta_{11} \neq \Delta_{12} \neq \Delta_{22}$. In Experiments II, III and IV, as shown in

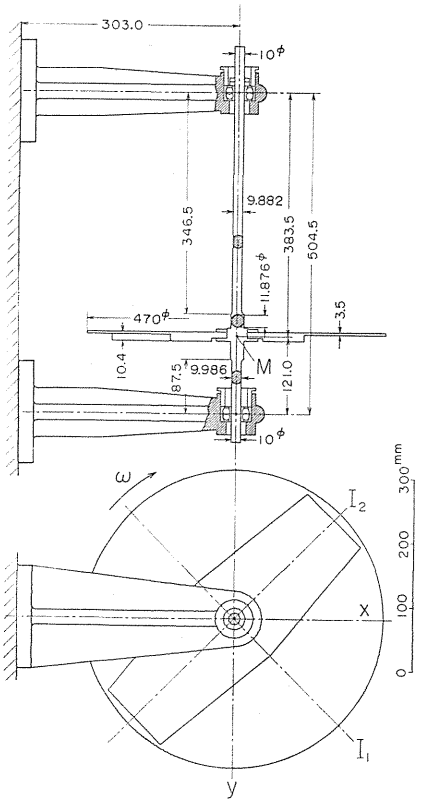

FIG. 1.10. Experimental apparatus (Experiment I).

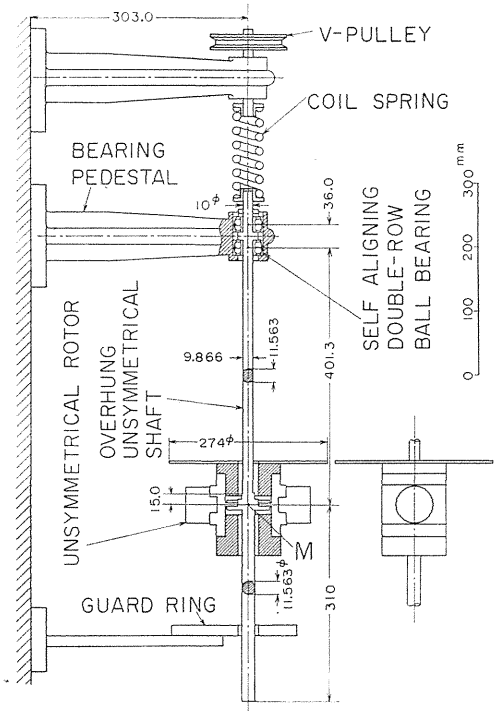

FIG. 1.11. Experimental apparatus (Experiment II, III and IV).

Fig. 1.11, the vertical shaft of length $l=$ 401.3 mm with unequal stiffness is supported by ball bearings only at the upper shaft end and the unsymmetrical rotor with $i_p<1$, $\Delta=0.1207$ (Experiment II), or $\Delta=0.1744$ (Experiment III), or $\Delta=0.0903$ (Experiment IV) is mounted at the free lower shaft end. In the upper shaft end the shaft are supported by two ball bearings equiped at a distance of $l_0=36.0$ mm. Ball bearings used in Experiments I, II, III and IV are the type of self-aligning double-row ball bearing with 10 ϕ bore of #1200. All spring constants in Table 1.1 are calculated by beam theory.

1.5.2. Forced vibrations and static unstable region

In Fig. 1.13 the response curves of Experiment I in the neighborhood of the lower major critical speed ω_{c2} are shown

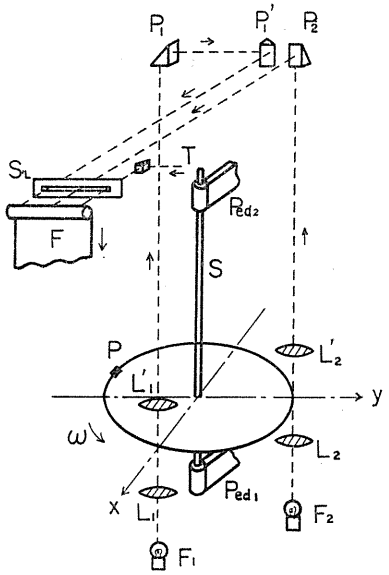

FIG. 1.12. Optical method of experiments.

TABLE 1.1. Dimensions of Experimental Apparatus

		Experiment I	Experiment II	Experiment III	Experiment IV
Mg	kg	10.433	11.894	13.681	12.179
I_p	kg cm s^2	2.1790	0.4300	0.5512	0.3725
I	kg cm s^2	1.0935	0.5276	0.6072	0.4943
ΔI	kg cm s^2	0.3325	0.0637	0.1059	0.0446
α	kg/cm	3.3617×10^2	0.2659×10^2	0.2659×10^2	0.2659×10^2
$-\gamma$	kg/rad	3.5773×10^3	0.5456×10^3	0.5456×10^3	0.5456×10^3
δ	kg cm/rad	6.2036×10^4	1.4993×10^4	1.4993×10^4	1.4993×10^4
$\Delta\alpha$	kg/cm	0.1945×10^2	0.0274×10^2	0.0274×10^2	0.0274×10^2
$-\Delta\gamma$	kg/rad	0.1838×10^3	0.0480×10^3	0.0480×10^3	0.0480×10^3
$\Delta\delta$	kg cm/rad	0.4258×10^4	0.1169×10^4	0.1169×10^4	0.1169×10^4
$\sqrt{\alpha/M}$	rpm	1697.0	446.9	416.9	441.9
$\sqrt{I/M}$	cm	10.135	6.593	6.595	6.307
i_p		1.9927	0.8150	0.9079	0.7536
δ		1.7966	12.9729	12.9665	14.1786
$-\gamma$		1.0499	3.1123	3.1108	3.2525
Δ		0.3041	0.1207	0.1744	0.0903
Δ_{11}		0.0579	0.1032	0.1032	0.1032
Δ_{12}		0.0514	0.0880	0.0880	0.0880
Δ_{22}		0.0686	0.0780	0.0780	0.0780

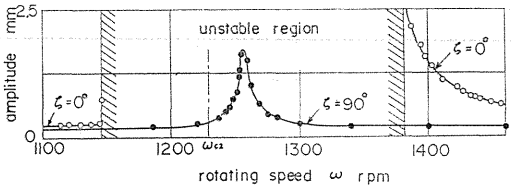

FIG. 1.13. Response curves at ω_{c2} (Experiment I).

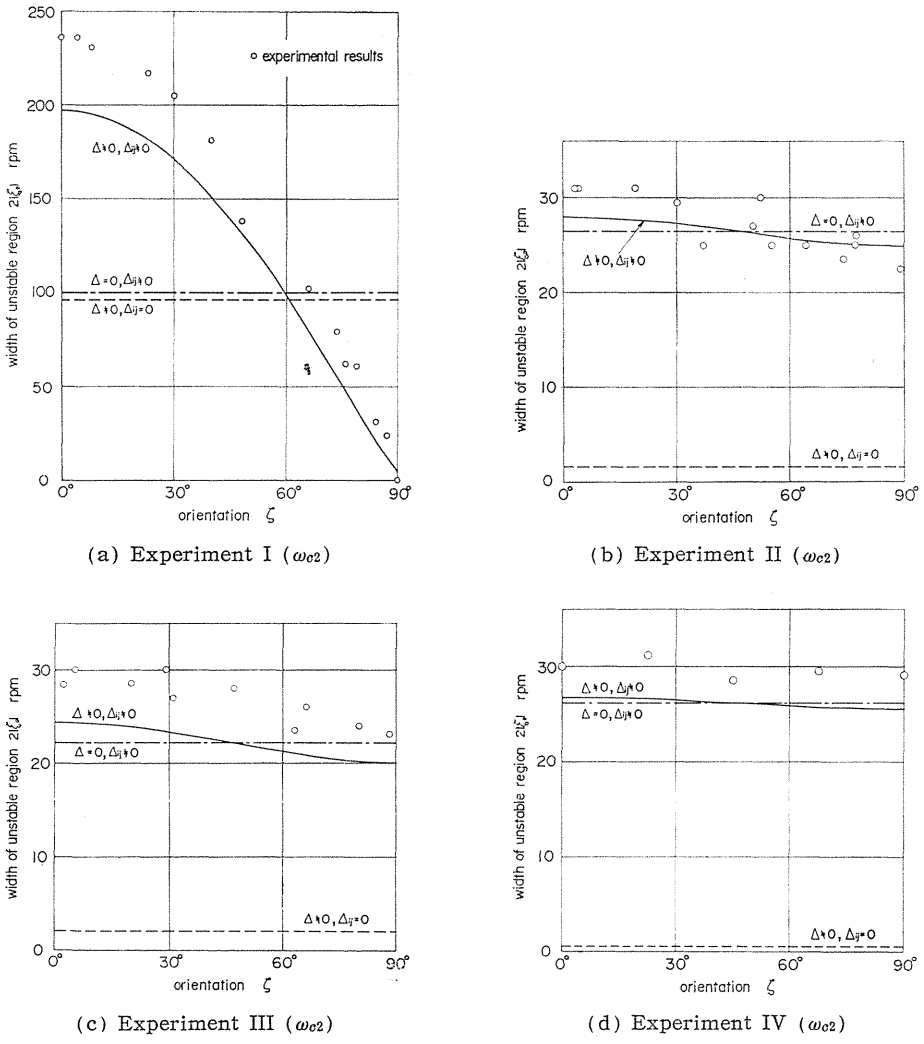

FIG. 1.14. $2|\xi_0|-\zeta$ diagram.

in case of $\zeta=0°$ and $\zeta=90°$ by the symbol ○ and ● respectively. In case of $\zeta=0°$ the width of unstable region $2|\xi_0|$ is 1382 rpm − 1146 rpm = 236 rpm, and there is no unstable region in case of $\zeta=90°$. The width $2|\xi_0|$ near ω_{c2} obtained by

Experiments I, II, III and IV are plotted against the orientation ζ in Figs. 1.14 (a), (b), (c) and (d) where the approximate results through Eq. (1.38 a) and the experimental results are shown by full line curves and symbols ○ severally; the calculated results when $\Delta=0$, $\Delta_{ij}\neq 0$ and $\Delta\neq 0$, $\Delta_{ij}=0$ of Experiments I, II, III and IV are added by chain and broken lines separately. It is seen from Eq. (1.38 a) that in Experiment I the widths $2|\xi_0|$ when $\zeta=0°$ and $\zeta=90°$ are approximately equal to 197.3 rpm and 4.6 rpm respectively. Since in Experiment II, III and IV θ_x, θ_y are smaller than x, y in the neighborhood of ω_{c2}, the effect of inertia asymmetry Δ induced by the motions of θ_x, θ_y is also smaller than that of stiffness asymmetry Δ_{ij}, and hence the broken line of case $\Delta\neq 0$, $\Delta_{ij}=0$ locates remarkably lower than the chain line of case $\Delta=0$, $\Delta_{ij}\neq 0$, and further the simultaneous effect of Δ and Δ_{ij} becomes somewhat small as shown in Figs. 1.14 (b), (c) and (d). Through Experiments I, II, III and IV, QR takes positive value in the neighborhood of the lower major critical speed ω_{c2}.

Figs. 1.15 (a), (b) show the four natural frequencies p_{10}, p_{20}, $\overline{p}_{30}$ and $\overline{p}_{40}$ of free vibration $\omega=0$, against the orientation ζ with experimental and analytical results which are denoted by ○ ⊖ ◒ ◓ and full-line curves, respectively. The difference between two natural frequencies p_{20}, $\overline{p}_{30}$ and the difference between p_{10}, $\overline{p}_{40}$ increase with ζ and take maximum values at $\zeta=90°$. This fact is in contrary to the width of the unstable region at major critical speed ω_c where $QR>0$, *i.e.* for case of $\gamma=0$ or case of the flat uniform shaft ($\Delta_{ij}=\Delta_s$).

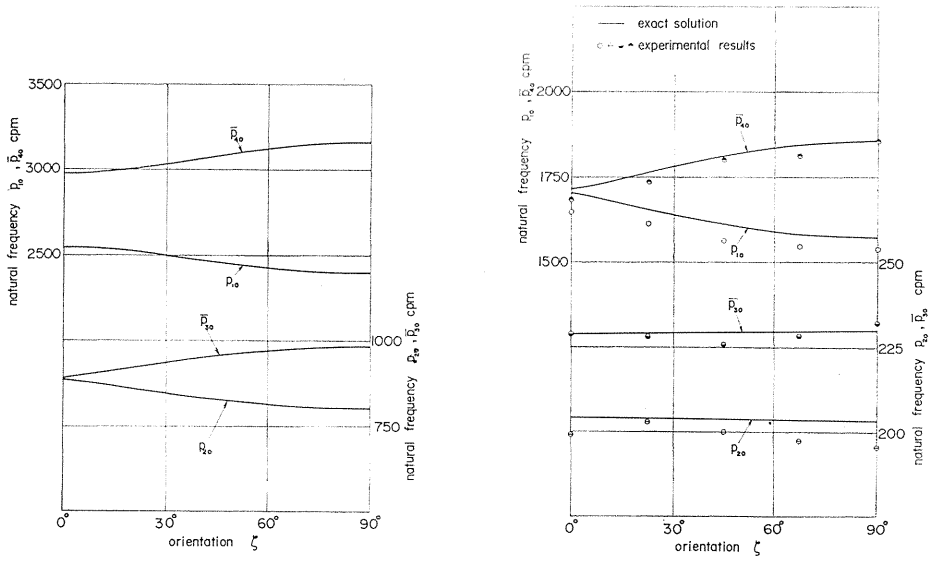

(a) Experiment I ($\omega=0$) (b) Experiment IV ($\omega=0$)

FIG. 1.15. p_{io}, $\overline{p}_{io}-\zeta$ diagrams.

1.5.3. Free vibrations and dynamic unstable region

Though the dynamic unstable region does not appear in Experiment I because of $i_p\fallingdotseq 2$[13], in Experiment II, III, IV there are unstable regions near $\omega=\omega_d=1216$ rpm, 1205 rpm, 1190 rpm respectively.

In Experiment II, IV for various values of ζ experimental and analytical results of the negative damping coefficient m are denoted by ● and full-line curves in Figs. 1.16, 1.17, respectively. The actual unstable regions come slightly lower than the analytical values because a massless shaft was assumed. Therefore, the latter is shifted to the lower side by 10 rpm (II), by 37 rpm (IV) in Figs. 1.16, 1.17, respectively. The magnitudes of m and $2|\xi_0|$ increase with the orientation ζ. Inserting the dimensionless quantities of Experiment IV ($i_p=0.7536$, $\delta=14.1786$, $\gamma=-3.2525$, $\Delta_{11}=0.1032$, $\Delta_{12}=0.0880$, $\Delta_{22}=0.0780$, $\omega_d=2.7771$, $p_1=5.0103$, $p_2=0.5438$) into Eq. (1.41), it wil be seen that the negative sign corresponding to $\zeta=0°$ must be taken because it provides the positive value of Δ. Although Eq. (1.41) provides the value $\Delta=0.0887$, which is slightly different from the actual value $\Delta=0.0903$ of the experimental apparatus used, inevitable damping forces[15] existing in the apparatus entirely remove unstable vibrations near the rotating speed ω_d as shown in Fig. 1.17.

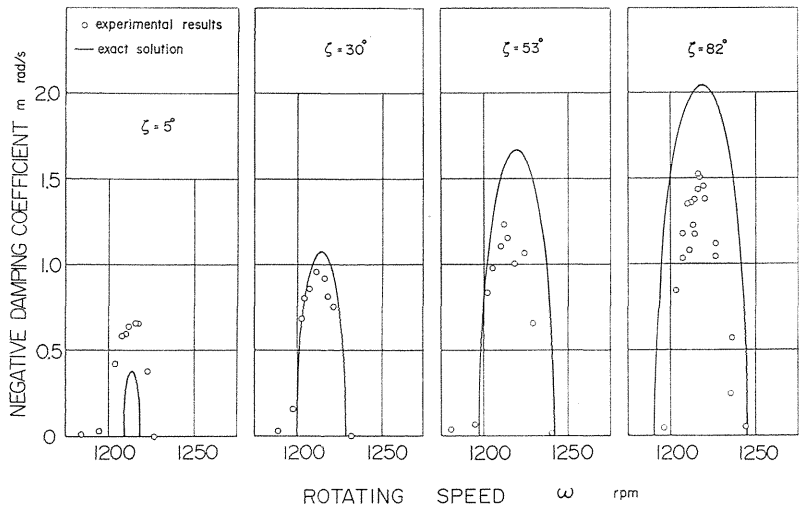

FIG. 1.16. $m-\omega$ diagrams for $\zeta=5°$, 30°, 53° and 82° (Experiment II, ω_d).

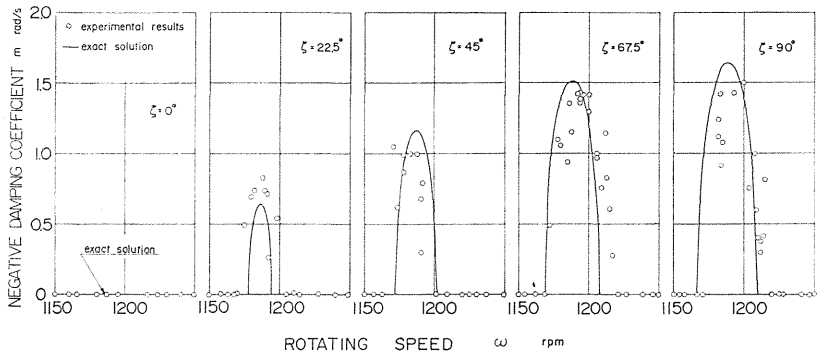

FIG. 1.17. $m-\omega$ diagrams for $\zeta=0°$, 22.5°, 45°, 67.5° and 90° (Experiment IV, ω_d).

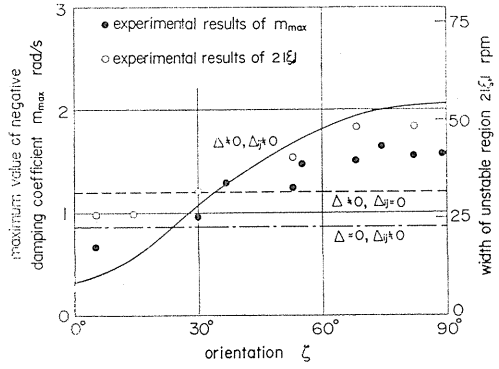

(a) Experiment II (ω_d)

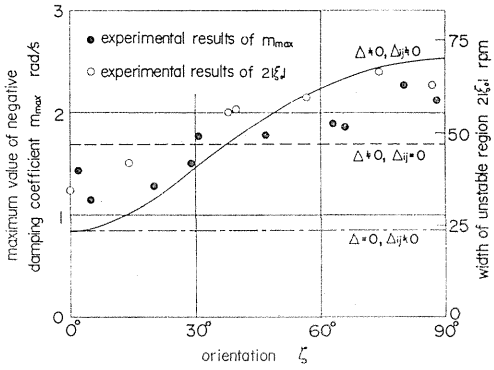

(b) Experiment III (ω_d)

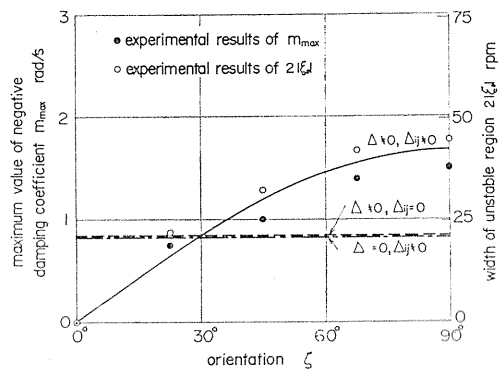

(c) Experiment IV (ω_d)

FIG. 1.18. $m_{\max}$, $2|\xi_0| - \zeta$ diagram.

The approximate results of $m_{\max}$ and $2|\xi_0|$ through Eqs. (1.36 a), (1.38 a) are shown in Figs. 1.18 (a), (b) and (c) for Experiments II, III and IV where an appropriate scales are adopted so that the magnitudes of both $m_{\max}$ and $2|\xi_0|$ can coincide each other, because the magnitude of $m_{\max}$ is in proportion to that of $2|\xi_0|$. In Fig. 1.18, the symbols ● and ○ show the experimental results of

TABLE 1.2. Comparison between Experimental and Analytical Results

		Experiment I	Experiment II	Experiment III	Experiment IV
Static unstable region	ω_{c2} rpm	1228.8 (1256)	223.8 (220)	209.5 (209)	221.4 (219)
	$2\|\xi_0\|$ at $\zeta=0°$ rpm	197.3 (236)	28.0 (31)	24.3 (29)	26.7 (30)
Dynamic unstable region	ω_d rpm		1228.4 (1216)	1197.0 (1205)	1227.2 (1190)
	$m_{\max}$ at $\zeta=90°$ rad/s		2.07 (1.6)	2.54 (2.3)	1.68 (1.5)
	$2\|\xi_0\|$ at $\zeta=90°$ rpm		54.1 (48)	70.3 (55)	41.9 (44)

Experimental results are shown in ( ).

m_{max} and $2|\xi_0|$ respectively. Further the approximate analytical results for case $\Delta=0$, $\Delta_{ij}\neq 0$ and $\Delta\neq 0$, $\Delta_{ij}=0$ are added by chain and broken lines severally. In Experiments II, III and IV, $2|\xi_0|$ and m_{max} take their minimum and maximum values at $\zeta=0°$ and $\zeta=90°$ separately at ω_d because $QR<0$. Comparison between the analytical and experimental results is shown in Table 1.2 where the values in ( ) are the experimental results, and $2|\xi_0|$ at ω_{c2} is the value at $\zeta=0°$ where it becomes maximum, and m_{max}, $2|\xi_0|$ at ω_d is the value at $\zeta=90°$ where it takes maximum value.

1.6. Conclusions

Obtained conclusions may be summed up as follows:

(1) In damped systems as well as in systems without damping, the approximate analytical values of the width of unstable region $2|\xi_0|$, the negative damping coefficient m of the unstable vibrations agree well with their exact values.

(2) The values of $2|\xi_0|$ and m_{max} of unstable vibrations appearing at both ω_c and ω_d are proportional to the magnitude of $\sqrt{\varphi_2}=\sqrt{Q^2+R^2+2QR\cos 2\zeta}$ and the sign of QR becomes positive or negative according to dimensions of the apparatus and whether $\omega=\omega_c$ or ω_d. If $QR>0$, φ_2 takes its maximum and minimum values at $\zeta=0°$ and $\zeta=90°$ respectively, vice versa if $QR<0$. Incidentally for case of $\gamma=0$ or case of the flat shaft having $\Delta_{ij}\equiv\Delta_s$, QR at ω_c is always positive.

(3) By means of an appropriate combination of Δ and Δ_{ij} so that $|Q|=|R|$ and $\cos 2\zeta=-QR/|QR|$, φ_2 becomes equal to zero, and hence the unstable vibrations at ω_c are removed perfectly and they at ω_d can almost vanish even though there is the term of φ_4.

(4) Even when the static unstable region at ω_c vanishes by large enough damping and the steady forced vibrations take place, the orientation ζ has large effect on the response curves of the forced vibrations. This effect is similar to that on unstable region when $c_1=c_2=0$.

(5) The difference between two natural frequencies p_{20}, $\bar{p}_{30}$, and the difference between p_{10}, $\bar{p}_{40}$ of free vibration when $\omega=0$, increase with ζ and take maximum values at $\zeta=90°$. This fact is in contrary to the width of the unstable region at major critical speed ω_c, for case of $\gamma=0$ or case of the flat uniform shaft ($\Delta_{ij}=\Delta_s$).

(6) The results of the analysis thus obtained were verified by four series of experiment and elimination of the unstable regions at both ω_c and ω_d was demonstrated.

Chapter 2. On Elimination of the Unstable Regions in a Rotating Shaft System Carrying an Unsymmetrical Rotor[21]

2.1. Introduction

When an elastic shaft carrying an unsymmetrical rotor with unequal diametral moments of inertia I_1 and I_2 ($I_1>I_2$) is supported at its both shaft ends by rigid pedestals, the system can be treated as a four-degree-of-freedom one.

In this chapter, the authors have verified analytically and experimentally that increase of degree-of-freedom of the system is effective for elimination of static unstable regions[10][11] and dynamic unstable regions[13]. There are two

theoretical methods for increasing the degree-of-freedom for the system. One is adoption of a flexible pedestal and the other is putting a mass on the shaft at the appropriate position. In this chapter the former method is mainly treated, and several series of experiments are carried out and are compared with the analytical results which give good agreement with the experimental results.

2.2. Equations of motion

The shaft carrying an unsymmetrical rotor with mass M is supported by a rigid pedestal B and a flexible pedestal A as shown in Fig. 2.1 (a). It is assumed that there is no unbalance in the rotor; it follows there from that the center of the rotor coincides with the center of gravity G. Points o and o_a are the equilibrium positions of the center of the rotor and the center of the equivalent mass M_a of the flexible bearing pedestal A, respectively, and o-xyz and o_a-$x_a y_a z$ are coordinate systems of the points G and G_a severally, G-$X_2Y_2Z_1$ is the coordinate system of the point G consisting of the principal moments of inertia of the rotor. The directions of plus sign of the deflection r and the inclination angle θ are as shown in Fig. 2.1 (a). The vibratory system considered here is a massless, uniform elastic shaft carrying an unsymmetrical rotor and supported by a flexible pedestal having mass M_a. Influence number of the shaft system $a_{ij}(=a_{ji})$ is introduced as follows:

$$\begin{pmatrix} x, & y \\ \theta_x, & \theta_y \\ x_a, & y_a \end{pmatrix} = \begin{pmatrix} a_{11} & a_{12} & a_{13} \\ a_{21} & a_{22} & a_{23} \\ a_{31} & a_{32} & a_{33} \end{pmatrix} \begin{pmatrix} P_x, & P_y \\ M_{ty}, & -M_{tx} \\ P_{ax}, & P_{ay} \end{pmatrix} \tag{2.1}$$

where P_x, P_y : Components of inertia force of the rotor in x and y directions
M_{tx}, M_{ty}: Components of moment M_t, in x and y directions
P_{ax}, P_{ay}: Components of inertia force P_a caused by the concentrated mass M_a in x_a, y_a directions.

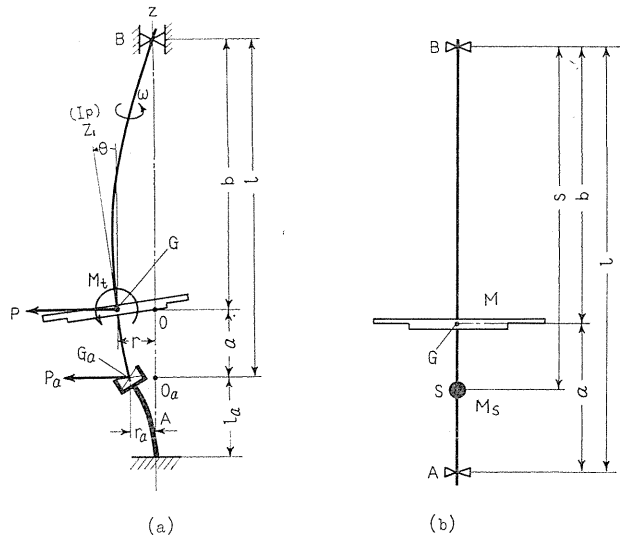

FIG. 2.1. Shaft system with a rotor and a mass.

The inertia forces arising at the points G and G_a are as follows:

$$P_x=-M\ddot{x},\ P_y=-M\ddot{y},\ P_{ax}=-M_a\ddot{x}_a,\ P_{ay}=-M_a\ddot{y}_a. \tag{2.2}$$

The torsional vibrations of the shaft, the magnitudes of which are smaller than θ_x^2 and θ_y^2, are neglected, and accordingly the rotating speed ω of the shaft is constant. Neglecting the powers higher than θ_x^3 and θ_y^3, the inertia moments about G are given by using Euler's equations of motion;

$$\left.\begin{aligned} M_{ty}&=-I\ddot{\theta}_x-I_p\omega\dot{\theta}_y+\Delta I\cdot\frac{d}{dt}(\dot{\theta}_x\cos 2\omega t+\dot{\theta}_y\sin 2\omega t)\\ -M_{tx}&=-I\ddot{\theta}_y+I_p\omega\dot{\theta}_x+\Delta I\cdot\frac{d}{dt}(\dot{\theta}_x\sin 2\omega t-\dot{\theta}_y\cos 2\omega t)\end{aligned}\right\} \tag{2.3}$$

Substituting Eq. (2.2) and (2.3) into Eq. (2.1), equations of motion of an unsymmetrical rotor are derived. In these equations, when the influence numbers a_{13}, a_{23}, a_{33} tend to zero, (or the mass of pedestal M_a tends to infinity), they coincide with equations of motion of a rotating shaft system carring an unsymmetrical rotor supported at both shaft ends by rigid pedestals[10].

2.3. Unstable regions in the neighborhood of the major critical speed

Existence of gyroscopic moment of the rotor results in whirling motion of the shaft, and there are two natural frequencies p and $\bar{p}=2\omega-p$ for each degree of freedom, because of unsymmetrical rotor. Accodingly free vibrations should take the form[10]

$$\begin{matrix}x\\y\end{matrix}=E\begin{matrix}\cos\\\sin\end{matrix}pt+\bar{E}\begin{matrix}\cos\\\sin\end{matrix}\bar{p}t,\ \begin{matrix}\theta_x\\\theta_y\end{matrix}=F\begin{matrix}\cos\\\sin\end{matrix}pt+\bar{F}\begin{matrix}\cos\\\sin\end{matrix}\bar{p}t,\ \begin{matrix}x_a\\y_a\end{matrix}=E_a\begin{matrix}\cos\\\sin\end{matrix}pt+\bar{E}_a\begin{matrix}\cos\\\sin\end{matrix}\bar{p}t \tag{2.4}$$

Substituting Eq. (2.4) into Eqs. (2.1), (2.2) and (2.3), and eliminating amplitudes E, $\bar{E}$, F, $\bar{F}$, E_a and $\bar{E}_a$, the following frequency equation is derived:

$$\Phi=\begin{vmatrix}
1-Mp^2a_{11} & 0 & -(Ip^2-I_p\omega p)a_{12} & -(\Delta I)p\bar{p}a_{12} & -M_ap^2a_{13} & 0\\
0 & 1-M\bar{p}^2a_{11} & -(\Delta I)p\bar{p}a_{12} & -(I\bar{p}^2-I_p\omega\bar{p})a_{12} & 0 & -M_a\bar{p}^2a_{13}\\
-Mp^2a_{12} & 0 & 1-(Ip^2-I_p\omega p)a_{22} & -(\Delta I)p\bar{p}a_{22} & -M_ap^2a_{23} & 0\\
0 & -M\bar{p}^2a_{12} & -(\Delta I)p\bar{p}a_{22} & 1-(I\bar{p}^2-I_p\omega\bar{p})a_{22} & 0 & -M_a\bar{p}^2a_{23}\\
-Mp^2a_{13} & 0 & -(Ip^2-I_p\omega p)a_{23} & -(\Delta I)p\bar{p}a_{23} & 1-M_ap^2a_{33} & 0\\
0 & -M\bar{p}^2a_{13} & -(\Delta I)p\bar{p}a_{23} & -(I\bar{p}^2-I_p\omega\bar{p})a_{23} & 0 & 1-M_a\bar{p}^2a_{33}
\end{vmatrix}=0 \tag{2.5}$$

Expanding Eq. (2.5) and using Laplacian expanding theorem, Eq. (2.5) reduces to

$$\Phi=f\bar{f}-(\Delta I)^2p^2\bar{p}^2g\bar{g}=0 \tag{2.6}$$

where

$$f=f(p)=\begin{vmatrix}
1-Mp^2a_{11} & -(Ip^2-I_p\omega p)a_{12} & -M_ap^2a_{13}\\
-Mp^2a_{12} & 1-(Ip^2-I_p\omega p)a_{22} & -M_ap^2a_{23}\\
-Mp^2a_{13} & -(Ip^2-I_p\omega p)a_{23} & 1-M_ap^2a_{33}
\end{vmatrix}$$

$$=-p(Ip-I_p\omega)g+h \tag{2.6 a}$$

$$g=g(p)=MM_a\begin{vmatrix} a_{11} & a_{12} & a_{13} \\ a_{12} & a_{22} & a_{23} \\ a_{13} & a_{23} & a_{33} \end{vmatrix} p^4-\left\{M\begin{vmatrix} a_{11} & a_{12} \\ a_{12} & a_{22} \end{vmatrix}+M_a\begin{vmatrix} a_{22} & a_{23} \\ a_{23} & a_{33} \end{vmatrix}\right\}p^2+a_{22} \quad (2.6\,\mathrm{b})$$

$$h=h(p)=MM_a\begin{vmatrix} a_{11} & a_{13} \\ a_{13} & a_{33} \end{vmatrix} p^4-(Ma_{11}+M_aa_{33})p^2+1 \quad (2.6\,\mathrm{c})$$

$$\bar{f}=\bar{f}(p)=f(\bar{p}),\ \bar{g}=g(\bar{p}),\ \bar{h}=h(\bar{p}) \quad (2.6\,\mathrm{d})$$

Putting $\Delta I=0$, natural frequencies of the system p_i $(i=1\sim6)$ carrying a symmetrical rotor are obtained from Eq. (2.6), and the following relation between natural frequencies p_i can always hold: $p_1>p_2>p_3>0>p_4>p_5>p_6$. Dynamically unstable vibrations arise at the rotating speed ω_d of the cross points of $p-\omega$ curves on the $p-\omega$ diagram, *i.e.*, at the rotating speed where the relation $p_i=\bar{p}_j$ is satisfied, and amplitudes of two vibrations of p_i and p_j build up exponentially as reported already[15)24)].

At the major critical speed, the relation $\omega=p_i=\omega_{ci}$ holds, and the major critical speed ω_{ci} is separated into ω_{ci1} and ω_{ci2} because of the existence of ΔI, and in the region of $\omega_{ci1}<\omega<\omega_{ci2}$ the so-called "static unstable vibration" takes place. As observed from the rotating coordinate system with ω, the amplitude becomes larger in the form of e^{mt}, so it is named static unstable vibration, but the circumstance is not the same as in case of recti-linear vibratory system with negative restoring force. Putting $p=\bar{p}=\omega$ in Eq. (2.5), the frequency equation becomes as follows:

$$\Phi=\Phi_1\cdot\Phi_2=0 \quad (2.5\,\mathrm{a})$$

where

$$\Phi_{1,2}=\begin{vmatrix} 1-M\omega^2a_{11} & -(I\pm\Delta I-I_p)\omega^2a_{12} & -M_a\omega^2a_{13} \\ -M\omega^2a_{12} & 1-(I\pm\Delta I-I_p)\omega^2a_{22} & -M_a\omega^2a_{23} \\ -M\omega^2a_{13} & -(I\pm\Delta I-I_p)\omega^2a_{23} & 1-M_a\omega^2a_{33} \end{vmatrix}=0 \quad (2.5\,\mathrm{b})$$

and ω_{ci1} is derived from the plus sign of $\pm\Delta I$ in Eq. (2.5 b), *i.e.*, $\Phi_1=0$, and ω_{ci2} is given from the minus sign, *i.e.*, $\Phi_2=0$.

At the major critical speeds ω_{ci}, when $\Delta I=0$ in Eq. (2.5 b), the relation $\omega_{c1}>\omega_{c2}>\omega_{c3}$ holds, and when $\Delta I\neq0$, the unstable regions are classified[10)] into the following three cases (a), (b) and (c), because the relation $I_1+I_2\geqq I_p\geqq I_1-I_2>0$ holds:

(a) When $I_p\geqq I_1>I_2$, there are two static unstable regions $[\omega_{c31},\ \omega_{c32}]$ and $[\omega_{c21},\ \omega_{c22}]$.

(b) When $I_1>I_2>I_p$, there are three static unstable regions $[\omega_{c31},\ \omega_{c32}]$, $[\omega_{c21},\ \omega_{c22}]$ and $[\omega_{c11},\ \omega_{c12}]$.

(c) When $I_1>I_p\geqq I_2$, there are three static unstable regions $[\omega_{c31},\ \omega_{c32}]$, $[\omega_{c21},\ \omega_{c22}]$ and $[\omega_{c11},\ \infty]$.

The amplitude of deflection is always larger than that of inclination angle in the unstable regions $[\omega_{c31},\ \omega_{c32}]$ and $[\omega_{c21},\ \omega_{c22}]$, and the deflected shaft whirls at the same angular velocity as the rotating speed ω of the shaft. In the unstable region $[\omega_{c31},\ \omega_{c32}]$, the deflections at the points G and G_a, *i.e.*, the centers of gravity of mass of the rotor and the concentrated mass of the flexible pedestals.

take the same phase, but in the unstable region [ω_{c21}, ω_{c22}], they take the opposite phase. In these vibratory modes, the inclination angle θ and the amplitude F can vanish by use of a pedestal having suitable mass and flexibility. Thus the unstable regions can be eliminated by omitting the dynamical effect of asymmetry ΔI which is induced by inclination angles θ_x, θ_y. Putting $F=0$ in Eq. (2.4), we have

$$\frac{E_a}{E} = -\frac{Ma_{12}}{M_a a_{23}} = \frac{1-M\omega^2 a_{11}}{M_a\omega^2 a_{13}} = \frac{M\omega^2 a_{13}}{1-M_a\omega^2 a_{33}} \tag{2.7}$$

The concentrated mass of pedestal M_a is given from Eq. (2.7) as follows:

$$\frac{M_a}{M} = \frac{a_{11}(a_{12}a_{23}) - a_{12}^2 a_{13}}{(a_{12}a_{23})a_{33} - a_{13}a_{23}^2} \tag{2.8}$$

which shows that M_a is defined by the known influence numbers of the system a_{ij}. The unstable region at the major critical speed vanishes only by adopting the value of M_a from Eq. (2.8) and the speed ω_c is obtained by Eq. (2.7) as follows:

$$\omega_c^2 = \left\{M\left(a_{11} - \frac{a_{12}a_{13}}{a_{23}}\right)\right\}^{-1} \tag{2.9}$$

From Eq. (2.5 b) the amplitude ratio E_a/E is derived as follows:

$$\frac{E_a}{E} = \frac{a_{13}a_{23} - a_{12}a_{33}}{a_{11}a_{23} - a_{12}a_{13}} \tag{2.10}$$

Since in the influence numbers of the system shown in Table 2.1, the relations $a_{11}>0$, $a_{13}>0$ and $a_{33}>0$ hold, and they result in $M_a>0$, $\omega_c^2>0$ and $E_a/E>0$ from Eq. (2.8), (2.9) hnd (2.7), respectively, the width of the unstable region [ω_{c31}, ω_{c32}], *i.e.*, $\Delta\omega_{c3}=\omega_{c32}-\omega_{c31}$ in the neighborhood of ω_{c3} can be always eliminated when $a_{12}/a_{23}<0$. On the other hand, at ω_{c2} where the relation $a_{12}/a_{23}>0$ holds and the phases of G and G_a are opposite, there is a possibility of elimination of the unstable region, *i.e.*, $\Delta\omega_{c2}=0$, but this possibility is restricted because signs of M_a and ω_c^2 in Eqs. (2.8) and (2.9) can not always become positive. As shown in Fig. 2.1 (a), there are the inertia force $P=Mr\omega^2$ at the center of gravity G of the rotor, the inertia force $P_a=M_a r_a\omega^2$ at the center of gravity G_a of the concentrated mass of the flexible pedestal and the gyroscopic moment $M_t=(I\pm\Delta I-I_p)\theta\omega^2$ about the point G, and hence the deflection curve of the shaft under these forces and moment give the mode of vibration at the major critical speed. When the relation $M_a=P_a=0$ holds, the inclination angle θ at the point G is not equal to zero, while when $M_a\neq 0$ in Eq. (2.7), the inertia force P_a at the point G_a grows, and the tangent of the deflection curve at G can become parallel to oz, hence, the moment M_t can vanish. From this it follows that there is no influence of asymmetry ΔI. It can be seen that the dynamical effect of the mass of the pedestal is not the same as that of the dynamic absorber in recti-linear vibrations, as above mentioned. In case of recti-linear vibration, the external force is canceled by the added mass of the absorber at the resonance. On the other hand, the force induced by the pedestal mass M_a has effect upon the elimination of the unstable region due to the asymmetry ΔI of the rotor, and it has no effect on

eliminating the external force.

In the rotating system carring an unsymmetrical rotor supported by a flexible pedestal, the unstable region $[\omega_{c11}, \omega_{c12}]$ in the neighborhood of the major critical speed ω_{c1} where $p_1=\omega$, can not be removed, because of inevitable presence of inclinational vibration. In the flat shaft system, it is impossible to eliminate the unstable regions at ω_c as well as ω_d, because there is always effect of unsymmetrical shaft stiffness, unless $E=F=E_a=0$.

For the system of additional mass on the shaft P_{ax}, P_{ay}, x_a and y_a should be replaced by P_{sx}, P_{sy}, x_s and y_s in Eq. (2.1); M_a by M_s in Eq. (2.2); and E_a by E_s in Eq. (2.4). From the condition $F=0$, *i.e.*, the condition that the rotor does not incline, M_s/M, ω_c and E_s/E can be obtained from Eq. (2.8), (2.9) and (2.10), respectively. It is noticeable that the influence number a_{ij} has to be recalculated from Eq. (2.1) for each shaft system.

2.3.1. Free-free supported systems supported by a rigid pedestal B and a flexible pedestal A

In a shaft system with uniform cross section freely supported at both shaft ends, the spring constants of the shaft are defined by Eq. (1.4) in Fig. 2.1 (a), and they are given as follows:

$$\left.\begin{aligned} \alpha &= 3lEI_0\frac{a^2-ab+b^2}{a^3b^3}, & \gamma &= 3lEI_0\frac{a-b}{a^2b^2} \\ \delta &= 3lEI_0\frac{1}{ab}, & k_a &= 3(EI)_a/l_a^3 \end{aligned}\right\} \tag{2.11}$$

where E is Young's modulus of elasticity, I_0 is moment of inertia of the area of cross section of shaft, k_a is spring constant of the flexible pedestal A. Using Eq. (2.11) influence numbers a_{ij} are as follows:

$$\left.\begin{aligned} a_{11} &= \frac{\delta}{\alpha\delta-\gamma^2}+\frac{b^2}{l^2k_a}, & a_{12} &= \frac{-\gamma}{\alpha\delta-\gamma^2}-\frac{b}{l^2k_a}, & a_{13} &= \frac{b}{lk_a} \\ a_{22} &= \frac{\alpha}{\alpha\delta-\gamma^2}+\frac{1}{l^2k_a}, & a_{23} &= -\frac{1}{lk_a}, & a_{33} &= \frac{1}{k_a} \end{aligned}\right\} \tag{2.12}$$

Observing Eqs. (2.8) and (2.12) it is seen that M_a is given as a function of α, γ, δ and k_a.

As is seen from Eqs. (2.11) and (2.12), the relations $\alpha\delta-\gamma^2>0$ and $a_{23}<0$ always hold; hence whenever $a_{12}>0$ holds, *i.e.*, whenever $P>0$ and $\theta>0$ holds, the unstable region $[\omega_{c31}, \omega_{c32}]$ can be eliminated completely. In order that $a_{12}>0$ can hold, the following two inequalities must be satisfied, as is seen from Eqs. (2.11) and (2.12):

$$a<b\,(i.e.,\ \gamma<0),\ \text{and}\ \ k_a\geqq-(\alpha\delta-\gamma^2)b/(\gamma l^2)>0 \tag{2.13}$$

Inserting Eq. (2.12) into Eqs. (2.8) and (2.9), the following three equations are derived from the condition for $\Delta\omega_{c3}=0$.

$$\frac{M_a}{M}=\frac{(\delta-\gamma b)\{k_a+(\alpha\delta-\gamma^2)b/(\gamma l^2)\}}{(\alpha\delta-\gamma^2)} \tag{2.8 a}$$

$$k_a = \frac{(\alpha\delta - \gamma^2)}{(\delta - \gamma b)}\left(\frac{M_a}{M}\right) - \frac{(\alpha\delta - \gamma^2)\, b}{\gamma l^2} \tag{2.8 b}$$

$$\omega_c^2 = \frac{\alpha\delta - \gamma^2}{M(\delta - \gamma b)} \tag{2.9 a}$$

Whenever Eq. (2.13) holds, the unstable region at ω_{c3} can always be eliminated, *i.e.*, $\Delta\omega_{c3}=0$ holds, because the signs of M_a, *i.e.*, Eq. (2.8 a), and k_a, *i.e.*, Eq. (2.8 b) are always positive. On the other hand, when $a>b$ (*i.e.*, $\gamma>0$), $a_{12}<0$ is obtained

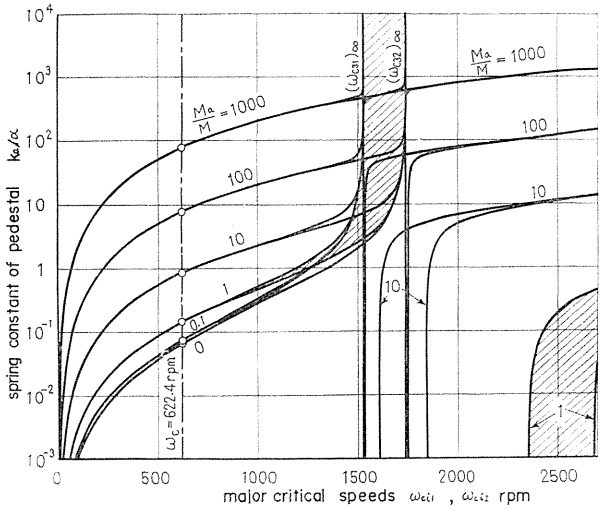

(a) $k_a-\omega_{ci}$ ($i=2, 3$)diagram

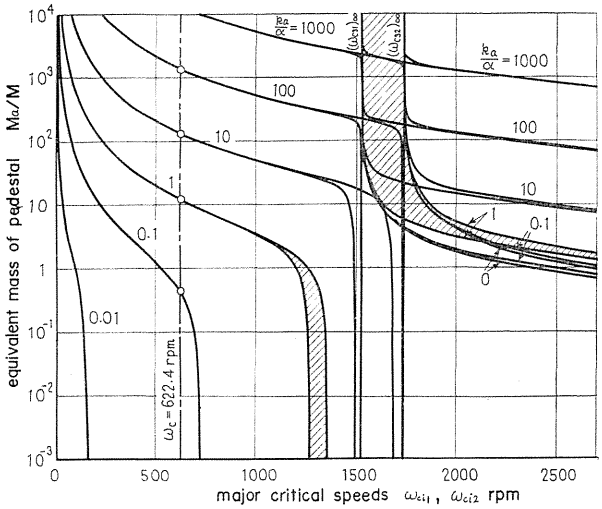

(b) $M_a-\omega_{ci}$ ($i=2, 3$) diagram

$(\omega_{c31})_\infty=1523.9$ rpm, $(\omega_{c32})_\infty=1736.0$ rpm, Dimensions of the shaft system are shown in Eq. (2.20).

FIG. 2.2. Boundaries of unstable region between ω_{ci1} and ω_{ci2}.

from Eq. (2.12), and the unstable region $[\omega_{c21}, \omega_{c22}]$ can be eliminated, while in order to remove the unstable region $[\omega_{c31}, \omega_{c32}]$, the rigid pedestal B and the flexible one A must be exchanged for each other, *i.e.*, $a<b$.

Fig. 2.2 (a), (b) show the relation between k_a/α and the major critical speeds ω_{ci} with a parameter M_a/M, and the relation between M_a/M and the major critical speeds ω_{ci} with a parameter k_a/α. Since the rotor with the relation $I_p>I_1>I_2$ is used in our experiments, there are two unstable regions $[\omega_{c31}, \omega_{c32}]$ and $[\omega_{c21}, \omega_{c22}]$. At the rotating speed $\omega_c=622.4$ rpm which is shown by vertical chain line in Fig. 2.2, and the value of which is given by Eq. (2.9 a), the width of unstable region $\Delta\omega_{c3}$ becomes equal to zero. The hatched ranges in Fig. 2.2 (a), (b) show the unstable regions for cases of $M_a/M=1$, $k_a/\alpha=1$,respectively. In Fig. 2.2 (a), when $k_a\to\infty$, the unstable region $[\omega_{c31}, \omega_{c32}]$ tends to the unstable region $[\omega_{c31}, \omega_{c32}]_\infty$ of the shaft system supported by rigid pedestals at both shaft ends. In case of somewhat large value of M_a/M, decrease of magnitude of k_a results in reduction of the unstable region $[\omega_{c31}, \omega_{c32}]$ appearing at the lower rotating speed, and further in a shift of the higher unstable region $[\omega_{c21}, \omega_{c22}]$ to the lower rotating speed. Accordingly in order to have no unstable region throughout certain range of rotating speeds, it is necessary to adopt a somewhat small value of M_a/M. Even in the extreme case of $M_a=0$, it is effective to eliminate the unstable region where k_a/α is small. For case of $a_{12}<0$, *i.e.*, $k_a/\alpha<0.06701$ from Eq. (2.12), there is no value of M_a in (2.8 a) realizing $\Delta\omega_{c3}=0$, because $M_a<0$, *i.e.*, because the ω_{ci} curves do not intersect with the vertical chain line $\omega=\omega_c$ in Fig. 2.2 (b). The width of unstable regions, however, becomes nearly equal to zero as easily seen from Fig. 2.2 (b). In Fig. 2.2, the width of the unstable region at the rotating speed $\omega=\sqrt{k_a/M_a}$, which is nearly equal to the major critical speed, is extremely narrow. It shows that only the vibration of flexible pedestal A takes place. The major critical speed at ω_{c3} where the phase of G is the same as that of G_a, comes close to $\omega=\sqrt{k_a/M_a}$ as k_a tends to zero or M_a tends to infinity, and the major critical speed ω_{c3} of the same phase (or ω_{c2} out of phase), comes close to the unstable region $[\omega_{c31}, \omega_{c32}]_\infty$ of the rigid pedestal as k_a tends to infinity (or M_a tends to infinity).

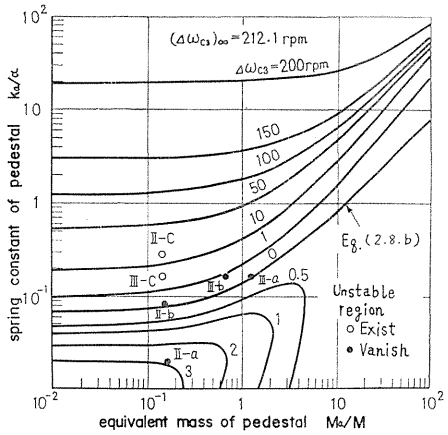

FIG. 2.3. The relation between k_a and M_a with a parameter $\Delta\omega_{c3}=\omega_{c32}-\omega_{c31}=$const. (Dimensions of the shaft system are the same as Eq. (2.20)).

The relation between k_a and M_a when $\Delta\omega_{c3}=\omega_{c32}-\omega_{c31}=$ constant is shown in Fig. 2.3. There is a linear relation $k_a/\alpha=0.07857\ (M_a/M)+0.06701$ which is derived from Eq. (2.8 b), *i.e.*, from the condition $\Delta\omega_{c3}=0$. A larger value of k_a gives a larger width of $\Delta\omega_{c3}$, and $\Delta\omega_{c3}$ comes close to $(\Delta\omega_{c3})_\infty=212.1$ rpm as k_a tends to infinity. Curves lying under the curve $\Delta\omega_{c3}=0$ furnish the narrow width of unstable regions shown in the left side of vertical chain line shown in

Fig. 2.2 (a), (b).

2.3.2. A rotating shaft system having a concentrated mass and free-free supported by rigid pedestals at both shaft ends

When, on the uniform elastic shaft supported by rigid pedestals A and B at both shaft ends, the mass M_s is mounted at the point S separated by the distance s from the pedestal B, M_a, E_a in Eqs. (2.7), (2.8) and (2.10) must be exchanged by M_s, E_s, respectively. It is assumed that the system considered here is a vertical shaft carrying an unsymmetrical rotor at the lower point from its mid-point, *i.e.* $a<b$. For the case of $a>b$ the relative position must be reversed. There are two cases of $s>b$ and $s<b$.

In the former case of $s>b$, the influence number a_{ij} of Eq. (2.1) is given as follows from beam theory:

$$a_{11}=\frac{\delta}{\alpha\delta-\gamma^2}=\frac{a^2b^2}{3\,lEI_0},\quad a_{12}=\frac{-\gamma}{\alpha\delta-\gamma^2}=\frac{ab(b-a)}{3\,lEI_0}$$

$$a_{13}=\frac{b(l-s)(2\,ls-s^2-b^2)}{6\,lEI_0},\quad a_{22}=\frac{\alpha}{\alpha\delta-\gamma^2}=\frac{a^2-ab+b^2}{3\,lEI_0}$$

$$a_{23}=-\frac{(l-s)(2\,ls-s^2-3\,b^2)}{6\,lEI_0},\quad a_{33}=\frac{s^2(l-s)^2}{3\,lEI_0} \tag{2.14}$$

It is seen from Eq. (2.14) that the relation $a_{12}>0$ always holds, and accordingly the following two conditions between b and s should be satisfied simultaneously in order that the relation $\Delta\omega_{c3}=0$ can hold:

$$l/\sqrt{3}>b>l/2,\quad l>s>l-\sqrt{l^2-3\,b^2} \tag{2.15}$$

which are derived from the condition $a_{23}<0$ in Eq. (2.14). If Eq. (2.15) is

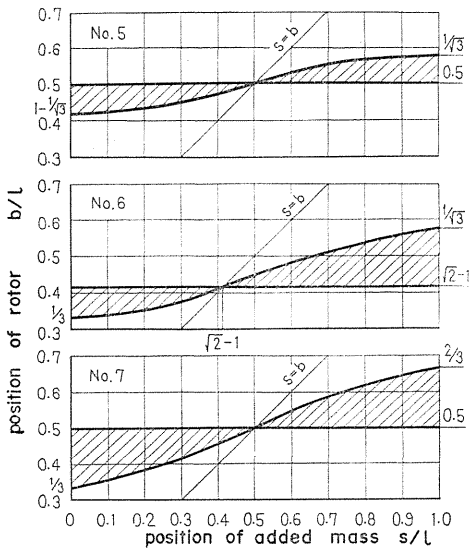

FIG. 2.4. Ranges of b and s for elimination of unstable region at ω_{c3} by added mass (in case of uniform shaft section).

satisfied, we have the relation $l-\sqrt{l^2-3b^2}>b$, from which the preliminary relation $s>b$ is derived.

In the case of $s<b$, a_{11}, a_{12}, a_{22} and a_{23} are the same as those in the case of $s>b$ as is seen in Eq. (2.14), and a_{13}, a_{23} are as follows:

$$a_{13}=\frac{as(2ab+b^2-s^2)}{6lEI_0},\quad a_{23}=\frac{s\{2a(b-a)+(b^2-s^2)\}}{6lEI_0} \tag{2.16}$$

Since the relation $a_{23}>0$ in Eq. (2.16) always holds, the condition $\Delta\omega_{c3}=0$ can not be realized. Consequently it can be concluded that the condition of elimination of unstable region, *i.e.* $\Delta\omega_{c3}=0$ is Eq. (2.15) (cf. No. 5 in Fig. 2.4).

2.3.3. In the case of other supported conditions of rotating shaft system

When a flexible pedestal and a rigid pedestal are used at each end of the shaft, there are four cases of No. 1~No. 4 shown in Table 2.1. In the case of No. 1 the influence number a_{ij} is represented in rather simple form as a function of spring constants of the shaft and spring constant of pedestal k_a. The problem in the systems having fixed support is not treated in this paper, because a_{ij} of such a system contains bending stiffnesses (EI_0), $(EI_0)_a$, and l_a, a and b, and should be expressed in complicated form.

There are three cases of No. 5, 6 and 7, when the additional mass M_a is used, as shown in Table 2.1. In the case of uniform shaft, a_{ij} of the case No. 5 is given by Eqs. (2.14) and (2.16), and in order to eliminate the unstable region of the lower rotating speed side of the major critical speeds, the locations of the rotor

TABLE 2.1. Various Cases of Support Condition.

	No.	Type	Note
When a flexible pedestal is furnished	1	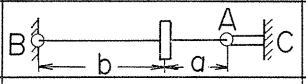	cf. section 2.3.1
	2	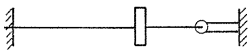	2.3.3
	3	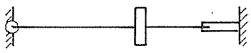	2.3.3
	4	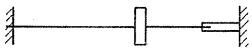	2.3.3
When a mass is added	5	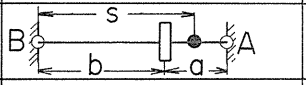	2.3.2
	6	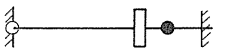	2.3.3
	7	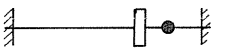	2.3.3

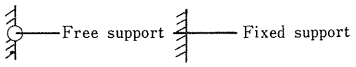

and the additional mass, *i.e.*, b and s should satisfy the condition (2.15). Ranges of b and s satisfying the condition Eq. (2.15) are shown in shaded zones in Fig. 2.4 (No. 5). For the case of $l/2>b>0$ which is not treated in Eq. (2.15), such zones are located in symmetrical positions with the point of symmetry $s=b=l/2$.

Similar procedure leads to the conclusions that, in the case of No. 6 in Table 2.1, the conditions of $\Delta\omega_{c3}=0$ are

$$\left.\begin{aligned} &l/\sqrt{3}>b>(\sqrt{2}-1)\,l \\ &l>s>2b^2l/(l^2-b^2) \end{aligned}\right\} \tag{2.17}$$

for $s>b$, and

$$\left.\begin{aligned} &(\sqrt{2}-1)\,l>b>l/3 \\ &l\sqrt{(3b-l)/(l+b)}>s>0 \end{aligned}\right\} \tag{2.18}$$

for $s<b$. In Fig. 2.4 (No. 6), the values of b and s in shaded zones satisfy the above conditions.

In case of No. 7, the following relations are derived:

$$2l/3>b>l/2, \quad l>s>bl/\{2(l-b)\} \tag{2.19}$$

and b and s satisfying Eq. (2.19) lie also in the shaded zones of Fig. 2.4 (No. 7).

2.4. *Experimental apparatus and experimental results*

Experimental apparatus is shown in Fig. 2.5. The vertical shaft S of diameter $d=11.60$ mm, is supported at its upper and lower ends by self-aligning double-row ball bearings with $10\,\phi$ bore (#1200). The rigid pedestals are shown by B and C. By changing the length l_a of the flexible pedestal A which is chucked on the rigid pedestal C, the flexibility of pedestal can be varied. And by changing the magnitude of attached weight of the flexible pedestal, we can vary the value of M_a. Motions of the center of gravity G of the rotor, and the center of gravity G_a of the flexible pedestal are recorded optically in y-direction. The influence number a_{ij} (in case of No. 1 in Table 2.1) in our experiment is obtained from Eqs. (2.11) and (2.12). Dimensions of our experimental apparatus are as follows:

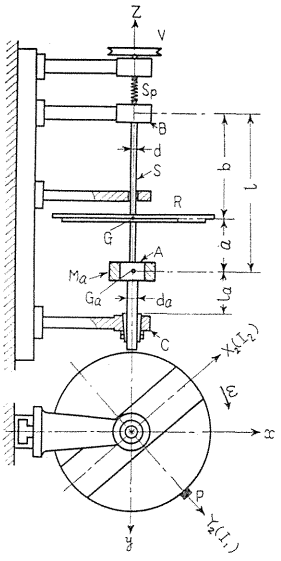

FIG. 2.5. Experimental apparatus (in case of the system supported by a flexible pedestal).

$$\left.\begin{aligned} &I_p=2.390 \text{ kg cm s}^2,\ I_1=1.590 \text{ kg cm s}^2,\ I_2=0.815 \text{ kg cm s}^2, \\ &Mg=9.746 \text{ kg},\ a=10.19 \text{ cm},\ b=40.36 \text{ cm},\ d=1.160 \text{ cm} \\ &d_a=1.80 \text{ cm},\ \alpha=5.377\times10^2 \text{ kg/cm},\ \gamma=-5\,049\times10^3 \text{ kg/rad}, \\ &\delta=6.882\times10^4 \text{ kg cm/rad}. \end{aligned}\right\} \tag{2.20}$$

Spring constants of the shaft α, γ and δ are derived from Eq. (2.11) for the

value $E=2.1\times10^6$ kg/cm^2. The value of k_a is directly measured. The value of M_a is derived from the natural frequency of the flexible pedestal A obtained experimentally. The unsymmetrical rotor with $I_p>I_1>I_2$ is used in our experiments, and hence there are two unstable regions $[\omega_{c31}, \omega_{c32}]$ and $[\omega_{c21}, \omega_{c22}]$. For elimination of the region $[\omega_{c31}, \omega_{c32}]$, the flexible pedestal A which has M_a satisfying Eq. (2.8 a) or k_a satisfying Eq. (2.8 b) must be used.

Several series of response curves in the neighborhood of the major critical speed ω_{c3} are shown in Fig. 2.6, where the rotor is supported with two rigid pedestals at both ends in Experiment I, and in Expriment II-a, b, c, the flexible pedestal A having several values of k_a is used. Throughout Experiments II-a, b, c, weight M_a has nearly the same magnitude. On the other hand, in Experiments III-a, b, c, response curves of which are shown in Fig. 2.7, k_a is common and M_a takes several values.

As shown in Fig. 2.6, in Experiment I the unstable region near the major critical speed ω_{c3} is the rotating speed range of 1518~1697 rpm, hence $(\Delta\omega_{c3})_\infty=$ 179 rpm. When the flexible pedestal having suitable values of k_a and M_a is adopted, the unstable region appearing in the neighborhood of the major critical speed is removed, and the locations of the major critical speeds move to the considerably lower rotating speed side, as shown in Experiment II-a, b and Experiments III-a, b of Figs. 2.6, 2.7.

Although in these figures, only the response curves near the major critical speed ω_{c3} are shown, there is another major critical speed ω_{c2} at a fairly higher rotating speed side shown in Table 2.2, because of $M_a/M\leqq1.25$. Further, experiments are performed in the range of the rotating speed $\omega=170\sim1850$ rpm; no vibration, however, takes place, except for ω_{c3}. The relations between k_a and M_a of Experiments II, III are shown in Fig. 2.3 by symbols ○ and ●. The former ○ means that the unstable region exists, and the latter ● shows that the unstable region can be eliminated. It is seen from Fig. 2.3 that the unstable

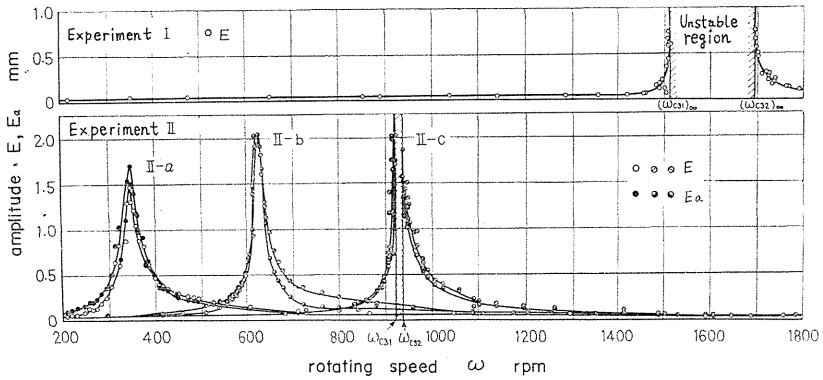

Experiment I ($k_a=\infty$, $M_ag=0$, $l_a=0$)
Experiment II-a ($k_a=11.0$ kg/cm, $M_ag=1.60$ kg, $l_a=65.0$ cm)
Experiment II-b ($k_a=45.1$ kg/cm, $M_ag=1.48$ kg, $l_a=40.7$ cm)
Experiment II-c ($k_a=152.8$ kg/cm, $M_ag=1.36$ kg, $l_a=26.1$ cm)
Dimensions of the shaft system are the same as Eq. (2.20).

FIG. 2.6. Response curves and unstable regions at ω_{c3} (Experiment I, II)

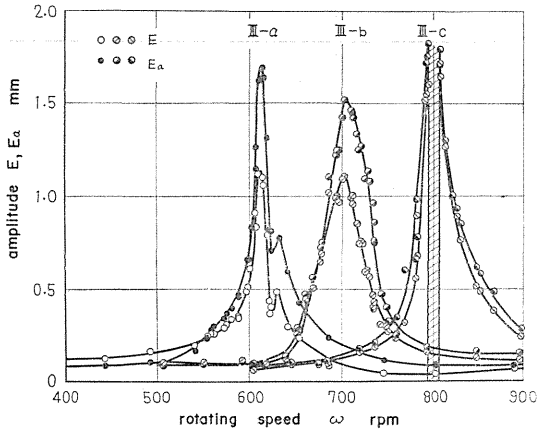

Experiment III-a ($M_a g = 12.20$ kg)
Experiment III-b ($M_a g = 6.60$ kg)
Experiment III-c ($M_a g = 1.40$ kg)
$k_a = 88.90$ kg/cm, $l_a = 31.6$ cm
Dimensions of the shaft system are the same as Eq. (2.20).

FIG. 2.7. Response curves and unstable region at ω_{c3} (Experiment III).

TABLE 2.2. Comparison between Experimental and Analytical Results of Static Unstable Regions (Experiment I, II, III)

Experiment		I	Ⅱ			Ⅲ		
			a	b	c	a	b	c
M_a/M		0	0.164	0.152	0.140	1.252	0.677	0.144
k_a/α		∞	0.0205	0.0839	0.2842	0.1653	0.1653	0.1653
Static unstable region [ω_{c31}, ω_{c32}]	ω_{c31} rpm	1523.9 (1518)	346.9	637.2	959.9 (922)	622.4	709.2	814.0
	ω_{c3} rpm	1642.4 (1607)	348.2 (349)	637.2 (626)	968.9 (930)	622.4 (613)	709.5 (706)	816.4 (800)
	ω_{c32} rpm	1736.0 (1697)	349.6	637.2	976.2 (938)	622.4	709.8	818.3
	$\Delta\omega_{c3}$ rpm	212.1 (179)	2.84 (0)	0.018 (0)	16.35 (16)	0.00002 (0)	0.54 (0)	4.29 (13)
	$(E_a/E)\,\omega_{c31}$	0	1.18	0.945	0.612 (0.849)	0.936	0.856	0.754 (1.13)
	$(E_a/E)\,\omega_{c3}$	0	1.20 (1.16)	0.954 (1.06)	0.635	0.936 (1.51)	0.861 (1.34)	0.765
	$(E_a/E)\,\omega_{c32}$	0	1.21	0.962	0.658 (0.846)	0.936	0.867	0.775 (1.04)
Static unstable region [ω_{c21}, ω_{c22}]	ω_{c21} rpm	∞	5417.4	5818.2	6637.3	2279.9	2906.8	6216.8
	ω_{c2} rpm	∞	5576.4	5960.1	6745.0	2467.1	3097.9	6342.1
	ω_{c22} rpm	∞	5658.3	6033.3	6800.8	2583.6	3206.8	6406.9
	$\Delta\omega_{c2}$ rpm	0	240.9	215.1	163.6	303.7	299.9	190.0

( ): experimental results

regions are eliminated by using M_a and k_a furnished by the point near the curve Eq. (2.8 b) and as the point deviates far from the curve, the width of the unstable region increases, and finally it tends to $(\Delta\omega_{c3})_\infty$.

The calculated values of the major critical speeds ω_{c31}, ω_{c3}, ω_{c32}, ω_{c21}, ω_{c2} and ω_{c22} from Eq. (2.5 b), and the amplitude ratios $(E_a/E)_{\omega_{c31}}$, $(E_a/E)_{\omega_{c3}}$ and $(E_a/E)_{\omega_{c32}}$ derived from the ratio of cofactors A_{13}/A_{11} of the determinant (2.5 b) are shown in Table 2.2. The experimental results are shown in brackets, and they have good agreement with the analytical results.

2.5. Elimination of dynamic unstable vibration

Generally speaking, when the number n of degrees of freedom ($n=4$ in this paper) increases by 2, one static unstable region and $(n/2)$ dynamic unstable regions appear additionally. The relations between the natural frequency p_i, $\bar{p}_i$ and the rotating speed of the shaft ω of unsymmetrical rotor with $I_1>I_2>I_p$ are shown in Fig. 2.8 in which the shaft systems are the same as those used in Experiment I in Fig. 2.6 and III-c in Fig. 2.7 except for the rotor. In Fig. 2.8 (a) and (b), $p-\omega$ diagrams of the case of the rigid pedestal (Experiment I′) and of the case of the flexible one (Experiment III′-c) are shown respectively. Natural frequency p_i (*i.e.* roots of $f=0$) of the symmetrical rotor (with $\Delta I=0$) and $\bar{p}_i=2\omega-p_i$ (*i.e.* roots of $\bar{f}=0$) are shown by full and broken lines respectively, and

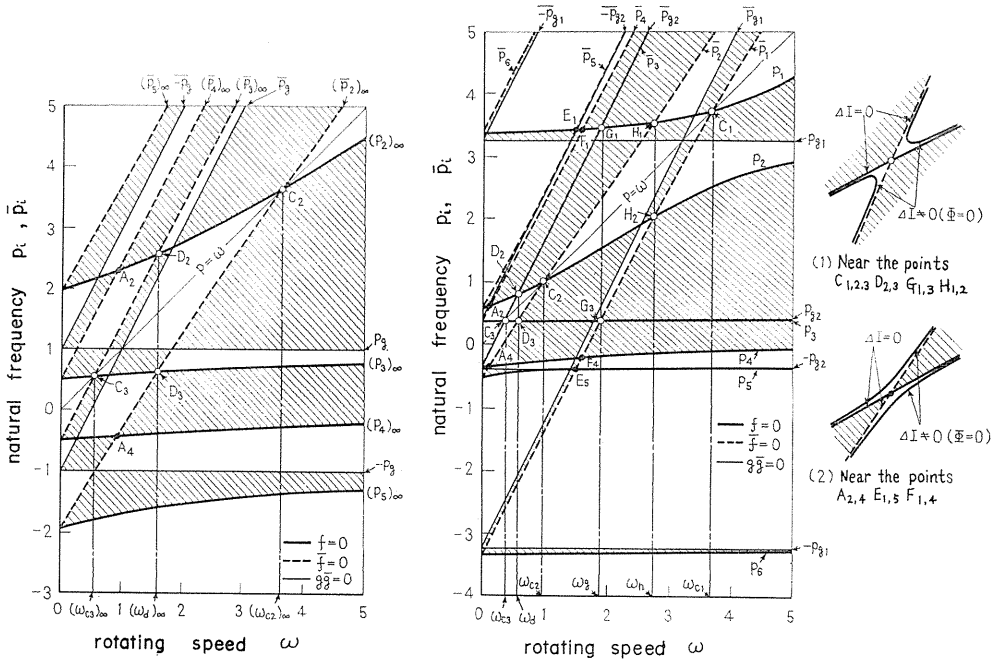

$k_a=\infty$, $M_ag=0$ $\qquad$ $k_a=88.90$ kg/cm, $M_ag=1.40$ kg

(a) Rigid pedestal used, Experiment I′ $\qquad$ (b) Flexible pedestal used, Experiment III′-c

$I_p=0.3725$ kg cm s^2, $I_1=0.5314$ kg cm s^2, $I_2=0.4572$ kg cm s^2, $Mg=11.668$ kg, $\sqrt{a/M}=2030.4$ rpm. Other dimensions are the same as Eq. (2.20).

FIG. 2.8. $f=0$, $\bar{f}=0$ diagram expressed in dimensionless quantities (1.12).

the straight lines $p=\pm p_g$ (roots of $g=0$) and $p=\overline{\pm p_g}=2\omega\mp p_g$ (roots of $\bar{g}=0$) are shown by fine lines. Real roots of Eq. (2.6) can exist only in unhatched regions where the sign of $f\bar{f}$ is the same as that of $g\bar{g}$ as shown in Fig. 2.8. When the unsymmetrical rotor is used, in the neighborhood of intersecting points $C_{1,2,3}$, $D_{2,3}$, $G_{1,3}$ and $H_{1,2}$ of curves $f=0$ and $\bar{f}=0$ shown by symbol ○, there are unstable regions where the root p, $\bar{p}$ can not be shown by a curve because it becomes a complex number[13] in these ranges of ω as shown in Fig. 2.8(b. 1). Meanwhile, in the neighborhood of the points $A_{2,4}$, $E_{1,5}$ and $F_{1,4}$ shown by the symbol ●, there are no unstable regions where the root becomes a real as shown in Fig. 2.8 (b. 2). It is verified, generally speaking, that $g=0$ in Eq. (2.6 b) [or $h=0$ in Eq. (2.6c)] has two positive roots p_{g1}^2 and p_{g2}^2 (or p_{h1}^2 and p_{h2}^2). And further the following relation holds:

$$p_1>p_{g1}\geqq p_2>p_{g2}\geqq p_3>0>p_4>-p_{g2}\geqq p_5>-p_{g1}\geqq p_6 \tag{2.21}$$

because the roots of $f=0$, *i.e.* p_1, p_2, p_3, p_4, p_5 and p_6 tend to $I_p\omega/I$, p_{g1}, p_{g2}, 0, $-p_{g2}$ and $-p_{g1}$, respectively, as ω tends to ∞. Denoting the ultimate value of p_i ($i=2\sim5$) when the rigidity k_a of the pedestal tends to ∞ as $(p_i)_\infty$, we have the relation

$$p_1>(p_2)_\infty>p_2>(p_3)_\infty>p_3>0>p_4>(p_4)_\infty>p_5>(p_5)_\infty>p_6 \tag{2.22}$$

and hence the following relations are derived from the relations (2.21) and (2.22).

$$\left.\begin{aligned}&\omega_{c1}>\omega_h>\omega_g>\omega_{c2}>\omega_d>\omega_{c3}\\&\omega_{c1}>(\omega_{c2})_\infty>\omega_{c2}>(\omega_{c3})_\infty>\omega_{c3}\end{aligned}\right\} \tag{2.23}$$

As is seen from Eq. (2.6 a) the common root p^2 which is independent of ω is also the root of $f=0$, provided that either of two positive roots p^2 of two quadratic equations $g=0$ and $h=0$, which is independent of ω, is a common root. Accordingly the relation $g=0$ holds at the intersecting point of $f=0$ and $\bar{f}=0$, and hence no unstable region arises in spite of $\Delta I\neq 0$.

2.5.1. Case of two common roots

When both two positive roots p^2 of equations $g=0$ and $h=0$ are common roots, all ratios between coefficients of the same order with respect to p in Eq. (2.6 b) and Eq. (2.6 c) become equal. If

$$a_{12}=a_{23}=0 \tag{2.24}$$

all the other unstable regions vanish except the unstable region in the neighborhood of ω_{c1}.

2.5.2. Case of single common root

When either of two positive roots p^2 of eqations $g=0$ and $h=0$ is common, the common root p^2 is derived from (2.6 b)$-a_{22}\times$(2.6 c)$=0$ as follows:

$$p^2=\left(\frac{a_{12}^2}{Ma}+\frac{a_{23}^2}{M}\right)\Big/\left\{a_{12}\begin{vmatrix}a_{12}&a_{23}\\a_{13}&a_{33}\end{vmatrix}+a_{23}\begin{vmatrix}a_{11}&a_{13}\\a_{12}&a_{23}\end{vmatrix}\right\} \tag{2.25}$$

Inserting the value p^2 denoted by Eq. (2.25) into Eq. (2.6 c), roots of the quadratic

equation with respect to M_a/M coincide with Eq. (2.8), and substituting Eq. (2.8) into Eq. (2.25), p^2 coincides with Eq. (2.9) and the amplitude ratio E_a/E coincides with Eq. (2.10), and also $F/E=0$ yields easily.

In case that the relation $a_{12}/a_{23}<0$ (*i.e.*, $E_a/E>0$) holds, the unstable regions in the neighborhood of the rotating speeds ω_{c3}, ω_d and ω_g which are the cross points of the two straight lines $p_3=p_{g2}$ and $p_5=-p_{g2}$ and the curves $\bar{p}_{3,2,1}$ can be eliminated completely, provided that the value M_a/M calculated from Eq. (2.8) is adopted. And in case that the relation $a_{12}/a_{23}>0$ (*i.e.*, $E_a/E<0$) holds, the value M_a/M calculated from Eq. (2.8) is not always positive. If the value M_a/M is positive, the unstable regions in the neighborhood of the rotating speeds ω_d, ω_{c2} and ω_h are eliminated completely, which are the cross points of the two straight lines $p_2=p_{g1}$ and $p_6=-p_{g1}$ and the curves $\bar{p}_{3.2,1}$. And further adoption of suitable values of M_a and k_a can result in that ω_{c2} takes place at the adequately higher rotating speed than $(\omega_{c3})_\infty$. Accordingly, as shown in Fig. 2.6, the system is thoroughly stable over the rotating speed range $\omega=0\sim(\omega_{c3})_\infty\sim\omega_{c2}$. The exact solutions of the unstable vibrations in the neighborhood of ω_{c3}, ω_d, ω_{c2}, ω_g, ω_h and ω_{c1} in Experiment III′-a, b, c are shown in Table 2.3. In this experiment, the value M_a/M derived from Eq. (2.8 a) is 1.252.

As the relation $I_p\fallingdotseq I_1+I_2$ holds in our experimental apparatus, only a static unstable region $(\omega_{c3})_\infty$ appears in Experiment I, where the shaft is supported by rigid pedestals at both shaft ends. In Experiment II and III where degree-of-freedom increases by two, there are two static unstable regions near the rotating speeds ω_{c3}, ω_{c2}, and also a dynamic unstable region in the neighborhood ω_d where the relations $\omega_{c2}>\omega_d>\omega_{c3}$ and $P_2+P_3=2\,\omega_d$ hold, and where two vibrations of frequency P_2, P_3 build up exponentially at the same time[24]. In Fig. 2.9 and 2.10, the negative damping coefficient m and the frequency P_3 are shown for the rotating speed of the shaft ω, where the positive value m represents the degree of instability of dynamic unstable vibrations. Experimental results are expressed by circular marks, and exact solutions derived from $\Phi=0$, *i.e.*, Eq. (2.6) are shown by full lines. In Table 2.4 both analytical and experimental results of width of unstable regions, maximum value of m, *i.e.*, $m_{\max}$ are given. The analytical values show good coincidence with the experimental results except for the values m. Values m obtained from experiments are smaller than calculated ones. Especially in Experiment II-b, III-a and III-b with small values of m, the dynamic unstable vibrations do not take place in experiments, because of somewhat large damping effect of a chuck between the flexible pedestal A and the rigid one C. In Experiments III-a and II-b, conditions for elimination of the width of static unstable region $\Delta\omega_{c3}$, *i.e.*, Eq. (2.8 a) and Eq. (2.8 b), are nearly satisfied. In these experiments it is interesting that the dynamic unstable regions $\Delta\omega_d$ in the neighborhood of rotating speed ω_d are eliminated simultaneously.

2.6. Conclusions

Conclusions obtained in this chapter are as follows:

(1) The unstable regions in the neighborhood of the major critical speed $(\omega_{c3})_\infty$ supported by rigid pedestals at both shaft ends are almost eliminated or completely removed by using an appropriate flexible pedestal at one shaft end side (or by putting an additional mass M_s at the suitable position of the shaft).

TABLE 2.3. Comparison between Experimental and Analytical Results of Dynamic Unstable Regions (Experiment I, II, III)

Experiment		I	II			III		
			a	b	c	a	b	c
M_a/M		0	0.164	0.152	0.140	1.252	0.677	0.144
k_a/α		∞	0.0205	0.0839	0.2842	0.1653	0.1653	0.1653
Dynamic unstable region $[\omega_{d1}, \omega_{d2}]$	ω_{d1} rpm	—	1934.0 (1888)	2538.2	3328.1 (3237)	1277.9	1552.6	2935.1 (2846)
	ω_{d2} rpm	—	2038.7 (2002)	2543.9	3437.0 (3347)	1277.9	1569.4	3003.7 (2895)
	$\Delta\omega_d$ rpm	—	104.7 (114)	5.77 (0)	108.9 (110)	0.0003 (0)	16.83 (0)	68.63 (49)
	$m_{\max}$ rad/sec	—	1.908 (1.08)	0.128 (0)	3.217 (0.31)	0.0055 (0)	0.571 (0)	1.771 (0.24)

( ): experimental values

TABLE 2.4. Analytical Results of Static and Dynamic Unstable Regions (Experiment III')

Experiment		III'		
		a	b	c
M_a/M		1.046	0.566	0.120
k_a/α		0.1653	0.1653	0.1653
Static unstable region $[\omega_{c31}, \omega_{c32}]$	ω_{c31} rpm	594.5	664.0	735.7
	ω_{c3} rpm	594.6	664.5	738.3
	ω_{c32} rpm	594.6	664.9	740.6
	$\Delta\omega_{c3}$ rpm	0.036	0.91	4.82
Dynamic unstable region $[\omega_{d1}, \omega_{d2}]$	ω_{d1} rpm	883.5	1069.3	1256.2
	ω_{d2} rpm	885.8	1083.9	1300.0
	$\Delta\omega_d$ rpm	2.35	14.63	43.79
	$m_{\max}$ rad/sec	0.106	0.587	1.647
Static unstable region $[\omega_{c21}, \omega_{c22}]$	ω_{c21} rpm	1201.4	1339.0	1685.3
	ω_{c2} rpm	1308.2	1493.8	2028.0
	ω_{c22} rpm	1439.0	1701.1	2712.1
	$\Delta\omega_{c2}$ rpm	237.6	362.1	1026.8
Dynamic unstable region $[\omega_{g1}, \omega_{g2}]$	ω_{g1} rpm	2205.5	2455.7	3846.9
	ω_{g2} rpm	2208.0	2466.3	3859.6
	$\Delta\omega_g$ rpm	2.53	10.60	12.68
	$m_{\max}$ rad/sec	0.166	0.506	0.645
Dynamic unstable region $[\omega_{h1}, \omega_{h2}]$	ω_{h1} rpm	2709.8	3082.7	5291.1
	ω_{h2} rpm	3174.1	3653.0	6258.9
	$\Delta\omega_h$ rpm	464.3	570.3	967.5
	$m_{\max}$ rad/sec	17.32	20.98	33.32
Static unstable region $[\omega_{c11}, \omega_{c12}]$	ω_{c11} rpm	4197.8	4585.4	7138.9
	ω_{c1} rpm	4890.9	5211.0	7500.3
	ω_{c12} rpm	7116.3	7319.2	8949.2
	$\Delta\omega_{c1}$ rpm	2918.5	2733.8	1810.3

I_p=0.3725 kg cm s^2, I_1=0.5314 kg cm s^2, I_2=0.4572 kg cm s^2, Mg=11.668 kg. Other dimensions are the same as Experiment III (Fig. 2.7).

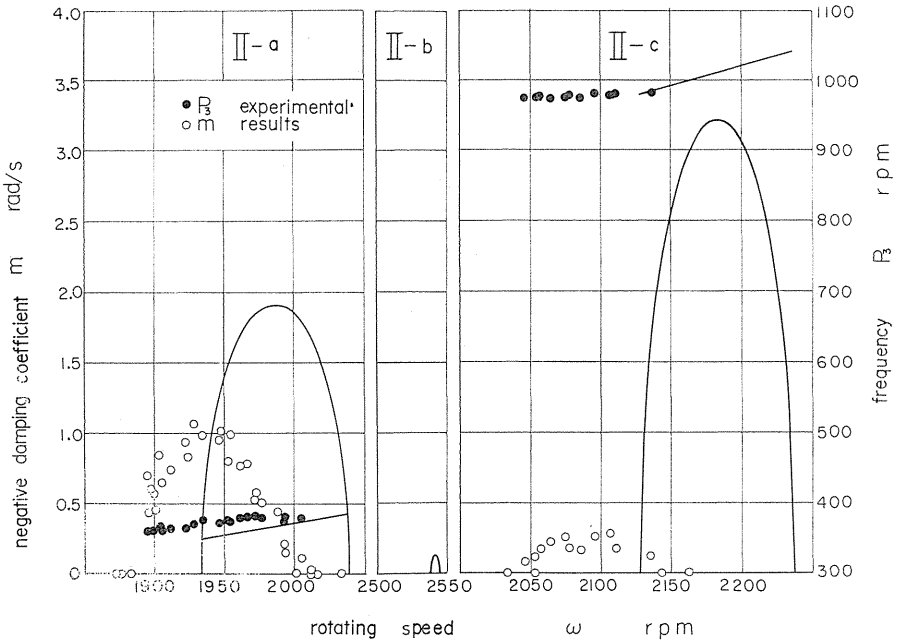

FIG. 2.9. m, $P_3-\omega$ diagram (Experiment II, ω_d).

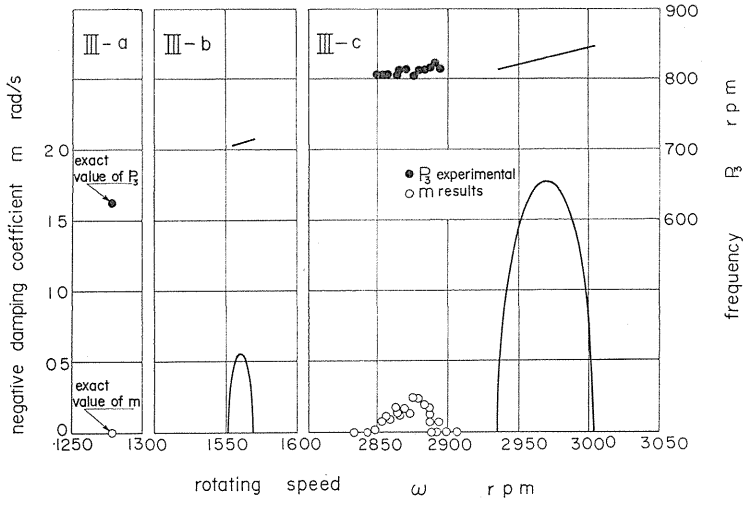

FIG. 2.10. m, $P_3-\omega$ diagram (Experiment III, ω_d).

(2) Dynamic effect of the method mentioned here is different from that of dynamic absorber used in recti-liner vibratory system: that is, the modification of mode of vibrations due to the inertia force of the mass of flexible pedestal or the additional mass on the shaft results in elimination of influence of asymmetry of the rotor.

(3) Although the adoption of the methods mentioned here results in a new static unstable region because of an increase of two-degree-of-freedom, it can be expected from adoption of appropriate values of k_a and M_a (or M_s) that a new unstable region appears at a higher rotating speed than $(\omega_{c3})_\infty$.

(4) The method mentioned here is useful for elimination of the unstable regions in the neighborhood ω_{c3}, ω_d and ω_g (in case $a_{12}/a_{23}<0$, *i.e.*, $E_a/E>0$), or ω_{c2}, ω_d and ω_h (in case $a_{12}/a_{23}>0$, *i.e.*, $E_a/E<0$). But it cannot be applied to the rotating shaft system with unsymmetrical stiffness.

(5) Experiments using the most popular type of rotating shaft system show that the experimental results in regard to the position of the major critical speed, width of unstable region and amplitude ratio between the flexible pedestal and the rotor agree with the analytical results.

Chapter 3. Unstable Vibrations Induced by Rotationally Unsymmetric Inertia and Stiffness Properties[22]

3.1. Introduction

It has been already mentioned that there exist two kinds of unstable region [10)13)] in the system having such a rotor with unsymmetric moment of inertia and in the system having such a shaft with unequal stiffness in lateral deflection, and that they are affected remarkably by the combined orientation angle ζ between unsymmetrical rotor and flat shaft[18)~20)].

These two unstable regions are called "static unstable region" and "dynamic unstable region", and in the former an unstable vibration grows according as $e^{mt}\cos\omega t$, and in the latter it grows according as $e^{mt}(A\cos P_1 t+B\cos P_2 t)$ where the relation $P_1+P_2=2\omega$ holds. Mathematically speaking, when a free vibration observed from the coordinate rotating at an angular velocity ω is expressed in the form of e^{st}, one is statically unstable in the vicinity of $\omega=\omega_c$ where the eigenvalue s has a real number $m>0$, and the other is dynamically unstable near $\omega=\omega_d$ where s is a conjugate complex $s=m\pm ip'$. By solving the characteristic equation we can find out the position and width of the unstable domain and the exact value of m and p' of the root s, but can not obtain the whole nature of the unstable vibrations. On the other hand, using the approximate solution[12)13)15)18)20)] obtained by applying the Taylor's expansion theorem to the characteristic equation near the rotating speed ω_c or ω_d, we can easily obtain the approximate values of the unstable vibrations. Moreover the obtained values fairly coincide with the exact values, and therefore this approximate method is satisfactory for practical uses. It is important to obtain the quantitative values related to unstable vibrations, but it is also necessary to elucidate the mechanism introducing energy into the shaft system and the physical condition that causes self-excited vibrations. This chapter deals with the mechanism of input energy into system and the physical meaning of the system of flat shaft having an unsymmetrical rotor.

3.2. Static unstable vibration in the vicinity of the major critical speed

In Fig. 1.1, the terms of higher order than θ^3 being neglected, the sum of kinetic energy T of the translation and rotation of an unsymmetrical rotor is derived from Eq. (1.1), $\Theta=\varphi+\psi=\omega t-\pi/2$ and $\dot{\Theta}=\omega$ as follows:

$$2T = M(\dot{x}^2 + \dot{y}^2) + I_p\omega_{Z1}^2 + I_1\omega_{Y2}^2 + I_2\omega_{X2}^2$$
$$= M(\dot{r}^2 + \dot{\phi}^2 r^2) + I_p(\omega^2 - \omega\dot{\varphi}\theta^2) + I(\dot{\theta}^2 + \dot{\varphi}^2\theta^2) + \Delta I\{(\dot{\theta}^2 - \dot{\varphi}^2\theta^2)\cos 2\psi + 2\dot{\varphi}\dot{\theta}\theta \sin 2\psi\} \tag{3.1}$$

The potential energy V stored in the flat shaft is given as follows:

$$2V = \{\alpha + \Delta\alpha \cos 2(\psi + \zeta + \xi)\}r^2 + 2\{\gamma \cos\xi + \Delta\gamma \cos(2\psi + 2\zeta + \xi)\}r\theta$$
$$+ \{\delta + \Delta\delta \cos 2(\psi + \zeta)\}\theta^2 \tag{3.2}$$

3.2.1. Dynamical equilibrium of force and moment, and torque at the shaft end

Now we consider the statically unstable vibration in which the deflection of the shaft gradually grows up and the deflection curve whirls at the angular velocity of $\dot{\phi} = \dot{\varphi} = \omega$ in the vicinity of the major critical speed ω_c. As the oG component of the rate of change of momentum about G is equal to the oG component of the restoring force of flat shaft, the following equation holds.

$$-M\ddot{r} + M\omega^2 r - \{\alpha + \Delta\alpha \cos 2(\psi + \zeta + \xi)\}r - \{\gamma \cos\xi + \Delta\gamma \cos(2\psi + 2\zeta + \xi)\}\theta = 0 \tag{3.3}$$

From the dynamic equilibrium of the forces in the direction GT perpendicular to oG,

$$-2M\omega\dot{r} - \Delta\alpha \sin 2(\psi + \zeta + \xi)\cdot r - \{\gamma \sin\xi + \Delta\gamma \sin(2\psi + 2\zeta + \xi)\}\theta = 0 \tag{3.4}$$

The first term in Eq. (3.4) is called "Coriolis' force". Also as the GL component of the rate of change of angular momentum about G is equal to the GL component of the restoring moment of shaft, the following holds.

$$(2I - I_p)\omega\dot{\theta} + \Delta I(\ddot{\theta} + \omega^2\theta)\sin 2\psi - \{\gamma \sin\xi - \Delta\gamma \sin(2\psi + 2\zeta + \xi)\}r$$
$$+ \Delta\delta \sin 2(\psi + \zeta)\cdot\theta = 0 \tag{3.5}$$

The first term agrees with "Coriolis' moment" which is the integrated moment about the axis GL due to the Coriolis' force over the whole rotor. The GK component of the rate of change of angular momentum is the same with the GK component of the restoring moment, and, therefore, we have

$$-(I + \Delta I\cos 2\psi)\ddot{\theta} - (I_p - I + \Delta I\cos 2\psi)\omega^2\theta$$
$$- \{\gamma \cos\xi + \Delta\gamma \cos(2\psi + 2\zeta + \xi)\}r - \{\delta + \Delta\delta \cos 2(\psi + \zeta)\}\theta = 0 \tag{3.6}$$

In addition, oz component of the rate of change of angular momentum is the sum of the moment about oz of $2M\omega\dot{r}$ which is the GT component of the rate of momentum change about G, and the GZ component of the rate of change of angular momentum about G. However, since the restoring moment of the shaft causing the change of angular momentum about oz does not exist, it is necessary to apply the torque T_r to shaft end from external source.

$$T_r = 2M\omega\dot{r}r + 2(I - I_p)\omega\dot{\theta}\theta + \Delta I\{(\dot{\theta}^2 + \ddot{\theta}\theta)\sin 2\psi - 2\omega\dot{\theta}\theta\cos 2\psi\} \tag{3.7}$$

The work done by torque applied to the shaft from external source in unit time is the same as the increasing rate of total energy of the system, and, therefore,

the following equation holds.

$$\omega T_r = \frac{d}{dt}(T+V) \tag{3.8}$$

It should be noted that r and θ vary with time exponentially as follows:

$$r = r_0 e^{mt}, \quad \theta = \theta_0 e^{mt} \tag{3.9}$$

where m is the negative damping coefficient.

3.2.2. Exact solution of statically unstable vibration (Case of flat shaft)

We have treated so far the particular case, *i.e.* an unsymmetrical rotor combined with a flat shaft. We are now going to treat the most simple case in which there is a symmetrical rotor mounted at the middle point of flat shaft supported with ball bearings on both ends. In this case $\theta=\gamma=\Delta r=\Delta I=\xi=0$ can be assumed, and Eqs. (3.3) and (3.4) expressing the dynamic equilibrium of force in the direction oG and GT are shown as follows:

$$-M\ddot{r}+M\omega^2 r-\{\alpha+\Delta\alpha\cos 2(\psi+\zeta)\}r=0 \tag{3.3 a}$$

$$-2M\omega\dot{r}-\Delta\alpha\sin 2(\psi+\zeta)\cdot r=0 \tag{3.4 a}$$

By substituting Eq. (3.9) into Eqs. (3.4 a) and (3.3 a), m and ω are derived as follows:

$$m=-\Delta\alpha\sin 2(\psi+\zeta)/(2M\omega) \tag{3.10}$$

$$\omega^2=m^2+\{\alpha+\Delta\alpha\cos 2(\psi+\zeta)\}/M \tag{3.11}$$

By eliminating $\psi+\zeta$ from Eqs. (3.10) and (3.11), we have the relation of m and ω as follows:

$$m^4+2(\omega^2+\alpha/M)m^2+(\omega^2-\alpha/M)^2-(\Delta\alpha/M)^2=0 \tag{3.12}$$

The calculated results from Eq. (3.12) are shown by full line in Fig. 3.1, parameter being taken as $\Delta\alpha/\alpha$. To eliminate $\Delta\alpha$ in Eqs. (3.10) and (3.11) gives the following relation between m and ω.

$$m^2-2\omega\cot 2(\psi+\zeta)\cdot m+(\alpha/M-\omega^2)=0 \tag{3.13}$$

And also the values of Eq. (3.13) are shown by broken line with parameter $\psi+\zeta$ in Fig. 3.1. The vertical double dotted chain line shows the major critical speed $\omega_c=\sqrt{\alpha/M}$ in the case of $\Delta\alpha=0$. There are two roots of m in Eq. (3.12), and the one is positive and the other negative. From Eq. (3.10), m takes positive or negative value according to negative or positive value of $\sin 2(\psi+\zeta)$, and only the former case (*i.e.*, $m>0$) is shown in Fig. 3.1. Explaining physically, when the flat shaft is held by the angle $\psi+\zeta=90°\sim180°$, the total energy of the system is increased because of the existence of two components of the restoring force of flat shaft, *i.e.*, not only Go component, but also tangential GT component $-\Delta\alpha\sin 2(\psi+\zeta)\cdot r>0$. Coriolis' force $-2M\omega\dot{r}$ in GT direction is generated as the reaction that the restoring force accelerates the rotor in GT direction. In order to keep the speed of rotor constant, it is necessary to apply the torque

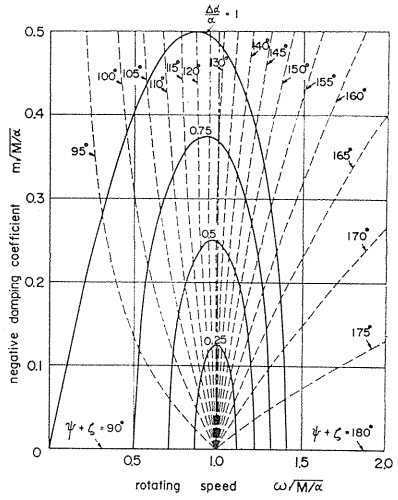

FIG. 3.1. Relation between m and ω (exact solution of flat shaft when $\gamma=\Delta\gamma=0$ and $\Delta\alpha/\alpha=0\sim1$).

Tr (the first term in Eq. (3.7)) against that due to Goriolis' force $-2M\omega\dot{r}r$ about oz. By using Eq. (3.11) the power $\omega Tr=2M\omega^2r^2m$ applied to the shaft end is assumed to coincide with the increasing rate of the total energy $\frac{d}{dt}(T+V)=\{M(m^2+\omega^2)+\alpha+\Delta\alpha\cos 2(\psi+\zeta)\}r^2m$, and it is evident that Eq. (3.8) holds. The critical speed $\omega=\sqrt{(\alpha\pm\Delta\alpha)/M}$ at the limit of unstable region is derived by putting $m=0$, or $\psi+\zeta=0°$, 90°, respectively, in Eq. (3.11). Putting $\partial(m^2)/\partial(\omega^2)=0$ in Eq. (3.12), we have the maximum value of negative damping coefficient $m_{\max}$ and the rotating speed ω when m is maximum in the following forms.

$$m_{\max}=\frac{\Delta\alpha}{2\alpha}\sqrt{\frac{\alpha}{M}},\quad \omega=\sqrt{1-\left(\frac{\Delta\alpha}{2\alpha}\right)^2}\sqrt{\frac{\alpha}{M}} \tag{3.12 a}$$

3.2.3. Exact solution of static unstable vibration (Case of unsymmetrical rotor)

Now we consider the system in which an unsymmetrical rotor is mounted at the middle point of round shaft, and inclination θ and deflection r are not co-related with each other. In this case, $r=\gamma=\Delta\alpha=\Delta\gamma=\Delta\delta=\xi=\zeta=0$ holds, and Eqs. (3.5) and (3.6) are given as

$$(2I-I_p)\omega\dot{\theta}+\Delta I(\ddot{\theta}+\omega^2\theta)\sin 2\psi=0 \tag{3.5 a}$$

$$-(I+\Delta I\cos 2\psi)\ddot{\theta}-(I_p-I+\Delta I\cos 2\psi)\omega^2\theta-\delta\theta=0 \tag{3.6 a}$$

Substituting Eq. (3.9) into Eq. (3.5 a) yields

$$\sin 2\psi=-(2I-I_p)\omega m/\{\Delta I(m^2+\omega^2)\} \tag{3.14}$$

As $2I-I_p>0$ holds generally for any rotor, we have $m\lesseqgtr 0$ according to $\sin 2\psi\gtreqless 0$. From Eq. (3.14) m is derived as follows:

$$m=-\frac{(2I-I_p)\omega-\omega\sqrt{(2I-I_p)^2-(2\Delta I\sin 2\psi)^2}}{2\Delta I\sin 2\psi}\fallingdotseq-\frac{\Delta I\omega\sin 2\psi}{(2I-I_p)} \tag{3.14 a}$$

When ω is kept constant, provided that θ is constant, *i.e.* $m=\dot{\theta}=\ddot{\theta}=0$, the GK component of gyroscopic moment $-(I_p-I+\Delta I\cos 2\psi)\omega^2\theta$ is balanced with the restoring moment of the shaft $-\delta\theta$, but the GL component $\Delta I\omega^2\sin 2\psi\cdot\theta<0$ increases the whirling motion of rotor, and, as the results, the energy of shaft system is raised. Consequently, "Coriolis' moment" $(2I-I_p)\omega\dot{\theta}>0$ arises as the reaction of the GL component of the gyroscopic moment which is the integrated moment about G due to the centrifugal force. By substituting Eq. (3.9) into Eq. (3.6 a), the equation

$$(I+\Delta I\cos 2\psi)m^2+\{\delta+(I_p-I+\Delta I\cos 2\psi)\omega^2\}=0 \tag{3.15}$$

is derived. Eliminating ψ or ΔI from Eq. (3.14) and (3.15) gives the following $m-\omega$ relations[10].

$$(I+\Delta I)(I-\Delta I)\,m^4+[2I\{\delta+(I_p-I)\,\omega^2\}+(2I-I_p)^2\omega^2-2(\Delta I)^2\omega^2]m^2 + \{\delta+(I_p-I-\Delta I)\,\omega^2\}\{\delta+(I_p-I+\Delta I)\,\omega^2\}=0 \quad (3.16)$$

$$Im^2-(2I-I_p)\,\omega\cot 2\psi\cdot m+\{\delta+(I_p-I)\,\omega^2\}=0 \quad (3.17)$$

The torque T_r (the 2nd and 3rd terms in Eq. (3.7)) applied to shaft end from external source becomes $\omega T_r=2\omega\theta^2 m\{(I-\Delta I\cos 2\psi-I_p)\,\omega+\Delta Im\sin 2\psi\}$. This value ωT_r also agrees with the increasing rate of the total energy by the use of Eq. (3.15). The critical speed of unstable region is derived by putting $\psi=0°$, 90° in Eq. (3.15) as $\omega=\sqrt{\delta/(I\mp\Delta I-I_p)}$. Rearranging Eq. (3.16), we have a quadratic equation in $m^2_{\max}$ derived from the condition of ω having equal roots.

$$I_p^2(2I-I_p)^2m^4_{\max}+4\delta(2I-I_p)\{(3I-I_p)\,I_p-2I^2+2(\Delta I)^2\}\,m^2_{\max}+(2\delta\Delta I)^2=0 \quad (3.11\,a)$$

The value of ω having $m_{\max}$ is derived from $\partial(m^2)/\partial(\omega^2)=0$ as follows:

$$\omega^2=\frac{2\delta(I-I_p)-\{(I-I_p)^2+I^2-2(\Delta I)^2\}\,m^2_{\max}}{2\{(I-I_p)^2-(\Delta I)^2\}} \quad (3.16\,a)$$

In Fig. 3.2 the calculated values of Eqs. (3.16) and (3.17) are shown with full and broken lines, respectively. And the vertical double-dotted chain line is the major critical speed $\omega_c=\sqrt{\delta/(I-I_p)}$ in case of $\Delta I=0$.

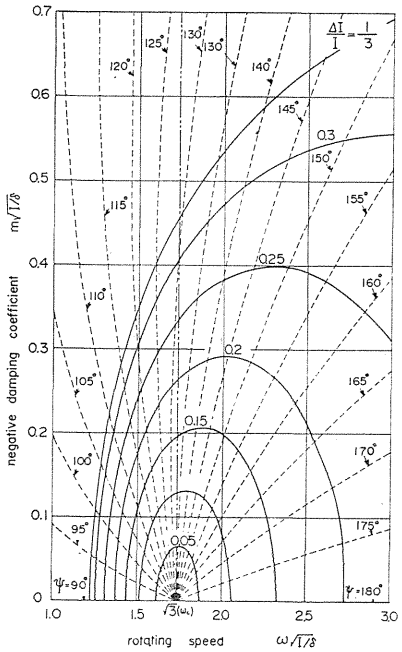

FIG. 3.2. Relation between m and ω (exact solution of unsymmetrical rotor when $I_p/I=2/3$ and $\Delta I/I=0\sim1/3$).

3.2.4. Exact and approximate solutions of static unstable vibration (Case of an unsymmetrical rotor mounted on a flat shaft)

By substituting Eq. (3.9) into Eqs. (3.3), (3.4), (3.5) and (3.6), we obtain three equations containing unknown values ξ, θ/r, m, ω having ψ as parameter. Eq. (3.3 b) is derived from Eq. (3.3).

$$\omega^2 - m^2 = A(\xi,\ \theta/r) \tag{3.3 b}$$

Eliminating $m\omega$ from Eqs. (3.4) and (3.5) gives Eq. (3.4 b).

$$\omega^2 + m^2 = B(\xi,\ \theta/r) \tag{3.4 b}$$

And Eq. (3.6) becomes as follows:

$$\omega^2 + Cm^2 = D(\xi,\ \theta/r) \tag{3.6 b}$$

where C is determined only by ψ, and A, B, and D are determined from ψ, ξ and θ/r. By eliminating m^2 and ω^2 from the above three equations, a quadratic equation in term of θ/r is derived. Since the unknown value ξ is included in the coefficients of the quadratic equation, we must determine the exact value of ξ which satisfies Eq. (3.4).

The calculated results by the use of dimensions of shaft system in Chapter 1, *i.e.*, $Mg=10.433$ kg, $I_p=2.179$ kg cm s^2, $I_1=1.426$ kg cm s^2, $I_2=0.761$ kg cm s^2, $\alpha \pm \Delta\alpha = (3.3617 \pm 0.1945) \times 10^2$ kg/cm, $\gamma \pm \Delta\gamma = -(3.5773 \pm 0.1838) \times 10^3$ kg/rad, $\delta \pm \Delta\delta = (6.2036 \pm 0.4258) \times 10^4$ kg cm/rad, $\omega_c = 1228.8$ rpm, are shown in Fig. 3.3. The exact solutions of ξ for $\psi = 0° \sim 180°$ are shown in Fig. 3.3 (a). They are shown by the marks of ⊘ ($\zeta = 0°$), ⊗ ($\zeta = 45°$) and ⦸ ($\zeta = 90°$) in the case that $\Delta I \neq 0$; $\Delta\alpha$, $\Delta\gamma$, and $\Delta\delta \neq 0$ hold, by the mark ● when $\Delta I \neq 0$; $\Delta\alpha = \Delta\gamma = \Delta\delta = 0$, and by the mark ○ when $\Delta I = 0$; $\Delta\alpha$, $\Delta\gamma$, $\Delta\delta \neq 0$, and $\zeta = 0°$. We know that the inequality in inertia gives larger effect on ξ than that of inequality in stiffness. And the value of ξ is very small when rotating inequality is small. Using the exact solution of ξ in Fig. 3.3 (a), θ/r is derived as shown in Fig. 3.3 (b). By substituting ξ and θ/r into Eq. (3.3 b) and (3.4 b), we have the result of ω and m as shown in Fig. 3.3 (b) and 3.3 (c), respectively. From Fig. 3.3 (b) and 3.3 (c), the relation between m and ω is obtained as shown in Fig. 3.3 (d). Exact solutions of m agree with the positive real part calculated from the characteristic equation[20] which is obtained by substituting Eq. (3.25) into Eq. (3.24).

As the combined effect of the asymmetry in rotor and inequality in shaft is not made clear by the aforementioned method, approximate treatment is given here by adding a suitable constraint to the shaft system. The shaft end torque T_r required to keep the shaft at a constant angular velocity ω under the constraint of $\xi = m = 0$, which holds in case without rotating inequality, is given as a generalized force with respect to ψ, by using Lagrange's equation of motion

$$T_r = \frac{d}{dt}\left(\frac{\partial T}{\partial \dot{\psi}}\right) - \frac{\partial T}{\partial \psi} + \frac{\partial V}{\partial \psi} \tag{3.18}$$

Substituting T and V obtained by putting $\dot{\theta} = \dot{\psi} = \omega$ and $\xi = m = 0$ in Eqs. (3.1) and (3.2) into Eq. (3.18), we have

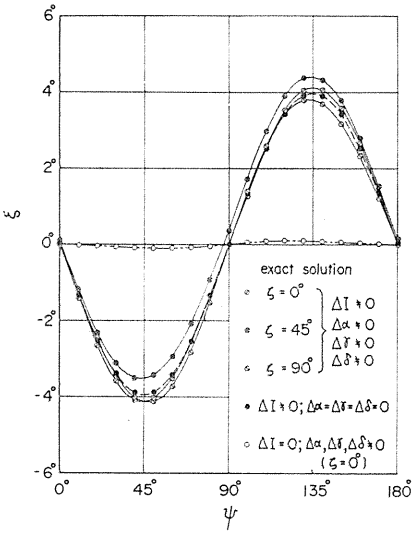

(a) Relation between ξ and ψ (exact solution)

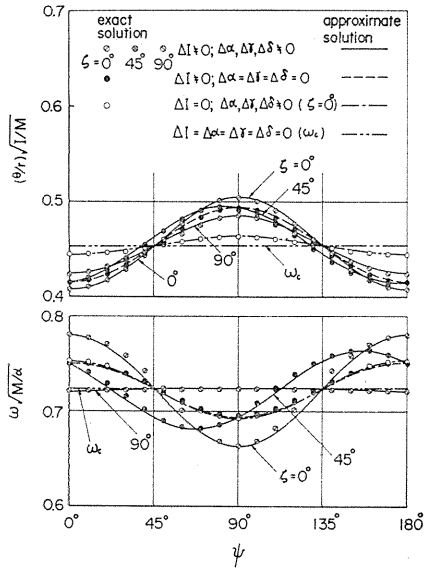

(b) Relation between ω, θ/r and ψ (exact and approximate solution)

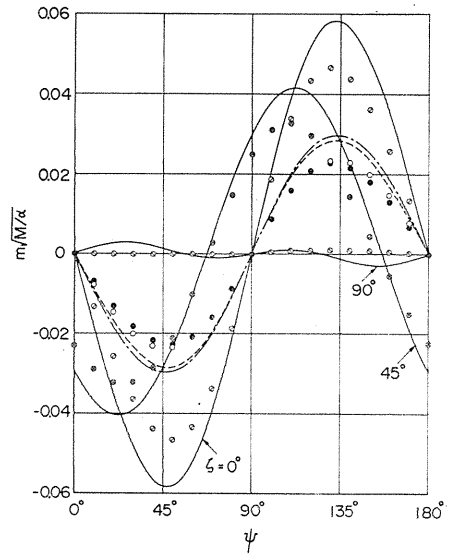

(c) Relation between m and ψ (exact and approximate solution)

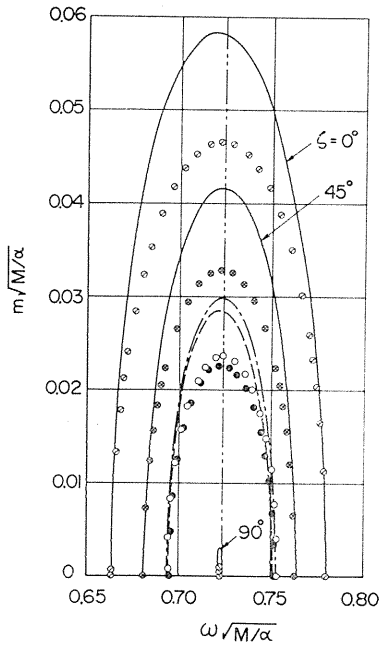

(d) Relation between m and ω (exact and approximate solution)

FIG. 3.3. Case of flat shaft having an unsymmetrical rotor (near major critical speed ω_c).

$$T_r = -\Delta I\omega^2\theta^2 \sin 2\psi - (\Delta\alpha r^2 + 2\,\Delta\gamma r\theta + \Delta\delta\theta^2)\sin 2(\psi+\zeta) \tag{3.19}$$

By equating the amplitude ratios θ/r obtained by putting $\xi=m=0$ in Eqs. (3.3) and (3.6), the following is resulted.

$$-\frac{\theta}{r} = \frac{\alpha + \Delta\alpha\cos 2(\psi+\zeta) - M\omega^2}{\gamma+\Delta\gamma\cos 2(\psi+\zeta)} = \frac{\gamma+\Delta\gamma\cos 2(\psi+\zeta)}{\delta+\Delta\delta\cos 2(\psi+\zeta)+(I_p-I+\Delta I\cos 2\psi)\omega^2} \tag{3.20}$$

When the angles ψ and ξ are given, the values of ω and θ/r are determined. The second term $(\Delta\alpha r^2+2\,\Delta\gamma r\theta+\Delta\delta\theta^2)$ in Eq. (3.19) is positive and the absolute value of T_r of Eq. (3.19) takes the maximum and the minimum value at $\zeta=0°$ and $\zeta=90°$, respectively. By combining unsymmetrical rotor with flat shaft at $\zeta=90°$ and choosing the shape and dimensions of the rotor and shaft so that the relation $\Delta\alpha+2\,\Delta\gamma(\theta/r)+\Delta\delta(\theta/r)^2=\Delta I\omega^2(\theta/r)^2$ holds, the unstable vibration in the vicinity of $\omega=\omega_c$ is eliminated. The effect of ΔI becomes maximum at $\psi=135°$, and also those of $\Delta\alpha$, $\Delta\gamma$ and $\Delta\delta$ become maximum at $\psi+\zeta=135°$. The approximate values of θ/r and ω given by Eq. (3.20) are shown in Fig. 3.3 (b), but it is found, in general, that there is hardly any difference between the approximate value and the exact solution calculated by $\xi\fallingdotseq 0°$. Approximate solutions are shown by full line (when $\Delta I\fallingdotseq 0$; $\Delta\alpha$, $\Delta\gamma$, $\Delta\delta\fallingdotseq 0$), by broken line (when $\Delta I\fallingdotseq 0$; $\Delta\alpha=\Delta\gamma=\Delta\delta=0$), by single dotted chain line (when $\Delta I=0$; $\Delta\alpha$, $\Delta\gamma$, $\Delta\delta\fallingdotseq 0$, $\zeta=0°$), and by double dotted chain line (when $\Delta I=\Delta\alpha=\Delta\gamma=\Delta\delta=0$), respectively. While the condition of $\xi=0$ is kept, by assuming that the work ωT_r $(\xi=m=0)$ applied to the shaft end per unit time is nearly equal to the increasing rate of the total energy in the shaft system $(\xi=0°,\ m\fallingdotseq 0)$, the following cubic equation in m is obtained by the use of Eqs. (3.1), (3.2), and (3.8).

$$A_3m^3 + A_2m^2 + A_1m + A_0 = 0 \tag{3.21}$$

where

$$\left.\begin{aligned} A_3 &= M + (I + \Delta I\cos 2\psi)(\theta/r)^2 \\ A_2 &= 2\,\Delta I\omega\sin 2\psi\cdot(\theta/r)^2 \\ A_1 &= M\omega^2 + \alpha + \Delta\alpha\cos 2(\psi+\zeta) + 2\{\gamma+\Delta\gamma\cos 2(\psi+\zeta)\}(\theta/r) \\ &\quad + \{\delta+\Delta\delta\cos 2(\psi+\zeta) - (I_p - I + \Delta I\cos 2\psi)\omega^2\}(\theta/r)^2 \\ A_0 &= \Delta I\omega^3\sin 2\psi\cdot(\theta/r)^2 + \omega\{\Delta\alpha + 2\,\Delta\gamma(\theta/r) + \Delta\delta(\theta/r)^2\}\sin 2(\psi+\zeta) \end{aligned}\right\} \tag{3.22}$$

The approximate values of m, shown in Fig. 3.3 (c) by the use of the value θ/r and ω given in Eq. (3.20), are a little larger than the exact one. Fig. 3.3 (d) shows $m-\omega$ diagrams derived from Figs. 3.3 (b) and (c), and there is also a little difference between the approximate values and the exact ones, because of the constrained condition of $\xi=0°$ used.

3.3. Dynamic unstable vibration

3.3.1. Equations of motion on rotating coordinate system

The equations of motion about the center of gravity G of unsymmetrical rotor mounted on flat shaft are expressed[10] by using four variables x, y, θ_x and θ_y as follows:

$$\begin{matrix} x \\ y \end{matrix} = r \begin{matrix} \cos \\ \sin \end{matrix} \Phi, \qquad \begin{matrix} \theta_x \\ \theta_y \end{matrix} = \theta \begin{matrix} \cos \\ \sin \end{matrix} \varphi \tag{3.23}$$

We now consider the coordinate system o-$x'y'z$ rotating with the same angular velocity ω as the shaft. The plane $x'oz$ is parallel to the principal axis GY_2, and when ox' is determined so that it agrees with ox at the instant $t=0$, the equations of motion[20] about x', y', θ_x' and θ_y' which are the projections of r and θ on the planes $x'oz$ and $y'oz$ are given as follows:

$$\left.\begin{aligned}
&M\ddot{x}'+\{\alpha-\Delta\alpha\cos 2\zeta-M\omega^2\}x'-2M\omega\dot{y}'-\Delta\alpha\sin 2\zeta\cdot y'\\
&\quad+(\gamma-\Delta\gamma\cos 2\zeta)\theta_x'-\Delta\gamma\sin 2\zeta\cdot\theta_y'=0\\
&M\ddot{y}'+\{\alpha+\Delta\alpha\cos 2\zeta-M\omega^2\}y'+2M\omega\dot{x}-\Delta\alpha\sin 2\zeta\cdot x'\\
&\quad+(\gamma+\Delta\gamma\cos 2\zeta)\theta_y'-\Delta\gamma\sin 2\zeta\cdot\theta_x'=0\\
&(I-\Delta I)\ddot{\theta}'_x+\{\delta-\Delta\delta\cos 2\zeta+(I_p-I-\Delta I)\omega^2\}\theta_x'-(2I-I_p)\omega\dot{\theta}_y'\\
&\quad-\Delta\delta\sin 2\zeta\cdot\theta_y'+(\gamma-\Delta\gamma\cos 2\zeta)x'-\Delta\gamma\sin 2\zeta\cdot y'=0\\
&(I+\Delta I)\ddot{\theta}_y'+\{\delta+\Delta\delta\cos 2\zeta+(I_p-I+\Delta I)\omega^2\}\theta_y'+(2I-I_p)\omega\dot{\theta}_x'\\
&\quad-\Delta\delta\sin 2\zeta\cdot\theta_x'+(\gamma+\Delta\gamma\cos 2\zeta)y'-\Delta\gamma\sin 2\zeta\cdot x'=0
\end{aligned}\right\}\qquad(3.24)$$

$$x'=Ae^{st},\quad y'=Be^{st},\quad \theta_x'=Ce^{st},\quad \theta_y'=De^{st}\qquad(3.25)$$

By substituting the solutions of the free vibrations given by Eq. (3.25) into Eq. (3.24), the characteristic equation[13)15)18)] is derived.

$$z=x'+iy',\quad \bar{z}=x'-iy',\quad \theta_z=\theta_x'+i\theta_y',\quad \bar{\theta}_z=\theta_x'-i\theta_y'\qquad(3.26)$$

By using complex numbers z, $\bar{z}$, θ_z and $\bar{\theta}_z$ given in Eq. (3.26), instead of x', y', θ_x' and θ_y', Eq. (3.27) is derived from Eq. (3.24).

$$\left.\begin{aligned}
&M\ddot{z}+2iM\omega\dot{z}+(\alpha-M\omega^2)z-\Delta\alpha e^{i2\zeta}\cdot\bar{z}+\gamma\theta_z-\Delta\gamma e^{i2\zeta}\cdot\bar{\theta}_z=0\\
&I\ddot{\theta}_z-\Delta I\ddot{\bar{\theta}}_z+i(2I-I_p)\omega\dot{\theta}_z+\{\delta+(I_p-I)\omega^2\}\theta_z\\
&\quad-(\Delta\delta e^{i2\zeta}+\Delta I\omega^2)\bar{\theta}_z+\gamma z-\Delta\gamma e^{i2\zeta}\cdot\bar{z}=0
\end{aligned}\right\}\qquad(3.27)$$

When $\Delta I=\Delta\alpha=\Delta\gamma=\Delta\delta=0$, complex numbers z, θ_z in Eq. (3.26) should take the following form

$$z=Ee^{i(p't+\alpha)},\quad \theta_z=Fe^{i(p't+\alpha)}\qquad(3.28)$$

due to the existence of Coriolis' force $i2M\omega\dot{z}$ and Coriolis' moment $i(2I-I_p)\omega\dot{\theta}_z$. Eq. (3.28) shows that the shaft makes a circular whirling motion at the angular velocity of p' on the rotating coordinate system. As long as the relation $\gamma\neq 0$ holds, the arguments of z and θ_z have the same value and they are in phase.

In the cases of unsymmetrical rotor ($\Delta I\neq 0$; $\Delta\alpha=\Delta\gamma=\Delta\delta=0$) or flat shaft ($\Delta I=0$; $\Delta\alpha$, $\Delta\gamma$, $\Delta\delta\neq 0$, $\zeta=0°$ or $90°$), substituting z, θ_z of Eq. (3.28) into Eq. (3.27), and transposing the terms containing rotating inequality into the right hand side shows that there occurs another vibration $e^{-i(p't+\alpha)}$ making a pair to Eq. (3.28) because of the existence of external force $\pm(\Delta\alpha E+\Delta\gamma F)e^{-i(p't+\alpha)}$ in the first equation of Eq. (3.27) and also the external moment $\{\Delta I(\omega^2-p'^2)F\pm(\Delta\gamma E+\Delta\delta F)\}e^{-i(p't+\alpha)}$ in the second equation. Accordingly, z and θ_z should take the following form

$$z = Ee^{i(p't+\alpha)} + \bar{E}e^{-i(p't+\alpha)},\quad \theta_z = Fe^{i(p't+\alpha)} + \bar{F}e^{-i(p't+\alpha)} \tag{3.29}$$

The loci of z and θ_z on the rotating coordinate system (x', y'; θ'_x, θ'_y) become ellipses, and their two principal axes coincide with ox' and oy', respectively.

In general case that an unsymmetrical rotor is mounted on flat shaft at some orientation ζ, if we substitute Eq. (3.28) into Eq. (3.27), and transpose the terms containing rotating inequality into the right hand side, there occur an external force $(\Delta\alpha E + \Delta\gamma F)e^{-i(p't+\alpha-2\zeta)}$, and a moment $\Delta I(\omega^2 - p'^2)Fe^{-i(p't+\alpha)} + (\Delta\gamma E + \Delta\delta F)e^{-i(p't+\alpha-2\zeta)}$. Accordingly z and θ_z should take the following form.

$$z = Ee^{i(p't+\alpha)} + \bar{E}e^{-i(p't+\alpha_1)},\quad \theta_z = Fe^{i(p't+\alpha)} + \bar{F}e^{-i(p't+\alpha_2)} \tag{3.30}$$

3.3.2. Causes of dynamic unstable vibration

The principal axes of the ellipses of z, θ_z on the rotating coordinate given by Eq. (3.30) are advanced in the direction ω by $(\alpha-\alpha_1)/2$ and $(\alpha-\alpha_2)/2$ to ox' (GY_2), respectively. Since the relation $\alpha_1=\alpha_2=\alpha$ holds in the case of unsymmetrical rotor, and $\alpha_1=\alpha_2=\alpha-2\zeta$ in the case of flat shaft, it can be said, that $\alpha_1 \fallingdotseq \alpha_2$ holds in general case $\Delta I \neq 0$; $\Delta\alpha$, $\Delta\gamma$, $\Delta\delta \neq 0$. When we pose the condition of $\alpha_1=\alpha_2=\bar{\alpha}$ as is done in the Section 3.2.4 and restrict the whirling of rotor so that the locus takes steady elliptic form, we shall calculate the torque T_r required to rotate the shaft end at a constant angular velocity ω.

The principal axes of the ellipses of z, θ_z exist in the direction advanced by $(\alpha-\bar{\alpha})/2$ to $ox'(GY_2)$, and $oy'(GX_2)$ exists in the direction further advanced by $\beta=90°-(\alpha-\bar{\alpha})/2$ to the principal axes of z, θ_z. Putting $\varphi'=p't-180°+(\alpha+\bar{\alpha})/2$ and rewriting Eq. (3.30), we have

$$z_n = z\cdot e^{-i(90°-\beta)} = Ee^{i\varphi'} + \bar{E}e^{-i\varphi'},\quad \theta_{zn} = \theta_z\cdot e^{-i(90°-\beta)} = Fe^{i\varphi'} + \bar{F}e^{-i\varphi'} \tag{3.30 a}$$

and the principal axes $GX_2(I_2)$ and $GX_3(\alpha+\Delta\alpha, \gamma+\Delta\gamma, \delta+\Delta\delta)$ lie in the direction advanced by β, $\beta+\zeta$ to the axis ($\varphi'=0°$) of the ellipse, respectively. Rewriting Eq. (3.30 a) yields the following relations

$$\left.\begin{aligned}
&r=|z|,\ \dot{r}=\frac{d}{dt}|z|,\ \theta=|\theta_z|,\ \dot{\theta}=\frac{d}{dt}|\theta_z|,\\
&\Theta=\varphi+\psi=\omega t-90°\\
&\Phi=\omega t-180°+\arg z,\ \dot{\Phi}=\omega+\frac{d}{dt}(\arg z),\\
&\varphi=\omega t-180°+\arg\theta_z,\ \dot{\varphi}=\omega+\frac{d}{dt}(\arg\theta_z),\\
&\psi=\Theta-\varphi=90°-\arg\theta_z=\beta-\arg\theta_{zn}\\
&\xi=\varphi-\Phi=\arg\theta_z-\arg z=\arg\theta_{zn}-\arg z_n
\end{aligned}\right\} \tag{3.31}$$

where $|z|$ and $|\theta_z|$ are the absolute values of complex number z and θ_z, and $\arg z$, $\arg\theta_z$ are the arguments of z, θ_z. From Eq. (3.30 a) the following relations are derived.

$$
\left.\begin{aligned}
&|z_n|^2=|z|^2=E^2+\bar{E}^2+2E\bar{E}\cos 2\varphi',\ \tan(\arg z_n)=\{(E-\bar{E})/(E+\bar{E})\}\tan\varphi'\\
&|\theta_{zn}|^2=|\theta_z|^2=F^2+\bar{F}^2+2F\bar{F}\cos 2\varphi',\ \tan(\arg\theta_{zn})=\{(F-\bar{F})/(F+\bar{F})\}\tan\varphi'\\
&\frac{d}{dt}|z_n|=\frac{d}{dt}|z|=-2p'E\bar{E}/|z_n|\cdot\sin 2\varphi',\ \frac{d}{dt}|\theta_{zn}|=\frac{d}{dt}|\theta_z|=-2p'F\bar{F}/|\theta_{zn}|\cdot\sin 2\varphi'\\
&\frac{d}{dt}(\arg z_n)=\frac{d}{dt}(\arg z)=p'(E^2-\bar{E}^2)/|z_n|^2,\\
&\frac{d}{dt}(\arg z_n)=\frac{d}{dt}(\arg\theta_z)=p'(F^2-\bar{F}^2)/|\theta_{zn}|^2
\end{aligned}\right\}
\tag{3.32}
$$

The driving torque T_r of shaft at ω is the generalized force with respect to β in term of Lagrange's equation of motion, *i.e.*

$$
T_r=\frac{d}{dt}\left(\frac{\partial T}{\partial\dot{\beta}}\right)-\frac{\partial T}{\partial\beta}+\frac{\partial V}{\partial\beta} \tag{3.33}
$$

By calculating Eq. (3.33) by the use of Eqs. (3.1), (3.2), (3.31) and (3.32), T_r is obtained as the sum of the torques due to $\Delta\alpha$, $\Delta\gamma$, $\Delta\delta$ and ΔI, as follows:

$$
T_r=(T_r)_{\Delta\alpha}+(T_r)_{\Delta\gamma}+(T_r)_{\Delta\delta}+(T_r)_{\Delta I} \tag{3.34}
$$

$$
\begin{aligned}
(T_r)_{\Delta\alpha}&=-\Delta\alpha|z_n|^2\sin 2(\beta+\zeta-\arg z_n)\\
&=-\Delta\alpha\{\underline{2E\bar{E}\sin 2(\beta+\zeta)}+E^2\sin 2(\beta+\zeta-\varphi')+\bar{E}^2\sin 2(\beta+\zeta+\varphi')\}
\end{aligned}\tag{3.34 a}
$$

$$
\begin{aligned}
(T_r)_{\Delta\gamma}&=-2\Delta\gamma|z_n||\theta_{zn}|\sin\{2(\beta+\zeta)-\arg z_n-\arg\theta_{zn}\}\\
&=-2\Delta\gamma\{\underline{(E\bar{F}+\bar{E}F)\sin 2(\beta+\zeta)}+EF\sin(\beta+\zeta-\varphi')+\bar{E}\bar{F}\sin 2(\beta+\zeta+\varphi')\}
\end{aligned}\tag{3.34 b}
$$

$$
\begin{aligned}
(T_r)_{\Delta\delta}&=-\Delta\delta|\theta_{zn}|^2\sin 2(\beta+\zeta-\arg\theta_{zn})\\
&=-\Delta\delta\{\underline{2F\bar{F}\sin 2(\beta+\zeta)}+F^2\sin 2(\beta+\zeta-\varphi')+\bar{F}^2\sin 2(\beta+\zeta+\varphi')\}
\end{aligned}\tag{3.34 c}
$$

$$
\begin{aligned}
(T_r)_{\Delta I}&=\Delta I\left[\left(\frac{d}{dt}|\theta_{zn}|\right)^2-\left\{\omega+\frac{d}{dt}(\arg\theta_{zn})\right\}^2|\theta_{zn}|^2\right]\cdot\sin 2(\beta-\arg\theta_{zn})\\
&\quad-\Delta I\left\{\omega+\frac{d}{dt}(\arg\theta_{zn})\right\}\cdot\frac{d}{dt}|\theta_{zn}|^2\cdot\cos 2(\beta-\arg\theta_{zn})\\
&=-\Delta I\{\underline{2(\omega^2-p'^2)F\bar{F}\sin 2\beta}+(\omega+p')^2F^2\sin 2(\beta-\varphi')\\
&\quad+(\omega-p')^2\bar{F}^2\sin 2(\beta+\varphi')\}
\end{aligned}\tag{3.34 d}
$$

Since the each term of Eq. (3.34) has the period of π/p', there is possibility of torsional vibration of π/p' in period. The mean value T_{rm} of variational torque T_r with respect to time is given as follows:

$$
T_{rm}=\frac{1}{2\pi}\int_0^{2\pi}(T_r)\,d\varphi'=(T_{rm})_{\Delta\alpha}+(T_{rm})_{\Delta\gamma}+(T_{rm})_{\Delta\delta}+(T_{rm})_{\Delta I} \tag{3.35}
$$

Each term of Eq. (3.35) agrees with the first terms in Eq. (3.34 a) ~ (3.34 d).

3.3.3. Approximate solution of dynamic unstable vibration

Substituting z and θ_z of Eq. (3.30 a) into Eq. (3.27) gives the frequency

equation under the condition of dynamical balance at the instant $\tan\varphi'=0$, and ∞,

$$\begin{vmatrix} \alpha_a - M(\omega^2+p'^2) & -2M\omega p' & \gamma_a & 0 \\ -2M\omega p' & \alpha_b - M(\omega^2+p'^2) & 0 & \gamma_b \\ \gamma_a & 0 & \delta_a + (I_p - I_b)\omega^2 - I_a p'^2 & -(2I - I_p)\omega p' \\ 0 & \gamma_b & -(2I - I_p)\omega p' & \delta_b + (I_p - I_a)\omega^2 - I_b p'^2 \end{vmatrix} = 0 \tag{3.36}$$

where

$$\left.\begin{aligned} \begin{matrix} I_a \\ I_b \end{matrix} &= I \pm \Delta I \cos 2\beta, & \begin{matrix} \alpha_a \\ \alpha_b \end{matrix} &= \alpha \pm \Delta\alpha \cos 2(\beta+\zeta) \\ \begin{matrix} \gamma_a \\ \gamma_b \end{matrix} &= \gamma \pm \Delta\gamma \cos 2(\beta+\zeta), & \begin{matrix} \delta_a \\ \delta_b \end{matrix} &= \zeta \pm \Delta\delta \cos 2(\beta+\zeta) \end{aligned}\right\} \tag{3.36 a}$$

The quartic equation (3.37) in the term of p'^2 is derived by expanding Eq. (3.36).

$$K_8 p'^8 - K_6 p'^6 + K_4 p'^4 - K_2 p'^2 + K_0 = 0 \tag{3.37}$$

By putting $\Delta\alpha=\Delta\gamma=\Delta\delta=0$ and $\cos 2\beta=\pm 1$, Eqs. (3.36) and (3.36 a) agree with those of an unsymmetrical rotor mounted on circular shaft[10)13)]. Even if β and ζ are given, two unknown values of ω and p' are not determined only by Eq. (3.36). Since the two roots among four ones of p'^2 are always equal root in the dynamically unstable region, the discriminant $D(\omega)$ of Eq. (3.37) must be zero[13)]. Namely, we have

$$\begin{aligned} 27K_8^6 D(\omega) = 4(12K_0K_8 - 3K_2K_6 + K_4^2)^3 - (27K_2^2K_8 - 72K_0K_4K_8 \\ + 27K_0K_6^2 - 9K_2K_4K_6 + 2K_4^3)^2 = 0 \end{aligned} \tag{3.38}$$

By using the value of ω that satisfies Eq. (3.38), $K_8 \sim K_0$ are obtained, and the roots p' of Eq. (3.37) are calculated. As the relation $A_{11} : A_{12} : A_{13} : A_{14} = E + \bar{E} : E - \bar{E} : F + \bar{F} : F - \bar{F}$ holds, the amplitude ratios $\bar{E}/E$, $\bar{F}/F$ and F/E are obtained by substituting ω and p' into the cofactor of the determinant of Eq. (3.36). If β is assumed for arbitrary ω and ζ in the stable region, four real roots of p'^2 can be calculated, and the amplitude rations $\bar{E}/E$, $\bar{F}/F$ and F/E are obtained by Eq. (3.36) for each value of p'. If the relation $T_{rm}=0$ is satisfied by substitution of these values into Eq. (3.35), the value of β assumed is proved right.

The negative damping coefficient m is derived in the following way. The amplitudes E, $\bar{E}$, F and $\bar{F}$ are assumed to be raised exponentially in the form of Eq. (3.39).

$$E = E_0 e^{mt},\ \bar{E} = \bar{E}_0 e^{mt},\ F = F_0 e^{mt},\ \bar{F} = \bar{F}_0 e^{mt} \tag{3.39}$$

The amount of $(T+V)$ varies according to the change of torque T_r of π/p' in period, and when only the term varying gradually in form e^{mt} are picked up, ωT_{rm} in the left hand side of Eq. (3.8) is equal to $m\{2(T+V)_m - I_p\omega^2\}$ in the right hand one. Therefore, we have

$$m = \omega T_{rm} / \{2(T+V)_m - I_p\omega^2\} \tag{3.40}$$

The mean value of total energy with respect to time, $(T+V)_m=\frac{1}{2\pi}\int_0^{2\pi}(T+V)d\varphi'$, can be obtained by the use of Eqs. (3.1), (3.2), (3.31) and (3.32).

$$\begin{aligned}2(T+V)_m=&M\{(\omega^2+p'^2)(E^2+\bar{E}^2)+2\omega p'(E^2-\bar{E}^2)\}+I_p\{\omega^2-\omega^2(F^2+\bar{F}^2)\\&-\omega p'(F^2-\bar{F}^2)\}+I\{(\omega^2+p'^2)(F^2+\bar{F}^2)+2\omega p'(F^2-\bar{F}^2)\}\\&-2\Delta I(\omega^2-p'^2)F\bar{F}\cos 2\beta+\alpha(E^2+\bar{E}^2)+2\gamma(EF+\bar{E}\bar{F})+\delta(F^2+\bar{F}^2)\\&+2\{\Delta\alpha E\bar{E}+\Delta\gamma(E\bar{F}+\bar{E}F)+\Delta\delta F\bar{F}\}\cos 2(\beta+\zeta)\end{aligned}\tag{3.41}$$

The arithmetic mean value of $(T+V)$ at the instants of $\tan\varphi'=0$ and ∞ is found to be the same as $(T+V)_m$ of Eq. (3.41).

In case an unsymmetrical rotor is mounted on circular shaft, the dimensions in the previous papers[13)15)] are as follows; for example $Mg=11.637$ kg, $I_p=0.4300$ kg cm s^2, $I_1=0.5090$ kg cm s^2, $I_2=0.3816$ kg cm s^2, $\alpha=3.120\times10$ kg/cm, $\gamma=-6.450\times10^2$ kg/rad, $\delta=1.777\times10^4$ kg cm/rad, $\omega_d=1544$ rpm. By using Eqs. (3.36), (3.37), (3.38), (3.40) and (3.41), approximate solutions of ω, p', $\bar{E}/E$, $\bar{F}/F$, F/E and m for β are shown in Fig. 3.4 (a). And the approximate solutions of $\bar{E}/E$, $\bar{F}/F$ and F/E are nearly equal to exact ones for the frequency p_1 of Fig. 10 in reference[15)].

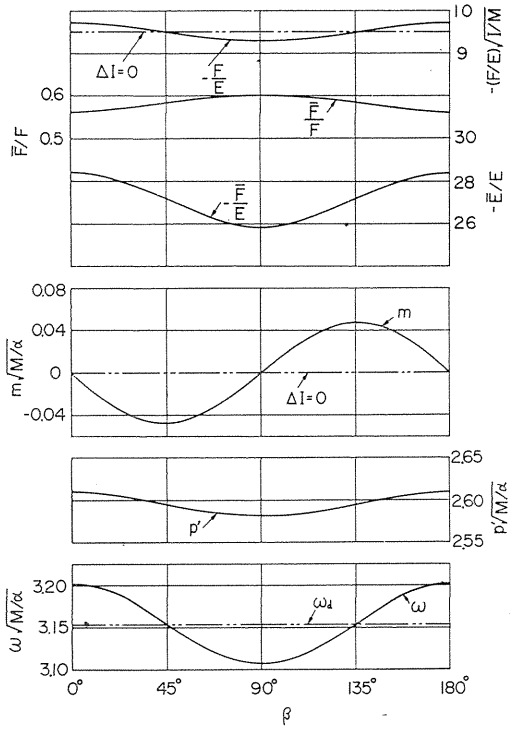

(a) Relation between ω, p', m, $\bar{E}/E$, $\bar{F}/F$, F/E and β (approximate solution)

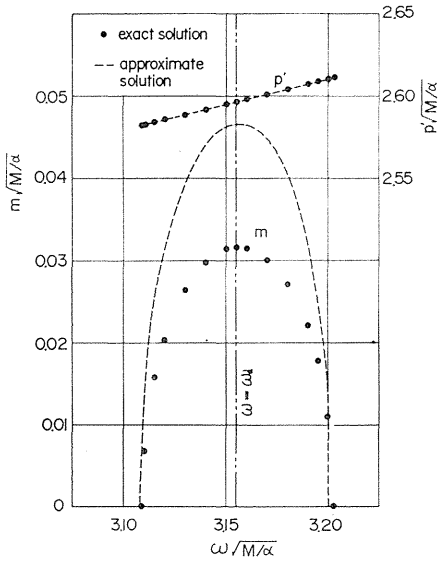

(b) Relation between m, p' and ω (exact and approximate solution)

FIG. 3.4. Case of shaft of circular cross-section having an unsymmetrical rotor (near ω_d where dynamic unstable vibrations occur).

Using the result in Fig. 3.4 (a), the approximate solution of the relation m and $p'-\omega$ is calculated and shown in Fig. 3.4 (b) by broken line. Exact solutions[13] calculated by the characteristic equation derived from Eq. (3.24) and (3.25) are shown by the mark ◉. The exact result shows good coincidence with the approximate one except for the values of m. The approximate values of m are larger by 30~40% than the exact ones as shown in Fig. 3.3 (d), because the restricted motion of rotor needs more torque T_{rm} than that without restriction. When the motion is left free, m becomes smaller.

As the second example we deal with the following case, whose dimensions are shown in Chapter 1 (Experiment IV), *i.e.*, $Mg=12.179$ kg, $I_p=0.3725$ kg cm s^2, $I_1=0.5389$ kg cm s^2, $I_2=0.4497$ kg cm s^2, $\alpha\pm\Delta\alpha=(2.6589\pm0.2744)\times10$ kg/cm, $\gamma\pm\Delta\gamma=-(5.4555\pm0.4801)\times10^2$ kg/rad, $\delta\pm\Delta\delta=(1.4993\pm0.1169)\times10^4$ kg cm/rad, $\omega_d=1227.2$ rpm. Approximate solutions of ω, p', $\bar{E}/E$, $\bar{F}/F$, F/E and m with respect to β are shown in Fig. 3.5 (a). In case the orientation ζ is equal to 0°, 45° and 90°,

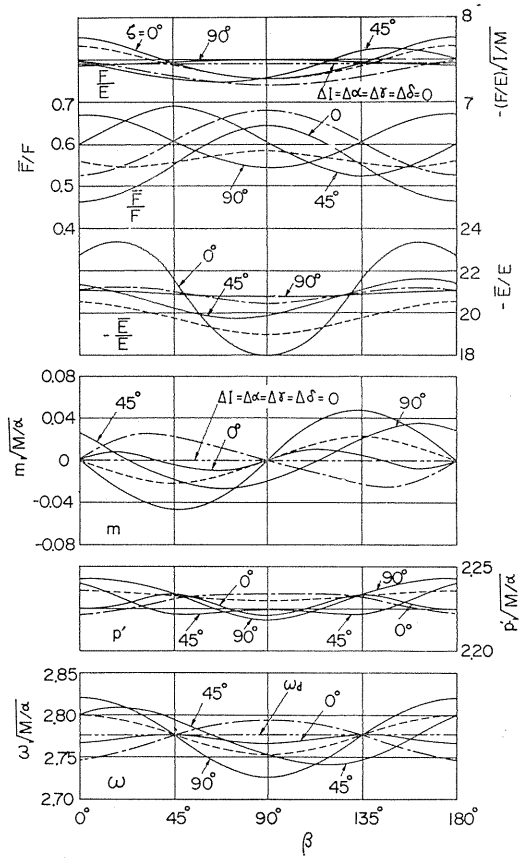

(a) Relation between ω, p', m, $\bar{E}/E$, $\bar{F}/F$, F/E and β (approximate solution)

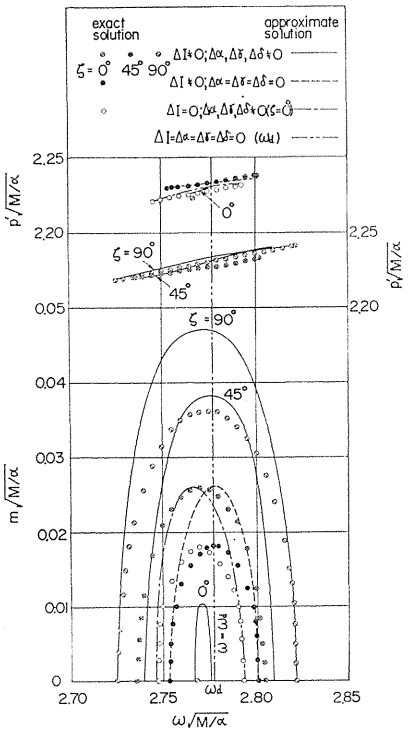

(b) Relation between m, p' and ω (exact and approximate solution)

FIG. 3.5. Case of flat shaft having an unsymmetrical rotor (near ω_d where dynamic unstable vibrations occur).

the approximate solutions are drawn by full line. In case $\Delta I \neq 0$; $\Delta\alpha = \Delta\gamma = \Delta\delta = 0$, and $\Delta I = 0$; $\Delta\alpha$, $\Delta\gamma$, $\Delta\delta \neq 0$, they are given by broken and single dotted chain line, respectively. The relation of m and $p' - \omega$ is also shown in Fig. 3.5 (b). Exact solutions corresponding to full line are shown by the marks ⊘ ($\zeta = 0°$), ⊗ ($\zeta = 45°$) ⃠ ($\zeta = 90°$), respectively. Also the exact ones corresponding to broken and chain line are shown by marks ●, ○, respectively. As in case of Fig. 3.4 (b) the approximate values of the location and the width of unstable region and the frequency p' agree well with the exact ones. However, the approximate ones of m take fairly larger value at ω_d than the exact ones, because the system must be restricted at ω_d to the most in order to keep steady ellipitical movement. Double dotted chain lines in Fig. 3.5 show the values of ω_d and $(F/E)_{\omega_d}$ when $\Delta I = \Delta\alpha = \Delta\gamma = \Delta\delta = 0$.

3.4. Conclusions

By considering an input energy from shaft end into the shaft system carrying an unsymmetrical rotor, or with unequal stiffness, we made clear the physical meaning and occurrence of two kinds of unstable vibrations. The approximate results derived from energy consideration coincide fairly well with the exact results obtained by numerical calculation of the characteristic equation.

Chapter 4. On the Forced Vibrations of a Rotor with Rotating Inequality [18) 19) 21)]

4.1. Introductions

A rotating shaft system with an unsymmetrical rotor, or the one with an unsymmetrical shaft stiffness may be regarded as be one of vibratory shaft systems having a rotating inequality which rotates with the rotor, *i.e.*, which rotates at an angular velocity of the shaft ω. In this chapter, the more general shaft system in which there exists the rotating anisotropy with any rotating velocity $\lambda\omega$ is treated, where λ is a certain constant, and the lateral vibrations appearing in such a shaft system are studied.

Since a free vibration of a natural frequency p appears with the free vibration of a frequency $\bar{p} = 2\lambda\omega - p$ in the shaft system having the rotating inequality[13], one external periodic force of a frequency ω_0 yields two forced vibrations of the frequency ω_0 and $\omega_0' = 2\lambda\omega - \omega_0$, and hence resonant phenomena are observed under the conditions of $\omega_0 \fallingdotseq \bar{p}$ as well as of $\omega_0 \fallingdotseq p$. Analytical results show that, in the state of resonance when $\omega_0 \fallingdotseq \bar{p}$, the predominant vibration is not the forced vibration of ω_0 but is always the forced vibration of frequency ω_0' ($= 2\lambda\omega - \omega_0$) which is apparently quite different from the frequency ω_0 of the external force, provided the rotating inequality is relatively small.

By using the above conclusion, elucidated physical meanings can be presented to the whirl of synchronous backward precession appearing in the rotating shaft supported by flexible bearing pedestals, the whirling of forward precession at the so-called secondary critical speed which takes place in the horizontal flat shaft and the whirling motion with a peculiar mode of backward precession caused by a small difference in diameter of balls in ball bearings.

4.2. Equations of motion, amplitude and amplitude ratio of forced vibrations

When there exists an anisotropy in shaft stiffness rotating at any angular velocity $\lambda\omega$ in a vibratory system consisting of a rotor and a light shaft, the system is governed by the following equations of motion[20]:

$$\left.\begin{aligned}
&M\ddot{x}+\alpha x+\gamma\theta_x-\Delta\alpha(x\cos 2\lambda\omega t+y\sin 2\lambda\omega t)\\
&\qquad-\Delta\gamma(\theta_x\cos 2\lambda\omega t+\theta_y\sin 2\lambda\omega t)=P\cos(\omega_0 t+\beta_1)\\
&M\ddot{y}+\alpha y+\gamma\theta_y-\Delta\alpha(x\sin 2\lambda\omega t-y\cos 2\lambda\omega t)\\
&\qquad-\Delta\gamma(\theta_x\sin 2\lambda\omega t-\theta_y\cos 2\lambda\omega t)=P\sin(\omega_0 t+\beta_1)\\
&I\ddot{\theta}_x+I_p\omega\dot{\theta}_y+\gamma x+\delta\theta_x-\Delta\gamma(x\cos 2\lambda\omega t+y\sin 2\lambda\omega t)\\
&\qquad-\Delta\delta(\theta_x\cos 2\lambda\omega t+\theta_y\sin 2\lambda\omega t)=M_t\cos(\omega_0 t+\beta_2)\\
&I\ddot{\theta}_y-I_p\omega\dot{\theta}_x+\gamma y+\delta\theta_y-\Delta\gamma(x\sin 2\lambda\omega t-y\cos 2\lambda\omega t)\\
&\qquad-\Delta\delta(\theta_x\sin 2\lambda\omega t-\theta_y\cos 2\lambda\omega t)=M_t\sin(\omega_0 t+\beta_2)
\end{aligned}\right\}\qquad(4.1)$$

where α, γ, δ are mean values of spring constants of the shaft, $\Delta\alpha$, $\Delta\gamma$, $\Delta\delta$ inequalities in shaft stiffness, P a magnitude of a periodic external force, M_t a magnitude of a periodic external moment, ω_0 a frequency of disturbances, β_1, β_2 phase angles, and t time. It is assumed that the anisotropies $\Delta\alpha$, $\Delta\gamma$, $\Delta\delta$ in stiffness are rather small quantities of order ε, *i.e.*, $\Delta\alpha/\alpha\ll 1$, $\Delta\gamma/\gamma\ll 1$, $\Delta\delta/\delta\ll 1$.

Since a gyroscopic moment acts to the rotor and there are the so-called gyroscopic terms $I_p\omega\dot{\theta}_y$, $-I_p\omega\dot{\theta}_x$ in Eq. (4.1), recti-linear vibrations can not take place in the system and all motions of the shaft of lateral vibrations become whirling motions. Accordingly, a frequency of vibration is regarded as to be an angular velocity of the whirl of the shaft and a positive frequency represents a whirling motion of forward precession in which the direction of whirl is the same as the direction of rotation of the shaft, and a negative frequency means a backward precession in which the whirl is in reversed direction.

There exist terms of the rotating anisotropies $\Delta\alpha$, $\Delta\gamma$, $\Delta\delta$ in the equations of motion as shown in Eq. (4.1), and hence free vibrations of a natural frequency p as well as a frequency $\bar{p}=2\lambda\omega-p$ appear in the system, and one external periodic force of a frequency ω_0 yields two forced vibrations of frequencies ω_0 and $\omega_0'=2\lambda\omega-\omega_0$. It follows that free and forced vibrations in the system should be represented by

$$\left.\begin{aligned}
\begin{matrix}x\\y\end{matrix}&=A\begin{matrix}\cos\\\sin\end{matrix}(p_i t+\beta)+\bar{A}\begin{matrix}\cos\\\sin\end{matrix}(\bar{p}_i t-\beta)\\
\begin{matrix}\theta_x\\\theta_y\end{matrix}&=B\begin{matrix}\cos\\\sin\end{matrix}(p_i t+\beta')+\bar{B}\begin{matrix}\cos\\\sin\end{matrix}(\bar{p}_i t-\beta')
\end{aligned}\right\}\qquad(4.2)$$

$$\left.\begin{aligned}
\begin{matrix}x\\y\end{matrix}&=E_P\begin{matrix}\cos\\\sin\end{matrix}(\omega_0 t+\beta_1)+E_P'\begin{matrix}\cos\\\sin\end{matrix}(\omega_0' t-\beta_1)+E_M\begin{matrix}\cos\\\sin\end{matrix}(\omega_0 t+\beta_2)+E_M'\begin{matrix}\cos\\\sin\end{matrix}(\omega_0' t-\beta_2)\\
\begin{matrix}\theta_x\\\theta_y\end{matrix}&=F_P\begin{matrix}\cos\\\sin\end{matrix}(\omega_0 t+\beta_1)+F_P'\begin{matrix}\cos\\\sin\end{matrix}(\omega_0' t-\beta_1)+F_M\begin{matrix}\cos\\\sin\end{matrix}(\omega_0 t+\beta_2)+F_M'\begin{matrix}\cos\\\sin\end{matrix}(\omega_0' t-\beta_2)
\end{aligned}\right\}\qquad(4.3)$$

where β, β' are phase angles, E_P, E_P', F_P, F_P' and E_M, E_M', F_M, F_M' are amplitudes of forced vibrations induced by the disturbance $P\cos(\omega_0 t+\beta_1)$, $P\sin(\omega_0 t+\beta_1)$ and

$M_t \cos(\omega_0 t+\beta_2)$, $M_t \sin(\omega_0 t+\beta_2)$ respectively, and E_P, E_M, F_P, F_M are amplitudes of forced vibrations of the frequency ω_0 and E'_P, E'_M, F'_P, F'_M are those of the frequency $\omega'_0 = 2\lambda\omega - \omega_0$.

Substituting Eq. (4.2) into Eq. (4.1) and eliminating all amplitudes A, $\bar{A}$, B, $\bar{B}$, one obtains the following frequency equation:

$$\Phi(p) = f(p)\cdot f(\bar{p}) + \varphi(p) = 0, \tag{4.4}$$

in which p is a natural frequency, $\bar{p}=2\lambda\omega-p$, and

$$\left.\begin{aligned} f(p) &= H(p)G(p) - \gamma^2 \\ \varphi(p) &= -G(p)G(\bar{p})(\Delta\alpha)^2 - \{G(p)H(\bar{p}) + H(p)G(\bar{p}) + 2\gamma^2\}(\Delta\gamma)^2 \\ &\quad - H(p)H(\bar{p})(\Delta\delta)^2 + 2\gamma\{G(p) + G(\bar{p})\}\Delta\alpha\cdot\Delta\gamma \\ &\quad - 2\gamma^2\cdot\Delta\alpha\cdot\Delta\delta + 2\gamma\{H(p) + H(\bar{p})\}\Delta\gamma\cdot\Delta\delta + \{\Delta\alpha\cdot\Delta\delta - (\Delta\gamma)^2\} \end{aligned}\right\} \tag{4.5}$$

$$H(p) = \alpha - Mp^2, \quad G(p) = \delta + I_p\omega p - Ip^2 \tag{4.6}$$

In the system without rotating anisotropy, *i.e.*, when all inequalities $\Delta\alpha$, $\Delta\gamma$, $\Delta\delta$ vanish, the frequency equation is reduced to

$$f(p) = (\alpha - Mp^2)(\delta + I_p\omega p - Ip^2) - \gamma^2 = 0. \tag{4.7}$$

Inserting Eq. (4.3) in Eq. (4.1) yields amplitudes of forced vibrations as follows:

$$\left.\begin{aligned} E_P &= P\{Gf(\omega'_0) - G'(\Delta\gamma)^2 - H'(\Delta\delta)^2 + 2\gamma\cdot\Delta\gamma\cdot\Delta\delta\}/\Phi(\omega_0) \\ E'_P &= P[GG'\cdot\Delta\alpha - \gamma(G+G')\Delta\gamma + \gamma^2\cdot\Delta\delta - \{\Delta\alpha\cdot\Delta\delta - (\Delta\gamma)^2\}\Delta\delta]/\Phi(\omega_0) \\ F_P &= P\{\gamma f(\omega'_0) - G'\cdot\Delta\alpha\cdot\Delta\gamma + \gamma\cdot\Delta\alpha\cdot\Delta\delta + \gamma(\Delta\gamma)^2 - H\cdot\Delta\gamma\cdot\Delta\delta\}/\Phi(\omega_0) \\ F'_P &= P[\gamma G\cdot\Delta\alpha - (GH' + \gamma^2)\Delta\gamma + \gamma H'\cdot\Delta\delta - \{\Delta\alpha\cdot\Delta\delta - (\Delta\gamma)^2\}\Delta\gamma]/\Phi(\omega_0) \\ E_M &= M_t\{\gamma f(\omega'_0) + \gamma(\Delta\gamma)^2 - G'\cdot\Delta\alpha\cdot\Delta\gamma + \gamma\cdot\Delta\alpha\cdot\Delta\delta - H'\cdot\Delta\gamma\cdot\Delta\delta\}/\Phi(\omega_0) \\ E'_M &= M_t[\gamma G'\cdot\Delta\alpha - (HG' + \gamma^2)\Delta\gamma + \gamma H\cdot\Delta\delta - \{\Delta\alpha\cdot\Delta\delta - (\Delta\gamma)^2\}\Delta\gamma]/\Phi(\omega_0) \\ F_M &= M_t\{Hf(\omega'_0) - G'(\Delta\alpha)^2 - H'(\Delta\gamma)^2 + 2\gamma\cdot\Delta\alpha\cdot\Delta\gamma\}/\Phi(\omega_0) \\ F'_M &= M_t[\gamma^2\cdot\Delta\alpha - \gamma(H+H')\Delta\gamma + HH'\cdot\Delta\delta - \{\Delta\alpha\cdot\Delta\delta - (\Delta\gamma)^2\}\Delta\alpha]/\Phi(\omega_0) \end{aligned}\right\} \tag{4.8}$$

in which

$$\left.\begin{aligned} H &= H(\omega_0) = \alpha - M\omega_0^2, \quad H' = H(\omega'_0) = \alpha - M\omega_0'^2 \\ G &= G(\omega_0) = \delta + I_p\omega\omega_0 - I\omega_0^2, \quad G' = G(\omega'_0) = \delta + I_p\omega\omega'_0 - I\omega_0'^2 \end{aligned}\right\} \tag{4.9}$$

Amplitude ratios between forced vibrations of frequencies ω_0 and $\omega'_0 = 2\lambda\omega - \omega_0$ are obtained from Eq. (4.8) as follows:

$$\left.\begin{aligned} \frac{E'_P}{E_P} &= \frac{GG'\cdot\Delta\alpha - \gamma(G+G')\Delta\gamma + \gamma^2\cdot\Delta\delta - \{\Delta\alpha\cdot\Delta\delta - (\Delta\gamma)^2\}\Delta\delta}{Gf(\omega'_0) - G'(\Delta\gamma)^2 - H'(\Delta\delta)^2 + 2\gamma\cdot\Delta\gamma\cdot\Delta\delta} \\ \frac{F'_P}{F_P} &= \frac{\gamma G\cdot\Delta\alpha - (GH' + \gamma^2)\Delta\gamma + \gamma H'\cdot\Delta\delta - \{\Delta\alpha\cdot\Delta\delta - (\Delta\gamma)^2\}\Delta\gamma}{\gamma f(\omega'_0) - G'\cdot\Delta\alpha\cdot\Delta\gamma + \gamma\cdot\Delta\alpha\cdot\Delta\delta + \gamma(\Delta\gamma)^2 - H\cdot\Delta\gamma\cdot\Delta\delta} \end{aligned}\right\} \tag{4.10}$$

$$\left.\begin{aligned}\frac{E'_M}{E_M}&=\frac{\gamma G'\cdot\Delta\alpha-(GH'+\gamma^2)\Delta\gamma+\gamma H'\cdot\Delta\delta-\{\Delta\alpha\cdot\Delta\delta-(\Delta\gamma)^2\}\Delta\gamma}{\gamma f(\omega'_0)-G'\cdot\Delta\alpha\cdot\Delta\gamma+\gamma\cdot\Delta\alpha\cdot\Delta\delta+\gamma(\Delta\gamma)^2-H'\cdot\Delta\gamma\cdot\Delta\delta}\\ \frac{F'_M}{F_M}&=\frac{\gamma^2\cdot\Delta\alpha-\gamma(H+H')\Delta\gamma+HH'\cdot\Delta\delta-\{\Delta\alpha\cdot\Delta\delta-(\Delta\gamma)^2\}\Delta\alpha}{Hf(\omega'_0)-G'(\Delta\alpha)^2-H'(\Delta\gamma)^2+2\gamma\cdot\Delta\alpha\cdot\Delta\gamma}\end{aligned}\right\}$$

The rotating shaft carrying an unsymmetrical rotor is also regarded as to be a vibratory system with the rotating anisotropy, and is governed by the following equations of motion[13]:

$$\left.\begin{aligned}&M\ddot{x}+\alpha x+\gamma\theta_x=P\cos(\omega_0 t+\beta_1)\\ &M\ddot{y}+\alpha y+\gamma\theta_y=P\sin(\omega_0 t+\beta_1)\\ &I\ddot{\theta}_x+I_p\omega\dot{\theta}_y+\gamma x+\delta\theta_x-\Delta I\cdot\frac{d}{dt}(\dot{\theta}_x\cos 2\omega t+\dot{\theta}_y\sin 2\omega t)=M_t\cos(\omega_0 t+\beta_2)\\ &I\ddot{\theta}_y-I_p\omega\dot{\theta}_x+\gamma y+\delta\theta_y-\Delta I\cdot\frac{d}{dt}(\dot{\theta}_x\sin 2\omega t-\dot{\theta}_y\cos 2\omega t)=M_t\sin(\omega_0 t+\beta_2)\end{aligned}\right\}\qquad(4.1\,a)$$

For the vibratory shaft system with an unsymmetrical rotor, the following relationships corresponding to Eqs. (4.5), (4.8), (4.10) are obtained in like manner[14].

$$\varphi(p)=-(\Delta I)^2(\alpha-Mp^2)(\alpha-M\overline{p}^2)p^2\overline{p}^2,\qquad(4.5\,a)$$

$$\left.\begin{aligned}&E_P=P\{Gf(\omega'_0)-(\Delta I)^2H'\omega_0^2\omega_0'^2\}/\Phi(\omega_0),\quad E'_P=P\cdot\Delta I\cdot\gamma^2\omega_0\omega'_0/\Phi(\omega_0),\\ &F_P=-P\gamma f(\omega'_0)/\Phi(\omega_0),\quad F'_P=-P\cdot\Delta I\cdot\gamma H'\omega_0\omega'_0/\Phi(\omega_0),\\ &E_M=-M_t\gamma f(\omega'_0)/\Phi(\omega_0),\quad E'_M=-M_t\cdot\Delta I\cdot\gamma H\omega_0\omega'_0/\Phi(\omega_0),\\ &F_M=M_tHf(\omega'_0)/\Phi(\omega_0),\quad F'_M=M_t\cdot\Delta I\cdot HH'\omega_0\omega'_0/\Phi(\omega_0),\end{aligned}\right\}\qquad(4.8\,a)$$

$$\left.\begin{aligned}&\frac{E'_P}{E_P}=\frac{\Delta I\cdot\gamma^2\omega_0\omega'_0}{Gf(\omega'_0)-(\Delta I)^2H'\omega_0^2\omega_0'^2},\quad \frac{E'_M}{E_M}=\frac{\Delta I\cdot H\omega_0\omega'_0}{f(\omega'_0)},\\ &\frac{F'_P}{F_P}=\frac{\Delta I\cdot H'\omega_0\omega'_0}{f(\omega'_0)},\quad \frac{F'_M}{F_M}=\frac{\Delta I\cdot H'\omega_0\omega'_0}{f(\omega'_0)}.\end{aligned}\right\}\qquad(4.10\,a)$$

4.3. Characteristics of the vibratory system with rotating inequality[14]

When the frequency ω_0 of disturbances comes near one of the roots of $f(p)=0$, *i.e.*, a natural frequency p, one has $f(\omega_0)\fallingdotseq 0$. Furthermore when ω_0 becomes nearly equal to $\overline{p}$, the relationship $\omega_0\fallingdotseq\overline{p}=2\lambda\omega-p$ leads to $2\lambda\omega-\omega_0=\omega'_0\fallingdotseq p$, and hence $f(\omega'_0)\fallingdotseq 0$. Since $\varphi(p)$ in Eq. (4.5) is small of order ε^2, the relationship $f(\omega'_0)\fallingdotseq 0$ or $f(\omega_0)\fallingdotseq 0$ yields $\Phi(\omega_0)=f(\omega_0)\cdot f(\omega'_0)+\varphi(\omega_0)\fallingdotseq 0$. Accordingly, it can be seen from Eq. (4.8) that, when $f(\omega'_0)\fallingdotseq 0$ or $f(\omega_0)\fallingdotseq 0$, all amplitudes of forced vibrations in Eq. (4.8) take large values and the system presents resonant phenomenon because of small $\Phi(\omega_0)$ of order ε^2.

In the resonant state of $\omega_0\fallingdotseq p$, $f(\omega'_0)$ in denominators of Eq. (4.10) is obviously not small and hence all amplitude ratios in Eq. (4.10) become small of order $\Delta\alpha$ etc., *i.e.*, of order ε. It follows that the forced vibration of the same frequency ω_0 as that of disturbances becomes remarkably larger than those of the frequency $\omega'_0=2\lambda\omega-\omega_0$ in the resonant state of $\omega_0\fallingdotseq p$. On the other hand, in the resonant state of $\omega_0\fallingdotseq\overline{p}$, $f(\omega'_0)$ becomes nearly equal to zero and all denominators in Eq.

(4.10) take small values of order ε^2, and hence one has large amplitude ratios of order ε^{-1}. It leads to the following general rule which can be applied to the vibratory shaft system with an anisotropy rotating at an angular velocity $\lambda\omega$: "In the resonant state of $\omega_0 \fallingdotseq \overline{p}$, the forced vibration of the frequency $\omega_0' = 2\lambda\omega - \omega_0$ which is apparently independent of the frequency ω_0 of the external periodic force builds up remarkably".

The above general rule can be also applied to the rotating shaft system with an unsymmetrical rotor, for which the relationships of Eqs. (4.1 a), (4.5 a), (4.10 a) hold.

In the case when the source of the disturbance exists in the rotating shaft system itself, the frequency ω_0 of the disturbance is usually proportional to the angular velocity ω of the shaft, and hence one has

$$\omega_0 = \kappa\omega, \tag{4.11}$$

where κ is a certain constant. The resonant condition $\omega_0 = \overline{p} = 2\lambda\omega - p$ and Eq. (4.11) yield the relationships

$$p = (2\lambda - \kappa)\omega = \nu\omega, \quad \omega = p/\nu, \tag{4.12}$$

in which

$$\nu = 2\lambda - \kappa. \tag{4.13}$$

Insertion of Eq. (4.12) in Eq. (4.7) leads to

$$f(\nu\omega) = (\alpha - M\nu^2\omega^2)\{\delta + \nu(I_p - \nu I)\omega^2\} - \gamma^2 = 0, \tag{4.14}$$

which can be solved analytically and yields

$$\omega^2 = p^2/\nu^2 = \frac{\{\alpha I_p - \nu(\alpha I + \delta M)\} \pm \sqrt{\{\alpha I_p - \nu(\alpha I + \delta M)\}^2 + 4\nu(\alpha\delta - \gamma^2) M(I_p - \nu I)}}{2\nu^2 M(I_p - \nu I)} \tag{4.15}$$

The rotating speed ω given by the above equation furnishes the so-called "resonant point" at which the frequency ω_0 of the disturbance becomes equal to $\overline{p} = 2\lambda\omega - p$.

In the case when ω_0 is proportional to ω, the general rule above mentioned can be rewritten as follows: "In the neighborhood of the resonant point given by Eq. (4.12) or (4.15), the system presents a resonant phenomenon because the frequency ω_0 of the disturbance becomes nearly equal to $\overline{p}$, and the forced vibration of the frequency

$$\omega_0' = 2\lambda\omega - \omega_0 = 2\lambda\omega - \kappa\omega = \nu\omega \fallingdotseq p, \tag{4.16}$$

which is apparently independent of ω_0 grows up remarkably".

In the following several sections, elucidated physical meanings will be presented to some sorts of forced vibrations upon use of the general rule obtained in this section.

4.4. *Forced vibrations of synchronous backward precession caused by flexible bearing pedestal*[4)6)12)]

The authors have pointed out[6)] that forced vibrations of synchronous back-

ward precession of frequency $-\omega$, whose absolute value is equal to the angular velocity of the shaft, take place when a circular shaft is supported by bearing pedestals which deflect slightly. In such a system, the pedestals hardly deform in their longitudinal direction (y-direction) in which they are subjected to tension or compression, while they can slightly deflect in their lateral direction (x-direction) in which bending moment acts to them. By taking into the deflection of pedestal, one has slightly larger spring constants of the shaft in y direction than those in x direction, and hence equations of motion of this system can take the following form:

$$\left.\begin{aligned} &M\ddot{x}+(\alpha-\Delta\alpha)x+(\gamma-\Delta\gamma)\theta_x=Me\omega^2\cos(\omega t+\beta_1)\\ &M\ddot{y}+(\alpha+\Delta\alpha)y+(\gamma+\Delta\gamma)\theta_y=Me\omega^2\sin(\omega t+\beta_1)\\ &I\ddot{\theta}_x+I_p\omega\dot{\theta}_y+(\gamma-\Delta\gamma)x+(\delta-\Delta\delta)\theta_x=(I_p-I)\tau\omega^2\cos(\omega t+\beta_2)\\ &I\ddot{\theta}_y-I_p\omega\dot{\theta}_x+(\gamma+\Delta\gamma)y+(\delta+\Delta\delta)\theta_y=(I_p-I)\tau\omega^2\sin(\omega t+\beta_2) \end{aligned}\right\} \tag{4.17}$$

Since the anisotropy in bearing pedestals does not rotate and hence the system governed by Eq. (4.17) can be regarded as the one of vibratory shaft systems with the rotating inequality which rotates at $\lambda\omega=0$, it follows that

$$\lambda=0, \tag{4.18}$$

and

$$\bar{p}=2\lambda\omega-p=-p. \tag{4.19}$$

Disturbances induced by unbalances e and τ have the frequency ω, as is seen from Eq. (4.17). Thus

$$\omega_0=\kappa\omega=\omega, \qquad \therefore \quad \kappa=1. \tag{4.20}$$

Hence by Eqs. (4.18), (4.20)

$$\nu=2\lambda-\kappa=0-1=-1. \tag{4.13 a}$$

Substituting $\nu=-1$ into Eq. (4.15), one gets the resonant point

$$\frac{\omega_{b1}^2}{\omega_{b2}^2}=\frac{\{\alpha(I_p+I)+\delta M\}\pm\sqrt{\{\alpha(I_p+I)-\delta M\}^2+4\gamma^2M(I_p+I)}}{2M(I_p+I)}, \tag{4.15 a}$$

at which $\omega_0(=\omega)$ becomes equal to $\bar{p}(=-p)$, *i.e.*, the relationship

$$\omega=p/\nu=-p \tag{4.12 a}$$

holds. Insertion of $\nu=-1$ into Eq. (4.16) yields the frequency

$$\omega_0'=\nu\omega=-\omega \tag{4.16 a}$$

of the forced vibration which builds up remarkably in the resonant state of $\omega_0\fallingdotseq\bar{p}$.

The above discussion leads to the following conclusion: "When bearing pedestals deflect slightly, the forced vibration of synchronous backward precession having frequency $-\omega$ which is induced by unbalances e, τ of the rotor builds up in the neighborhood of the resonant point ω_{b1} or ω_{b2} where the angular velocity ω becomes equal to $-p$".

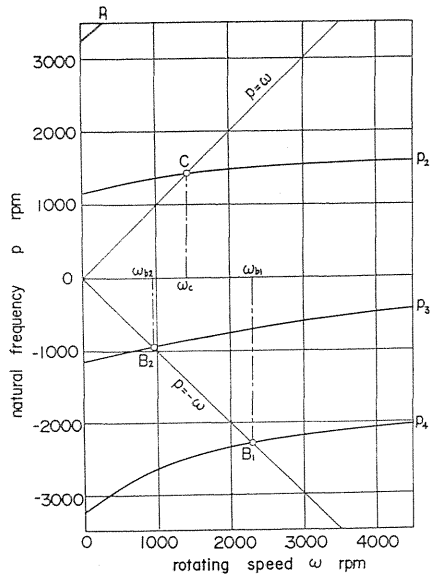

($Mg=6.927$ kg, $I=0.5769$ kg cm s^2, $I_p \fallingdotseq 2I$, $\alpha=2.505\times10^2$ kg/cm, $\gamma=-2.605\times10^3$ kg/rad, $\delta=5.58\times10^4$ kg cm/rad)

FIG. 4.1. $p-\omega$ diagram and the positions of the critical speeds of synchronous backward precession ($\lambda=0$, $\kappa=1$, $\nu=-1$).

One example of $p-\omega$ diagram obtained from Eq. (4.7) is illustrated in Fig. 4.1. As shown in Fig. 4.1, the resonant points ω_{b1}, ω_{b2} given by Eq. (4.15 a) can be obtained graphically from the intersecting points B_1, B_2 where the straight line $p=-\omega$ intersects curves of p_3, p_4 and the relationships $\omega_0=\omega=\overline{p}_4=-p_4$ and $\omega_0=\omega=\overline{p}_3=-p_3$ hold.

The intersecting point C where the straight line $p=\omega$ intersects the curve of p_2 gives the so-called major critical speed ω_c. In the neighborhood of ω_c, namely, in the resonant state of $\omega_0=\omega\fallingdotseq p$, the forced vibration of synchronous forward precession of frequency $\omega_0=+\omega$ grows up remarkably larger than that of frequency $\omega_0'=-\omega$.

One example of experimental results is shown in Fig. 4.2 where the peaks of synchronous backward and forward precessions appear in the neighborhood of ω_{b1}, ω_{b2} and ω_c in Fig. 4.1 respectively.

Amplitudes and amplitude ratios of forced vibrations of synchronous back-

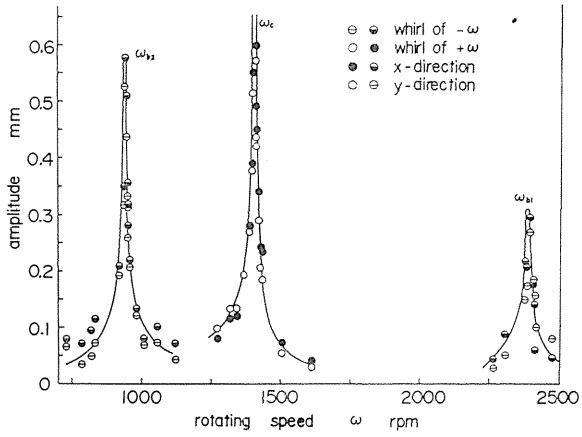

($\Delta\alpha=0.195\times10^2$ kg/cm, $\Delta\gamma=-0.115\times10^3$ kg/rad, $\Delta\delta=0.05\times10^4$ kg cm/rad, Other dimensions of the shaft system are the same as Fig. 4.1).

FIG. 4.2. Whirling of synchronous backward precession of frequency $-\omega$ (at ω_{b1}, ω_{b2}).

ward precession can be derived by putting $\lambda=0$, $\omega_0=\omega$, $P=Me\omega^2$, $M_t=(I_p-I)\tau\omega^2$ in Eqs. (4.8), (4.10), respectively.

4.5. The secondary critical speed

It has been known that, in a horizontal shaft with small inequalities $\Delta\alpha$, $\Delta\gamma$, $\Delta\delta$ of shaft stiffness like a horizontal flat shaft, the phenomenon of the so-called secondary critical speed caused by a gravity of the rotor takes place in the neighborhood of $\omega=\omega_c/2$[2)3)]. It is, however, not so easy to understand the reason why only the forced vibration of forward precession appears at the secondary critical speed. Furthermore, it has been not plainly explained yet that, even in the rotating shaft system in which the spring constant γ vanishes and deflections and inclinations of the rotor do not couple each other and hence the deflections are not subject to any influence of the gyroscopic moment, why the gravity of the rotor acting in the vertical direction (y-direction) causes the whirling motion of forward precession in xy-plane at the secondary critical speed.

Upon use of the general rule above mentioned, these questions can be made clear as follows. Since the inequalities $\Delta\alpha$, $\Delta\gamma$, $\Delta\delta$ in shaft stiffness rotate with the shaft and hence one has

$$\lambda\omega=\omega, \qquad \therefore\ \lambda=1. \tag{4.21}$$

Let the external forces in the right hand side of the first and second equations in Eq. (4.1), *i.e.*, the external forces in x, y directions be P_x, P_y respectively.

$$P_x=P\cos(\omega_0 t+\beta_1), \quad P_y=P\sin(\omega_0 t+\beta_1) \tag{4.22}$$

By putting $P=Mg$, $\beta_1=-\pi/2$, $\omega_0=0$, one has

$$P_x=0, \qquad P_y=-Mg, \tag{4.23}$$

which represents the gravity of the rotor acting vertically in y-direction. Accordingly, the gravity can be considered as an external force of frequency $\omega_0=0$. Thus one has

$$\omega_0=\kappa\omega=0, \qquad \therefore\ \kappa=0. \tag{4.24}$$

From Eqs. (4.21), (4.24), one obtains

$$\nu=2\lambda-\kappa=2-0=2, \tag{4.13 b}$$

$$\omega_0'=2\lambda\omega-\kappa\omega=\nu\omega=2\omega. \tag{4.16 b}$$

The resonant point is given by Eq. (4.12) as follows:

$$\omega=p/\nu=p/2. \tag{4.12 b}$$

Consequently, the phenomenon of the secondary critical speed can be explained as follows: "In the neighborhood of the resonant point $\omega=p/2$ at which the frequency $\omega_0\,(=0)$ of the external force, *i.e.*, the gravity becomes equal to $\overline{p}=2\lambda\omega-p=2\omega-p$, namely, in the neighborhood of the secondary critical speed, the forced vibration of forward precession having the frequency $\omega_0'=\nu\omega=+2\omega$ takes place remarkably".

By substituting $\nu=2$ in Eqs. (4.14), (4.15), one obtains analytically the secondary critical speed. As shown in Fig. 4.3, intersecting points S_1, S_2 at which a straight line $\omega=p/2$ $(p=+2\omega)$ intersects curves of p_1, p_2 furnish graphically the secondary critical speeds ω_{s1}, ω_{s2}. At rotating speed ω'_{s1}, ω'_{s2} determined by intersecting points S'_1, S'_2 at which a straight line $p=-2\omega$ crosses curves p_4, p_3, the phenomenon of the secondary critical speed does not occur, because the whirling motion of backward precession with a frequency -2ω cannot appear in the neighborhood of the secondary critical speed.

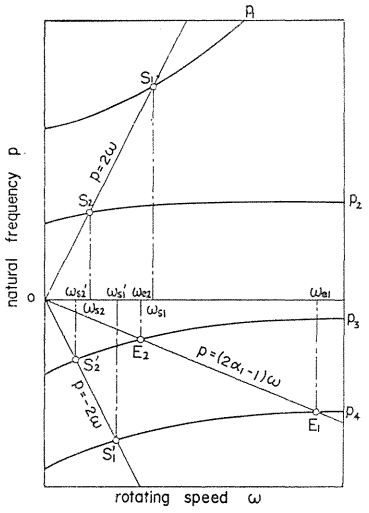

FIG. 4.3. $p-\omega$ diagram.

By putting $\lambda=1$, $\omega_0=0$, $P=Mg$, $M_t=0$ in Eqs. (4.8), (4.10), one obtains amplitudes and amplitude ratios in the neighborhood of the secondary critical speed.

Since the relationship $p=\omega_c$ holds in the rotating shaft system in which the spring constant γ becomes equal to zero, the resonant point of the secondary critical speed is given by $\omega=p/2=\omega_c/2$, which is a rotating speed of a half of the major critical speed ω_c.

It is easily seen from Eq. (4.10 a) that, when the rotating inequality takes its rise in the unsymmetrical rotor, the secondary critical speed does not appear because all numerators containing $\omega_0(=0)$ vanish.

4.6. The whirl of backward precession of shaft supported by ball bearing[7)16)]

Balls in a ball bearing rotate around the center of the inner ring at the following angular velocity ω_1 which is determined under the condition that the rolling contact is kept between balls and inner and outer rings:

$$\omega_1=D\omega/\{2(D+d)\}=\alpha_1\omega, \qquad (\alpha_1<1/2), \tag{4.25}$$

where D and d are diameters of inner ring and ball respectively. It has been reported by one of the authors that a difference in diameter of the balls results in the anisotropy[16)] of shaft stiffness rotating at ω_1 as shown in Fig. 4.4, and this anisotropy causes the whirl[16)] of backward precession of frequency $(2\alpha_1-1)\omega$ in cooperation with unbalances e, τ of the rotor.

The general rule previously mentioned can elucidate this vibratory phenomenon. In this case, the angular velocity of inequality $\lambda\omega$ is given by

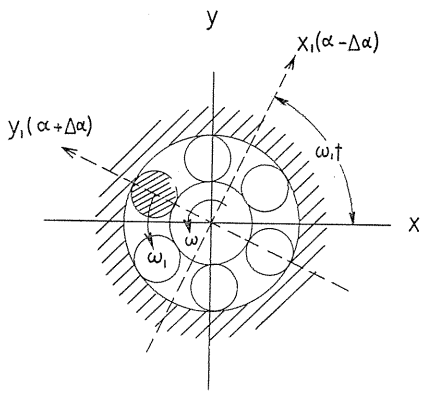

FIG 4.4. A difference in diameter of balls.

$$\lambda\omega = \omega_1 = \alpha_1\omega, \qquad \therefore \quad \lambda = \alpha_1, \tag{4.26}$$

so

$$\bar{p} = 2\lambda\omega - p = 2\alpha_1\omega - p. \tag{4.27}$$

The frequency ω_0 of disturbance induced by unbalances e, τ is obviously equal to the rotating speed ω of the shaft.

$$\omega_0 = \kappa\omega = \omega, \qquad \therefore \quad \kappa = 1 \tag{4.28}$$

From Eqs. (4.26), (4.28), one has

$$\nu = 2\lambda - \kappa = 2\alpha_1 - 1, \qquad (\nu < 0) \tag{4.13 c}$$

$$\omega_0' = 2\lambda\omega - \kappa\omega = \nu\omega = (2\alpha_1 - 1)\omega, \qquad (\omega_0' < 0) \tag{4.16 c}$$

Accordingly, the resonant point is given by

$$\omega = p/\nu = p/(2\alpha_1 - 1). \tag{4.12 c}$$

As is seen in Eq. (4.25), the value of α_1 is always smaller than 1/2, and hence $\nu = 2\alpha_1 - 1$ and $\omega_0' = \nu\omega$ take negative values. It follows that the vibration discussed in this section is always a whirl of backward precession. In experiments previously reported, self-aligning double-row ball bearing with $\alpha_1 \fallingdotseq 1/2.65$ was used, and hence one got $\omega_0' = \nu\omega = (2\alpha_1 - 1)\omega \fallingdotseq -\omega/4.1$.

The forced vibration studies in this section can be explained as follows: "In the neighborhood of the resonant point $\omega = p/\nu = p/(2\alpha_1 - 1)$ at which the frequency $\omega_0 (= \omega)$ of disturbances induced by unbalances e, τ of the rotor becomes equal to $\bar{p} = 2\alpha_1\omega - p$, the whirl of backward precession of frequency $\omega_0' = (2\alpha_1 - 1)\omega$ (< 0) grows up remarkably".

By substituting $\nu = (2\alpha_1 - 1)$ in Eqs. (4.14), (4.15), one obtains analytically the resonant point. As shown in Fig. 4.3, intersecting points E_1, E_2 at which a straight line $\omega = p/\nu$ $[p = \nu\omega = (2\alpha_1 - 1)\omega]$ intersects curves of p_4, p_3 determine the resonant points ω_{e1}, ω_{e2}.

By putting $\lambda = \alpha_1$, $\omega_0 = \omega$, $P = Me\omega^2$, $M_t = (I_p - I)\tau\omega^2$ in Eqs. (4.8), (4.10), one obtains amplitudes and amplitude ratios of vibrations of $\omega_0' = (2\alpha_1 - 1)\omega$.

4.7. Conclusions

Obtained conclusions in this chapter may be summarized as follows:

(1) In the rotating shaft system having an anisotropy which rotates at $\lambda\omega$, the system presents resonant phenomena when the frequency ω_0 of disturbances becomes nearly equal to $\bar{p} = 2\lambda\omega - p$ as well as when $\omega_0 = p$.

(2) In such a system, one external force of frequency ω_0 causes two forced vibrations of frequencies ω_0 and $\omega_0' = 2\lambda\omega - \omega_0$.

(3) In the resonant state of $\omega_0 \fallingdotseq p$, the forced vibration of frequency ω_0 builds up remarkably larger than that of frequency ω_0'.

(4) In the resonant state of $\omega_0 \fallingdotseq \bar{p}$, the forced vibration of frequency $\omega_0' = 2\lambda\omega - \omega_0$ grows up remarkably larger than that of frequency ω_0.

(5) When the frequency ω_0 of disturbance is proportional to the angular velocity ω of the shaft, the resonant point, the frequency ω_0' of forced vibration can be determined analytically even for the general vibratory system with $\gamma \neq 0$.

(6) Upon use of the general rule of (4), elucidated physical meanings can

be presented to some sorts of vibrations whose cause of occurrence is rather difficult to understand.

Chapter 5. On Vibrations of a Rotor with Variable Rotating Speed[23]

5.1. *Introduction*

There is, in general, the so called "gyroscopic term" in equations of motion of a rotor, whose magnitude is proportional to an angular velocity ω of the rotor. When the rotating speed ω of the rotor fluctuates periodically, equations of motion of the rotor turn into linear differential equations with variable coefficients[1]. In this chapter, effects of these gyroscopic terms, *i.e.*, the inertia terms with variable coefficients are investigated. In these systems governed by equations with variable inertia terms, likewise in a flat shaft system[2)3)], in a rotating shaft system with an unsymmetrical rotor[10)13)] and in a system governed by Mathieu's equation[17)], it is expected that there are unstable regions where unstable vibrations aggravate with time t. Analytical results in this chapter, however, show that there is no unstable region in the rotating shaft system with fluctuations of the angular velocity ω. It is also found that characteristics of forced vibrations appearing in such a system similar to those of the system with unsymmetrical rotor[14)] are furnished by variable inertia terms. Furthermore, it is pointed out that the variable inertia terms with a frequency $\nu\omega$ yield forced vibrations with frequencies $(1+\nu)\omega$ and $(1-\nu)\omega$ as well as the frequency ω.

5.2. *Equations of motion*

First, the procedure to introduce the equations of motion will be briefly explained. In this section, it is assumed that there is no unbalance in the rotor. It can be also assumed that lateral vibrations and torsional vibrations are not coupled, even if torsional vibrations are induced by periodic fluctuations of the angular velocity ω. Accordingly, elastic forces P_x, P_y and moments M_{tx}, M_{ty} of the shaft acting on the rotor are given by[6)]

$$\left.\begin{aligned} P_x &= -\alpha x - \gamma\theta_x, \quad M_{ty} = -\gamma x - \delta\theta_x, \\ P_y &= -\alpha y - \gamma\theta_y, \quad -M_{tx} = -\gamma y - \delta\theta_y \end{aligned}\right\} \tag{5.1}$$

where x, y are deflections of the rotor in x, y directions; θ_x, θ_y inclination angles of the rotor in x, y directions; α, γ, δ spring constants of the shaft.

Although equations of motion for x, y are given by rather simple forms

$$M\ddot{x} = P_x, \qquad M\ddot{y} = P_y \tag{5.2}$$

a relatively complicate procedure is needed to obtain equations of motion for θ_x, θ_y, as explained in the following.

In a fixed coordinate system o-xyz in Fig. 5.1, the z axis is a bearing center line, the origin o being an equilibrium position of a center of the rotor $M(x, y)$ which moves in the xy plane. Configurations of the rotor are illustrated by those of a disk, as shown in Fig. 5.1, where MK denotes the line of intersection of the disk and the xy plane, M-$X_2Y_2Z_1$ consists of three principal axes of the

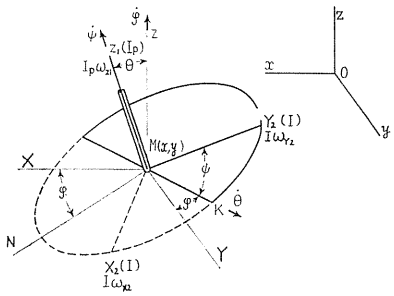

FIG. 5.1. Eulerian angles θ, φ, ψ.

rotor, and the polar moment of inertia I_p is the principal moment of inertia about MZ_1 axis, the diametral moment of inertia I is the principal moment of inertia about MX_2 and MY_2. A coordinate system M-XYZ is parallel to o-xyz, and MN is a projection of MZ_1 on the xy plane. Since angles

$$\angle Z_1MZ=\theta,\ \angle XMN=\varphi,\ \angle Y_2MK=\psi \tag{5.3}$$

are the so called "Eulerian angles", angular velocities in the system are $\dot{\theta}$, $\dot{\varphi}$ and $\dot{\psi}$, whose directions are MK, MZ and MZ_1 respectively. As direction cosines between three principal axes of moment of inertia MX_2, MY_2, MZ_1 and MZ-axis are $-\sin\theta\cos\psi$, $\sin\theta\sin\psi$ and $\cos\theta$ separately[6], angular velocities ω_{X2}, ω_{Y2}, and ω_{Z1} in the directions of the principal axes are as follows:

$$\left.\begin{aligned} &MX_2 \text{ direction}: && \omega_{X2}=\dot{\theta}\sin\psi-\dot{\varphi}\sin\theta\cos\psi \\ &MY_2 \text{ direction}: && \omega_{Y2}=\dot{\theta}\cos\psi+\dot{\varphi}\sin\theta\sin\psi \\ &MZ_1 \text{ direction}: && \omega_{Z1}=\dot{\varphi}\cos\theta+\dot{\psi} \end{aligned}\right\} \tag{5.4}$$

Since angular momentums in directions MX_2, MY_2 and MZ_1 are $I\omega_{X2}$, $I\omega_{Y2}$ and $I_p\omega_{Z1}$, respectively, the following Euler's equations furnish time rate of change of the angular momentums per unit time H_{X2}, H_{Y2} and H_{Z1} in these directions:

$$\left.\begin{aligned} H_{X2}&=I\dot{\omega}_{X2}-(I-I_p)\,\omega_{Y2}\omega_{Z1}, \\ H_{Y2}&=I\dot{\omega}_{Y2}-(I_p-I)\,\omega_{Z1}\omega_{X2}, \\ H_{Z1}&=I_p\dot{\omega}_{Z1}-(I-I)\,\omega_{X2}\omega_{Y2}=I_p\dot{\omega}_{Z1} \end{aligned}\right\} \tag{5.5}$$

Denoting direction cosines of three principal axes MX_2, MY_2 and MZ_1 with respect to o-xyz as l_1, l_2, l_3; m_1, m_2, m_3; n_1, n_2, n_3; time rate of change of the angular momentums in x, y and z directions as H_x, H_y and H_z, external moments acting on the rotor as M_{tx}, M_{ty} and M_{tz}, we get the following relationships:

$$\left.\begin{aligned} H_x&=H_{X2}l_1+H_{Y2}l_2+H_{Z1}l_3=M_{tx} \\ H_y&=H_{X2}m_1+H_{Y2}m_2+H_{Z1}m_3=M_{ty} \\ H_z&=H_{X2}n_1+H_{Y2}n_2+H_{Z1}n_3=M_{tz} \end{aligned}\right\} \tag{5.6}$$

When terms smaller than the third can be neglected, components θ_x, θ_y of an inclination angle θ of the rotor can be represented by

$$\theta_x = \theta \cos\varphi, \quad \theta_y = \theta \sin\varphi \tag{5.7}$$

By inserting values[6] of direction cosines l_1, l_2 etc. and Eqs. (5.1), (5.4), (5.5), (5.7) into Eqs. (5.2), (5.6), and by dropping terms smaller than the second, equations of motion of the rotor are obtained as follows:

$$\left.\begin{aligned} &I_p\ddot{\Theta} = M_{tz}, \\ &M\ddot{x} + \alpha x + \gamma\theta_x = 0 \\ &M\ddot{y} + \alpha y + \gamma\theta_y = 0 \\ &I\ddot{\theta}_x + I_p\frac{d}{dt}(\dot{\Theta}\theta_y) + \gamma x + \delta\theta_x = 0 \\ &I\ddot{\theta}_y - I_p\frac{d}{dt}(\dot{\Theta}\theta_x) + \gamma y + \delta\theta_y = 0 \end{aligned}\right\} \tag{5.8}$$

where

$$\dot{\Theta} = \dot{\varphi} + \dot{\phi} \tag{5.9}$$

Since the moment M_{tz} in Eq. (5.8) is determined by states of a driver and a follower of the shaft, *i.e.*, of a prime mover and a load on the shaft, it is independent of values x, y, θ_x, θ_y. When M_{tz} is given, $\ddot{\Theta}$ and $\dot{\Theta}$ can be determined from the first equation in Eq. (5.8). It is assumed here that the angular velocity $\dot{\Theta}$ fluctuates periodically with frequency $\nu\omega$, and is given by

$$\dot{\Theta} = \omega(1 - 2\varepsilon\nu\cos\nu\omega t) \tag{5.10}$$

in which ε is a small quantity and ν is a certain constant. By substituting Eq. (5.10) into Eq. (5.8), by introducing dimensionless quantities Eq. (1.12) and by omitting primes, Eq. (5.8) is reduced to

$$\left.\begin{aligned} &\ddot{x} + x + \gamma\theta_x = 0, \\ &\ddot{y} + y + \gamma\theta_y = 0, \\ &\ddot{\theta}_x + i_p\omega\dot{\theta}_y - 2\varepsilon\nu i_p\omega\frac{d}{dt}(\theta_y\cos\nu\omega t) + \gamma x + \delta\theta_x = 0, \\ &\ddot{\theta}_y - i_p\omega\dot{\theta}_x + 2\varepsilon\nu i_p\omega\frac{d}{dt}(\theta_x\cos\nu\omega t) + \gamma y + \delta\theta_y = 0 \end{aligned}\right\} \tag{5.11}$$

5.3. Free vibrations

In this section, a general form of solutions for free vibrations in the system governed by Eq. (5.8) having variable inertia terms is presented, and further it is verified that there exists no unstable region in such a system.

When the angular velocity $\dot{\Theta}$ pulsates periodically as shown in Eq. (5.10), free vibrations of frequencies $p-\nu\omega$, $p+\nu\omega$ with small amplitudes of order ε, those of $p-2\nu\omega$, $p+2\nu\omega$ with small amplitudes of order ε^2 as well as free vibrations of frequency p can occur. Accordingly free vibrations should be given by

$$\left.\begin{aligned}\begin{matrix}x\\y\end{matrix} &= a\begin{matrix}\cos\\\sin\end{matrix}(pt+\beta)+\varepsilon\bar{a}\begin{matrix}\cos\\\sin\end{matrix}(\bar{p}t+\beta)+\varepsilon a'\begin{matrix}\cos\\\sin\end{matrix}(p't+\beta)\\ &\quad+\varepsilon^2\bar{\bar{a}}\begin{matrix}\cos\\\sin\end{matrix}(\bar{\bar{p}}t+\beta)+\varepsilon^2 a''\begin{matrix}\cos\\\sin\end{matrix}(p''t+\beta)+\cdots,\\ \begin{matrix}\theta_x\\\theta_y\end{matrix} &= b\begin{matrix}\cos\\\sin\end{matrix}(pt+\beta)+\varepsilon\bar{b}\begin{matrix}\cos\\\sin\end{matrix}(\bar{p}t+\beta)+\varepsilon b'\begin{matrix}\cos\\\sin\end{matrix}(p't+\beta)\\ &\quad+\varepsilon^2\bar{\bar{b}}\begin{matrix}\cos\\\sin\end{matrix}(\bar{\bar{p}}t+\beta)+\varepsilon^2 b''\begin{matrix}\cos\\\sin\end{matrix}(p''t+\beta)+\cdots.\end{aligned}\right\}\tag{5.12}$$

where β is a phase angle, ... represents small terms of ε^3, ε^4, ..., and

$$\bar{p}=p-\nu\omega,\ p'=p+\nu\omega,\ \bar{\bar{p}}=p-2\nu\omega,\ p''=p+2\nu\omega \tag{5.13}$$

Since gyroscopic terms are contained in equations of motion, motions of the shaft are not rectilinear vibrations, but whirling motions. Consequently, a positive or a negative sign of the frequency means a forward precession whose direction of whirl is the same as that of the angular velocity ω of the shaft or a backward precession in which the shaft whirls in the opposite direction to that of ω[6]. It should be noticed that free vibrations of frequencies $p-\nu\omega$, $p+\nu\omega$ can appear but those of $\nu\omega-p$, $-p-\nu\omega$ do not exist in the system[10)13)].

Substituting Eq. (5.12) into Eq. (5.11), and dropping small terms of ε^3, ε^4, ..., we get

$$\left.\begin{aligned}&Ha+\gamma b=0,\ \gamma a+Gb-\varepsilon^2\nu i_p\omega p(\bar{b}+b')=0\\ &\bar{H}\bar{a}+\gamma\bar{b}=0,\ -\nu i_p\omega\bar{p}\bar{b}+\gamma\bar{a}+\bar{G}\bar{b}=0\\ &H'a'+\gamma b'=0,\ -\nu i_p\omega p'b+\gamma a'+G'b'=0\end{aligned}\right\}\tag{5.14}$$

in which

$$\left.\begin{aligned}&H=1-p^2,\ \bar{H}=1-\bar{p}^2,\ H'=1-p'^2\\ &G=\delta+i_p\omega p-p^2,\ \bar{G}=\delta+i_p\omega\bar{p}-\bar{p}^2,\ G'=\delta+i_p\omega p'-p'^2\end{aligned}\right\}\tag{5.15}$$

Eliminating amplitudes a, b etc. from Eq. (5.14) and putting

$$\left.\begin{aligned}&f(p)=HG-\gamma^2=(1-p^2)(\delta+i_p\omega p-p^2)-\gamma^2,\\ &\bar{f}=f(\bar{p}),\ f'=f(p'),\ \varphi=\nu^2 i_p^2\omega^2 pH(\bar{p}\bar{H}f'+p'H'\bar{f})\end{aligned}\right\}\tag{5.16}$$

we get the following frequency equation:

$$\Phi=f\bar{f}f'-\varepsilon^2\varphi=0 \tag{5.17}$$

A natural frequency vs. rotating speed diagram, *i.e.*, a $p-\omega$ diagram obtained from $f\bar{f}f'=0$, which is a frequency equation when $\varepsilon=0$, is illustrated in Fig. 5.2. When $\dot{\Theta}=$ constant, the frequency equation is reduced to $f=0$[6] whose roots p_1, p_2, p_3, p_4 are shown by full line curves in Fig. 5.2 where curves $\bar{f}=0$ and $f'=0$ are represented by broken and dotted line separately. Since the relationships Eq. (1.20) and

$$\left.\begin{aligned}&\text{(i)}\ \ p_3=-p_2,\ \ p_4=-p_1,\ \ \text{at}\ \ \omega=0\\&\text{(ii)}\ \ p_1\to i_p\omega,\ \ p_2\to 1,\ \ p_3\to 0,\ \ p_4\to -1,\ \ \text{as}\ \ \omega\to\infty\end{aligned}\right\}\qquad (5.18)$$

can be always satisfied[6)13)], all $p-\omega$ diagrams of the system consisting of the elastic shaft and the rotor are similar to Fig. 5.2, and the number of the intersections A, A', ..., F, F', between $f=0$, $\bar{f}=0$ and $f=0$, $f'=0$ is always twelve.

If there is an unstable region in which unstable vibrations aggravate, it should have a width of order ε, and it appears in the neighborhood of the intersecting points A, ..., F'[13)]. In the neighborhood of the intersection C of two curves $f=0$ and $\bar{f}=0$, there is an unstable region when curves $\Phi=0$ take forms as Fig. 5.3 (a), and no unstable region in the case of Fig. 5.3 (b)[13)18)]. In the neighborhood of C, the relations $f\fallingdotseq 0$, $\bar{f}\fallingdotseq 0$ are satisfied, and accordingly $\varphi\fallingdotseq\nu^2 i_p^2\omega^2 p\bar{p}H\bar{H}f'$, and Eq. (5.17) reduces to

$$\Phi=f'(f\bar{f}-\varepsilon^2\nu^2 i_p^2\omega^2 p\bar{p}H\bar{H})=0\qquad (5.17\,a)$$

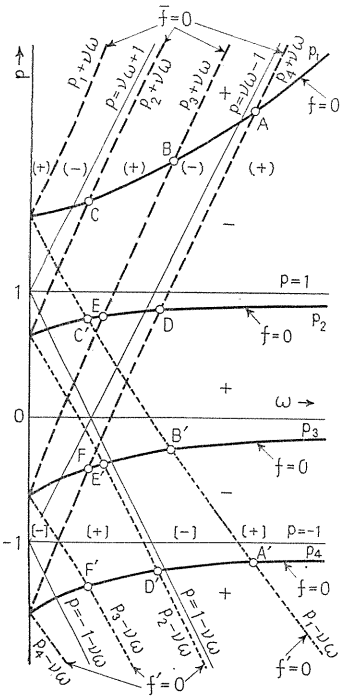

$f=0$: $+-$, $\bar{f}=0$: $(+)(-)$, $f'=0$: $[+][-]$

FIG. 5.2. $p-\omega$ diagram.

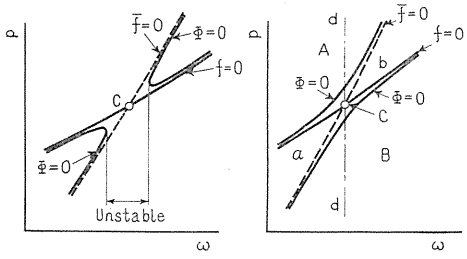

FIG. 5.3. $\Phi=0$ curves.

provided small terms of order ε^3 can be neglected. Since the curves $\Phi=0$ exist only in the region of the $p-\omega$ plane in which the sign of $f\bar{f}$ is the same as that of $p\bar{p}H\bar{H}$, then $f\bar{f}\cdot p\bar{p}H\bar{H}$ takes a positive value in the upper and lower regions A, B in Fig. 5.3 (b), and it is negative in the left and right hand side regions a, b in Fig. 5.3 (b). Accordingly, when $p\bar{p}H\bar{H}>0$, the positive value of $f\bar{f}$ in the regions A, B in Fig. 5.3 (b) changing its magnitude along the vertical chain line dd takes its minimum value zero at the point C, and accordingly $\dfrac{\partial^2(f\bar{f})}{\partial p^2}>0$ and $p\bar{p}H\bar{H}\dfrac{\partial^2(f\bar{f})}{\partial p^2}>0$ at C. When $p\bar{p}H\bar{H}<0$, the negative value of $f\bar{f}$ takes its maximum value zero at C, thus $\dfrac{\partial^2(f\bar{f})}{\partial p^2}<0$ and $p\bar{p}H\bar{H}\dfrac{\partial^2(f\bar{f})}{\partial p^2}>0$ are obtained. From the above discussion, it can be concluded that in the neighborhood of the

intersection C of two curves $f=0$ and $\bar{f}=0$, there is no unstable region under the condition $p\bar{p}H\bar{H}\dfrac{\partial^2(f\bar{f})}{\partial p^2}>0$. Since the relationship $\dfrac{\partial^2(f\bar{f})}{\partial p^2}=2\dfrac{\partial f}{\partial p}\dfrac{\partial \bar{f}}{\omega p}$ holds at C, the above condition can be rewritten as follows:

$$p\bar{p}H\bar{H}\frac{\partial f}{\partial p}\frac{\partial \bar{f}}{\partial p}>0 \tag{5.19a}$$

A similar procedure verifies that there exists no unstable region in the neighborhood of the intersection of two curves $f=0$ and $f'=0$ under the condition

$$pp'HH'\frac{\partial f}{\partial p}\frac{\partial f'}{\partial p}>0 \tag{5.19b}$$

It will be discussed whether the conditions (5.19a) and (5.19b) are satisfied or not in the neighborhood of the intersections A, B, ... in Fig. 5.2. Values of f, $\bar{f}$ and f' on the $p-\omega$ plane change their signs on the curves $f=0$, $\bar{f}=0$ and $f'=0$ respectively. Signs of f, $\bar{f}$ and f' are illustrated by notations $+$, $-$, $(+)$, $(-)$, $[+]$, $[-]$, separately in Fig. 5.2. For instance, at the intersection A of two curves $f=0$ and $\bar{f}=0$, relationships $\partial f/\partial p>0$, $\partial\bar{f}/\partial p<0$ hold, which can be easily obtained from Fig. 5.2. Further, it is seen from Eq. (5.18) that relations $p=p_1>0$, $\bar{p}=p_1-\nu\omega=p_4<0$, $H=1-p_1^2<0$ and $\bar{H}=1-\bar{p}^2=1-p_4^2<0$ are satisfied at the point A. Consequently, it can be found that condition Eq. (5.19a) holds at A and there is no unstable region in the neighborhood of A. Similar discussion as given in Table 5.1 leads to the conclusion that an unstable region does not develop in the neighborhoods of all intersecting points $A, A', \ldots, F, F'$ in Fig. 5.2. Thus it can be concluded that, although equations of motion belong to differential equations with variable coefficients, unstable lateral vibrations cannot appear in the rotating shaft system whose angular velocity fluctuates periodically with frequency $\nu\omega$.

As seen in Fig. 5.2, there are many intersections of two curves $\bar{f}=0$ and $f'=0$. In the neighborhood of these intersections, unstable regions with the width of order ε^2 may appear. These small unstable regions, however, are not discussed in the present paper.

TABLE 5.1. Signs at the Intersections $A, A', \ldots, F, F'$

	p	$\bar{p}$	H	$\bar{H}$	$\dfrac{\partial f}{\partial p}$	$\dfrac{\partial \bar{f}}{\partial p}$	$p\bar{p}H\bar{H}\dfrac{\partial f}{\partial p}\dfrac{\partial \bar{f}}{\partial p}$
A	+	−	−	−	+	−	+
B	+	−	−	+	+	+	+
C	+	+	−	+	+	−	+
D	+	−	+	−	−	−	+
E	+	−	+	+	−	+	+
F	−	−	+	−	+	−	+

	p	p'	H	H'	$\dfrac{\partial f}{\partial p}$	$\dfrac{\partial f'}{\partial p}$	$pp'HH'\dfrac{\partial f}{\partial p}\dfrac{\partial f'}{\partial p}$
A′	−	+	−	−	−	+	+
B′	−	+	+	−	+	+	+
C′	+	+	+	−	−	+	+
D′	−	+	−	+	−	−	+
E′	−	+	+	+	+	−	+
F′	−	−	−	+	−	+	+

5.4. *Forced vibrations*

5.4.1. *Forced vibrations induced by an external force of a frequency* ω_0

Since all vibrations appearing in the rotating shaft are whirling motions, an external force represented by a rotating vector like a centrifugal force should

be considered as one elementary force[6]. When there are many external forces, the principle of superposition may be adopted. When the external force of a frequency ω_0 acts on the system, equations of motion are given by

$$\left.\begin{aligned}
&\ddot{x}+x+\gamma\theta_x = P\cos(\omega_0 t+\beta')\\
&\ddot{y}+y+\gamma\theta_y = P\sin(\omega_0 t+\beta')\\
&\ddot{\theta}_x+i_p\omega\dot{\theta}_y-2\varepsilon\nu i_p\omega\frac{d}{dt}(\theta_y\cos\nu\omega t)+\gamma x+\delta\theta_x = M_t\cos(\omega_0 t+\beta'')\\
&\ddot{\theta}_y-i_p\omega\dot{\theta}_x+2\varepsilon\nu i_p\omega\frac{d}{dt}(\theta_x\cos\nu\omega t)+\gamma y+\delta\theta_y = M_t\sin(\omega_0 t+\beta'')
\end{aligned}\right\} \tag{5.20}$$

in which β' and β'' are phase angles. Forced vibrations of the system governed by Eq. (5.20) can be expressed by

$$\left.\begin{aligned}
\begin{matrix}x\\y\end{matrix} &= E_P\begin{matrix}\cos\\\sin\end{matrix}(\omega_0 t+\beta')+\varepsilon\bar{E}_P\begin{matrix}\cos\\\sin\end{matrix}(\bar{\omega}_0 t+\beta')+\varepsilon E'_P\begin{matrix}\cos\\\sin\end{matrix}(\omega'_0 t+\beta')\\
&\quad+E_M\begin{matrix}\cos\\\sin\end{matrix}(\omega_0 t+\beta'')+\varepsilon\bar{E}_M\begin{matrix}\cos\\\sin\end{matrix}(\bar{\omega}_0 t+\beta'')+\varepsilon E'_M\begin{matrix}\cos\\\sin\end{matrix}(\omega'_0 t+\beta'')+\cdots\\
\begin{matrix}\theta_x\\\theta_y\end{matrix} &= F_P\begin{matrix}\cos\\\sin\end{matrix}(\omega_0 t+\beta')+\varepsilon\bar{F}_P\begin{matrix}\cos\\\sin\end{matrix}(\bar{\omega}_0 t+\beta')+\varepsilon F'_P\begin{matrix}\cos\\\sin\end{matrix}(\omega'_0 t+\beta')\\
&\quad+F_M\begin{matrix}\cos\\\sin\end{matrix}(\omega_0 t+\beta'')+\varepsilon\bar{F}_M\begin{matrix}\cos\\\sin\end{matrix}(\bar{\omega}_0 t+\beta'')+\varepsilon F'_M\begin{matrix}\cos\\\sin\end{matrix}(\omega'_0 t+\beta'')+\cdots
\end{aligned}\right\} \tag{5.21}$$

where $\cdots$ represents small terms of order $\varepsilon^2, \varepsilon^3, \ldots$, and

$$\bar{\omega}_0 = \omega_0-\nu\omega, \quad \omega'_0 = \omega_0+\nu\omega \tag{5.22}$$

It should be noticed that, although only vibration of a frequency $2\omega-\omega_0$ can appear[14] in the flat shaft system and in the shaft system carrying an unsymmetrical rotor, in the system governed by Eq. (5.20) forced vibrations of $\omega_0-2\omega$ as well as $\omega_0+2\omega$ can take place when $\nu=2$. In Eq. (5.21), amplitudes E_P, $\bar{E}_P$ and E'_P are those of vibrations of the deflections with frequencies ω_0, $\bar{\omega}_0$ and ω'_0 respectively, which are caused by the external force P; and E_M, $\bar{E}_M$ and E'_M are amplitudes of forced vibrations of the deflections induced by the moment M_t. Amplitudes F_P, $\bar{F}_P$, F'_P and F_M, $\bar{F}_M$, F'_M are those of vibrations of the inclination angles θ_x, θ_y. Inserting Eq. (5.21) into Eq. (5.20), these amplitudes are determined as follows:

$$\left.\begin{aligned}
&E_P = P\{G_0\bar{f}_0 f'_0-\varepsilon^2\nu^2 i_p^2\omega^2\omega_0(\bar{\omega}_0\bar{H}_0 f'_0+\omega'_0 H'_0\bar{f}_0)\}/D,\\
&\bar{E}_P = P\nu\gamma^2 i_p\omega\bar{\omega}_0 f'_0/D,\quad E'_P = P\nu\gamma^2 i_p\omega\omega'_0\bar{f}_0/D,\\
&F_P = -P\gamma\bar{f}_0 f'_0/D,\quad \bar{F}_P = -P\nu\gamma i_p\omega\bar{\omega}_0\bar{H}_0 f'_0/D,\\
&F'_P = -P\nu\gamma i_p\omega\omega'_0 H'_0\bar{f}_0/D,\quad E_M = -M_t\gamma\bar{f}_0 f'_0/D,\\
&\bar{E}_M = -M_t\nu\gamma i_p\omega\bar{\omega}_0 H_0 f'_0/D,\quad E'_M = -M_t\nu\gamma i_p\omega\omega'_0 H_0\bar{f}_0/D,\\
&F_M = M_t H_0\bar{f}_0 f'_0/D,\quad \bar{F}_M = M_t\nu i_p\omega\bar{\omega}_0 H_0\bar{H}_0 f'_0/D,\\
&F'_M = M_t\nu i_p\omega\omega'_0 H_0 H'_0\bar{f}_0/D
\end{aligned}\right\} \tag{5.23}$$

where
$$D=f_0\bar{f}_0f_0'-\varepsilon^2\nu^2i_p^2\omega^2\omega_0H_0(\bar{\omega}_0\bar{H}_0f_0'+\omega_0'H_0'\bar{f}_0) \tag{5.24}$$
$$\left.\begin{aligned} &H_0=1-\omega_0^2,\quad \bar{H}_0=1-\bar{\omega}_0^2,\quad H_0'=1-\omega_0'^2\\ &G_0=\delta+i_p\omega\omega_0-\omega_0^2,\quad \bar{G}_0=\delta+i_p\omega\bar{\omega}_0-\bar{\omega}_0^2,\quad G_0'=\delta+i_p\omega\omega_0'-\omega_0'^2\\ &f_0=f(\omega_0),\quad \bar{f}_0=\bar{f}(\omega_0),\quad f_0'=f'(\omega_0)\end{aligned}\right\} \tag{5.25}$$

From Eq. (5.23), amplitude ratios between vibration of frequency $\omega_0-\nu\omega$ and ω_0, and between vibration of frequency $\omega_0+\nu\omega$ and ω_0 are derived as follows:

$$\left.\begin{aligned} &\frac{\varepsilon\bar{E}_P}{E_P}=\frac{\varepsilon\nu\gamma^2i_p\omega\bar{\omega}_0f_0'}{G_0\bar{f}_0f_0'-\varepsilon^2\nu^2i_p^2\omega^2\omega_0(\bar{\omega}_0\bar{H}_0f_0'+\omega_0'H_0'\bar{f}_0)}\\ &\frac{\varepsilon\bar{F}_P}{F_P}=\frac{\varepsilon\bar{F}_M}{F_M}=\frac{\varepsilon\nu i_p\omega\bar{\omega}_0\bar{H}_0}{\bar{f}_0},\quad \frac{\varepsilon\bar{E}_M}{E_M}=\frac{\varepsilon\nu i_p\omega\bar{\omega}_0H_0}{\bar{f}_0}\end{aligned}\right\} \tag{5.26 a}$$

$$\left.\begin{aligned} &\frac{\varepsilon E_P'}{E_P}=\frac{\varepsilon\nu\gamma^2i_p\omega\omega_0'\bar{f}_0}{G_0\bar{f}_0f_0'-\varepsilon^2\nu^2i_p^2\omega^2\omega_0(\bar{\omega}_0\bar{H}_0f_0'+\omega_0'H_0'\bar{f}_0)}\\ &\frac{\varepsilon F_P'}{F_P}=\frac{\varepsilon F_M'}{F_M}=\frac{\varepsilon\nu i_p\omega\omega_0'H_0'}{f_0'},\quad \frac{\varepsilon E_M'}{E_M}=\frac{\varepsilon\nu i_p\omega\omega_0'H_0}{f_0'}\end{aligned}\right\} \tag{5.26 b}$$

It is seen from Eq. (5.24) that the relations $f_0\fallingdotseq 0$, $\bar{f}_0\fallingdotseq 0$, $f_0'\fallingdotseq 0$, *i.e.*, $\omega_0\fallingdotseq p_i$ ($i=1, 2, 3, 4$), $\omega_0\fallingdotseq p_i+\nu\omega$ ($\bar{\omega}_0\fallingdotseq p_i$), $\omega_0\fallingdotseq p_i-\nu\omega$ ($\omega_0'\fallingdotseq p_i$) hold, the system presents the resonant condition because of $D\fallingdotseq 0$. Accordingly, when the frequency ω_0 becomes nearly equal to $p_i+\nu\omega$, $p_i-\nu\omega$ as well as p_i, forced vibrations occur and the resonant phenomena take place.

Furthermore, it can be seen from Eqs. (5.26 a), (5.26 b) that, for instance, $\bar{f}_0\fallingdotseq 0$, *i.e.*, $\omega_0\fallingdotseq p_i+\nu\omega$ results in large amplitude ratios in Eq. (5.26 a), and hence forced vibrations of the frequency $\bar{\omega}_0=\omega_0-\nu\omega\fallingdotseq p_i$ develop and their amplitudes become larger than those of the frequency ω_0. When $f_0'\fallingdotseq 0$, *i.e.*, $\omega_0\fallingdotseq p_i-\nu\omega$ holds, magnitudes of amplitude ratios given by Eq. (5.26 b) take large values, which results in larger amplitudes of vibration with frequency $\omega_0'=\omega_0+\nu\omega\fallingdotseq p_i$ than those of ω_0. Since at the resonance of $f_0\fallingdotseq 0$, *i.e.*, $\omega_0\fallingdotseq p_i$, all amplitude ratios in Eqs. (5.26 a), (5.26 b) take small values of order ε, forced vibrations occur with the same freqency ω_0 as the frequency of the external force. From the above discussion, it can be concluded that in the resonant vibrations of frequencies $\omega_0\fallingdotseq p_i+\nu\omega$ and $\omega_0\fallingdotseq p_i-\nu\omega$, forced vibrations of $\bar{\omega}_0\fallingdotseq p_i$ and $\omega_0'\fallingdotseq p_i$ become remarkably larger, their frequencies, *i.e.*, $\bar{\omega}_0$, ω_0' being apparently independent of the frequency ω_0 of the external force.

5.4.2. Forced vibrations caused by unbalances of the rotor

When an eccentricity e and a dynamic unbalance τ exist at the angular position ξ and η respectively, which are angles measured from the axis MY_2 in Fig. 5.1, coordinates of the gravitational center x_G, y_G, inclination angles of the principal axis of moment of inertia θ_{x1}, θ_{y1} are expressed by

$$\begin{matrix}x_G\\ y_G\end{matrix}=\begin{matrix}x\\ y\end{matrix}+e\begin{matrix}\cos\\ \sin\end{matrix}(\Theta+\xi),\quad \begin{matrix}\theta_{x1}\\ \theta_{y1}\end{matrix}=\begin{matrix}\theta_x\\ \theta_y\end{matrix}+\tau\begin{matrix}\cos\\ \sin\end{matrix}(\Theta+\eta) \tag{5.27}$$

provided that terms of $\varepsilon^3, \varepsilon^4, \ldots$ are neglected. In Eq. (5.27), the angle Θ is given by

$$\Theta = \varphi + \psi + \pi/2 \tag{5.28}$$

From Eqs. (5.9), (5.10), the angle $\varphi+\psi$ is represented by

$$\varphi + \psi = \omega t - 2\,\varepsilon \sin \nu\omega t + C_1 \tag{5.29}$$

where C_1 is an arbitrary constant determined by initial conditions. The eccentricity e in Eq. (5.27) is expressed by a dimensionless quantity, and the actual value of eccentricity is given by $e\sqrt{I/M}$. By being replaced x, y, θ_x and θ_y in inertia terms by x_G, y_G, θ_{x1} and θ_{y1} in Eq. (5.11), respectively, the following equations of motion for the rotor with unbalances e and τ can be obtained:

$$\left.\begin{aligned}
&\ddot{x}_G + x + \gamma\theta_x = 0,\\
&\ddot{y}_G + y + \gamma\theta_y = 0,\\
&\ddot{\theta}_{x1} + i_p\omega\dot{\theta}_{y1} - 2\,\varepsilon\nu i_p\omega\frac{d}{dt}(\theta_{y1}\cos\nu\omega t) + \gamma x + \delta\theta_x = 0,\\
&\ddot{\theta}_{y1} - i_p\omega\dot{\theta}_{x1} + 2\,\varepsilon\nu i_p\omega\frac{d}{dt}(\theta_{x1}\cos\nu\omega t) + \gamma y + \delta\theta_y = 0
\end{aligned}\right\} \tag{5.30}$$

When there exist unbalances e and τ, the moments of inertia $i_p(I_p)$ and $1(I)$ must be considered as the principal moments of inertia about the principal axes passing through the gravitational center. By substituting Eqs. (5.27), (5.28), (5.29) into Eq. (5.30) and by rejecting small quantities of order ε^2, Eq. (5.30) is rewritten as follows:

$$\left.\begin{aligned}
&\ddot{x} + x + \gamma\theta_x = e\omega^2[\cos(\omega t + \xi') + \varepsilon(1-\nu)^2\cos\{(1-\nu)\omega t + \xi'\}\\
&\qquad + \varepsilon(1+\nu)^2\cos\{(1+\nu)\omega t + \xi''\}],\\
&\ddot{y} + y + \gamma\theta_y = e\omega^2[\sin(\omega t + \xi') + \varepsilon(1-\nu)^2\sin\{(1-\nu)\omega t + \xi'\}\\
&\qquad + \varepsilon(1+\nu)^2\sin\{(1+\nu)\omega t + \xi''\}],\\
&\ddot{\theta}_x + i_p\omega\dot{\theta}_y - 2\,\varepsilon\nu i_p\omega\frac{d}{dt}(\theta_y\cos\nu\omega t) + \gamma x + \delta\theta_x\\
&\qquad = \tau\omega^2(1-i_p)[\cos(\omega t + \eta') + \varepsilon(1-\nu)^2\cos\{(1-\nu)\omega t + \eta'\}\\
&\qquad + \varepsilon(1+\nu)^2\cos\{(1+\nu)\omega t + \eta''\}],\\
&\ddot{\theta}_y - i_p\omega\dot{\theta}_x + 2\,\varepsilon\nu i_p\omega\frac{d}{dt}(\theta_x\cos\nu\omega t) + \gamma y + \delta\theta_y\\
&\qquad = \tau\omega^2(1-i_p)[\sin(\omega t + \eta') + \varepsilon(1-\nu)^2\sin\{(1-\nu)\omega t + \eta'\}\\
&\qquad + \varepsilon(1+\nu)^2\sin\{(1+\nu)\omega t + \eta''\}]
\end{aligned}\right\} \tag{5.31}$$

in which

$$\left.\begin{aligned}
&\xi' = \xi + C_1 + \pi/2, \quad \xi'' = \xi + C_1 - \pi/2\\
&\eta' = \eta + C_1 + \pi/2, \quad \eta'' = \eta + C_1 - \pi/2
\end{aligned}\right\} \tag{5.32}$$

Equation (5.31) shows that external forces of order ε with frequencies $(1-\nu)\omega$ and $(1+\nu)\omega$ are induced by the fluctuation of the rotating speed of the frequency $\nu\omega$. Since all lateral vibrations of the rotating shaft are whirling motions, except

for shaft systems in which the spring constant γ vanishes and hence deflections and inclinations of the rotor are not coupled, a mode of vibration of the frequency $(\nu-1)\omega$ is not the same as that of the frequency $(1-\nu)\omega$, and further peaks of forced vibrations of frequencies $(\nu-1)\omega$ and $(1-\nu)\omega$ at the resonance appear separately. For instance, in the rotating shaft driven by a universal joint, forced vibrations of $-\omega$ and $+3\omega$ take place because of $\nu=2$, and those of $+\omega$ and -3ω do not occur. In this case, peaks of $+\omega$ and $-\omega$, peaks of $+3\omega$ and -3ω appear separately.

Ratios of magnitudes of the external forces of frequencies ω, $(1-\nu)\omega$ and $(1+\nu)\omega$ are $1:\varepsilon(1-\nu)^2:\varepsilon(1+\nu)^2$ in the first and second equations as well as in the third and fourth equations of Eq. (5.31). If there is no variable inertia term in the third and fourth equations of Eq. (5.30), these ratios of magnitudes of the external forces in the first and second equations of Eq. (5.31) are different from those in the third and fourth equations. It is more clearly seen from the following fact that equations of motion must be represented by Eq. (5.30) and variable inertia terms must be given by $-2\varepsilon\nu i_p\omega\frac{d}{dt}(\theta_{y1}\cos\nu\omega t)$ and $+2\varepsilon\nu i_p\omega\frac{d}{dt}(\theta_{x1}\cos\nu\omega t)$: Since all external forces of ω, $(1-\nu)\omega$ and $(1+\nu)\omega$ in the third and fourth equations of Eq. (5.31) have a common coefficient of $(1-i_p)$, they vanish for the shaft system in which the shape of the rotor is a sphere and hence i_p is equal to unity. From this it follows that there is no external force induced by the dynamic unbalance τ, because there must exist no dynamic unbalance in the sphere. If there were no variable inertia term in Eq. (5.30), external forces in the third and fourth equations of Eq. (5.31) would not vanish even if $i_p=1$. This is followed by a contradictory fact that external forces induced by the dynamic unbalance τ appears in the system consisting of the sphere without the dynamic unbalance τ.

It is natural[1] that forced vibrations of frequencies ω, $(1-\nu)\omega$ and $(1+\nu)\omega$ take place because of an existence of external forces of ω, $(1-\nu)\omega$ and $(1+\nu)\omega$. However it should be noticed that, even if one assumes that only one external force of ω exists, three forced vibrations of ω, $(1-\nu)\omega$ and $(1+\nu)\omega$ induced by variable inertia terms can appear. Accordingly it can be concluded that forced vibrations of frequencies $(1-\nu)\omega$ and $(1+\nu)\omega$ are introduced by (i) external forces of frequencies $(1-\nu)\omega$ and $(1+\nu)\omega$ which are induced by the fluctuation of the rotating velocity of the frequency $\nu\omega$, and (ii) variable inertia terms.

5.5. *Conclusions*

Conclusions obtained from the above discussion can be summarized as follows:

(1) When the angular velocity of the rotating shaft fluctuates periodically with the frequency $\nu\omega$, as shown in Eq. (5.10), there are variable inertia terms $-2\varepsilon\nu i_p\omega\frac{d}{dt}(\theta_y\cos\nu\omega t)$ and $2\varepsilon\nu i_p\omega\frac{d}{dt}(\theta_x\cos\nu\omega t)$ in the gyroscopic terms of equations of motion.

(2) Although equations of motion belong to differential equations with variable coefficients when the angular velocity pulsates periodically, unstable vibration does not take place, appearance of which is usually expected.

(3) There exist only free vibrations of $p_i-\nu\omega$ and $p_i+\nu\omega$ as well as p_i. Those

of $\nu\omega-p_i$ and $-p_i-\nu\omega$ do not appear.

(4) The external force with the frequency ω_0 causes forced vibrations of frequencies $\omega_0-\nu\omega$, $\omega_0+\nu\omega$ as well as ω_0. Forced vibrations of $\nu\omega-\omega_0$, $-\omega_0-\nu\omega$, however, do not occur.

(5) When $\omega_0 \fallingdotseq p_i+\nu\omega$ and $\omega_0 \fallingdotseq p_i-\nu\omega$ as well as $\omega_0=p_i$ (p_i=natural frequencies), resonance phenomena take place.

(6) When $\omega_0 \fallingdotseq p_i$, forced vibrations of ω_0 aggravate.

(7) When $\omega_0 \fallingdotseq p_i+\nu\omega$ and $\omega_0 \fallingdotseq p_i-\nu\omega$ forced vibrations of $\bar{\omega}_0=\omega_0-\nu\omega$, $\omega_0'=\omega_0+\nu\omega$ build up remarkably, their frequencies being apparently independent of ω_0.

(8) External forces of $(1-\nu)\omega$ and $(1+\nu)\omega$ are induced by unbalances e and τ of the rotor. Those of $(\nu-1)\omega$ and $-(1+\nu)\omega$ do not appear.

(9) Forced vibrations of frequencies $(1-\nu)\omega$ and $(1+\nu)\omega$ are caused both by the fact (8) and by variable inertia terms in equations of motion.

References

1) O. Föpple, "Kritische Drehzahlen rasch umlaufender Welle", V.D.I., Bd. 63 (1919), S. 866.
2) H. D. Taylor, "Critical—Speed Behavior of Unsymmetrical Shaft", Jour. App. Mech., Vol. **7**, No. 2 (1940-6), pp. A 71-79.
3) W. Kellenberger, "Biegeschwingungen einer Unrunden Rotierenden Welle in Horizontaler Lage", Ing. Arch., Bd. **26**, (1958), S. 302-318.
4) Y. Shimoyama and T. Yamamoto, "On the Critical Speed of a Shaft due to the Deflections of Bearing Pedestals", Trans. of Japan Soc. of Mech. Engrs., Vol. **20**, No. 91 (1954-3), pp. 215-222.
5) T. Yamamoto, "On the Critical Speed of a Shaft Supported in Ball Bearing, (Part 2)", Trans. of Japan Soc. of Mech. Engrs., Vol. **20**, No. 99 (1954-11), pp. 755-760.
6) T. Yamamoto, "On the Critical Speeds of a Shaft", Memoirs of the Faculty of Engineering, Nagoya University, Vol. **6**, No. 2 (1954-11), pp. 106-174.
7) T. Yamamoto, "On the Vibrations of a Rotating Shaft", Memoirs of the Faculty of Engineering, Nagoya University, Vol. **9**, No. 1 (1957-5), pp. 19-115.
8) P. J. Brosens and S. H. Crandall, "Whirling of Unsymmetrical Rotors", Jour. App. Mech., Trans. ASME, Vol. **28**, Ser. E, No. 3 (1961-9), pp. 355-362.
9) S. H. Crandall and P. J. Brosens, "On the Stability of Rotation of a Rotor With Rotationally Unsymmetric Inertia and Stiffness Properties", Jour. App. Mech., Trans. ASME, Ser. E, Vol. **28**, No. 4 (1961-12), pp. 567-570.
10) T. Yamamoto and H. Ōta, "On the Vibrations of the Shaft Carrying an Asymmetrical Rotating Body", Bulletin of JSME, Vol. **6**, No. 21 (1963-2), pp. 29-36.
11) T. Yamamoto and H. Ōta, "On the Forced Vibrations of the Shaft Carrying an Unsymmetrical Rotating Body (Response Curves of the Shaft at the Major Critical Speeds)", Bulletin of JSME, Vol. **6**, No. 23 (1963-8), pp. 412-420.
12) T. Yamamoto and H. Ōta, "Unstable Vibrations of the Shaft Carrying an Unsymmetrical Rotating Body (Vibrations Induced by Flexibility of Bearing Pedestals)", Bulletin of JSME, Vol. **6**, No. 23 (1963-8), pp. 404-411.
13) T. Yamamoto and H. Ōta, "On the Unstable Vibrations of a Shaft Carrying an Unsymmetrical Rotor", Jour. App. Mech., Trans. ASME, Ser. E, Vol. **31**, No. 3 (1964-9), pp. 515-522.
14) T. Yamamoto, H. Ōta, and K. Sato, "On the Forced Vibrations of the Shaft Carrying an Unsymmetrical Rotor (Forced Vibrations Having the Circular Frequencies Differing from the Rotating Angular Velocity of the Shaft)", Bulletin of JSME, Vol. **9**, No. 33 (1966-2), pp. 58-66.
15) T. Yamamoto and H. Ōta, "The Damping Effect on Unstable Whirlings of a Shaft Carrying an Unsymmetrical Rotor", Memoirs of the Faculty of Engineering, Nagoya University,

Vol. **19**, No. 2 (1967-12), pp. 197-217.
16) T. Yamamoto, "On Critical Speeds of a Shaft Suppoted by a Ball Bearing", Jour. App. Mech., Trans. ASME, Ser. E, Vol. **26**, No. 2 (1959-6), pp. 199-204.
17) T. Yamamoto and A. Saito, "On the Vibrations of "Summed and Differential Types" under Parametric Excitation", Memoirs of the Faculty of Engineering, Nagoya University, Vol. **22**, No. 1 (1970-5), pp. 54-123.
18) T. Yamamoto, H. Ōta and K. Kōno, "The Effect of Flat Shaft on the Unstable Vibrations of a Shaft Carrying an Unsymmetrical Rotor (Part I. Analytical treatment)", Memoirs of the Faculty of Engineering, Nagoya University, Vol. **21**, No. 1 (1969-5), pp. 122-134.
19) T. Yamamoto, H. Ōta and K. Kōno, "The Effect of Flat Shaft on the Unstable Vibrations of a Shaft Carrying an Unsymmetrical Rotor (Part II. Experimental treatment)", Memoirs of the Faculty of Engineering, Nagoya University, Vol. **21**, No. 2 (1969-11), pp. 287-293.
20) T. Yamamoto, H. Ōta and K. Kōno, "On the Unstable Vibrations of a Shaft With Unsymmetrical Stiffness Carrying an Unsymmetrical Rotor", Jour. App. Mech., Trans. ASME, Ser. E, Vol. **35**, No. 2 (1968-6), pp. 313-321.
21) H. Ōta, K. Kōno and Y. Mitsuya, "On Elimination of the Unstable Region of the Major Critical Speed in a Rotating Shaft System Carrying an Unsymmetrical Rotor (Dynamical Effect of a Flexible Pedestal or Added Mass on the Shaft)", Bulletin of JSME, Vol. **12**, No. 51 (1969-6), pp. 470-481.
22) H. Ōta and K. Kōno, "Unstable Vibrations Induced by Rotationally Unsymmetric Inertia and Stiffness Properties", Bulletin of JSME, Vol. **14**, No. 67 (1971-1), pp. 29-38.
23) T. Yamamoto and K. Kōno, "On Vibrations of a Rotor with Variable Rotating Speed", Bulletin of JSME, Vol. **13**, No. 60 (1970-6), pp. 757-765.
24) T. Yamamoto and H. Ōta, "On the Vibrations of a Shaft Carrying an Unsymmetrical Rotor", Memoirs of the Faculty of Engineering, Nagoya University, Vol. **21**, No. 1 (1969-5), pp. 1-78.
25) H. Ōta and K. Kōno, "On Various Vibrations of a Shaft Carring an Unsymmetrical Rotor", Jour. Japan Soc. Mech. Engrs., Vol. **72**, No. 610 (1969-11), pp. 1537-1546.